University of Ljubljana
Faculty of Electrical Engineering

Boštjan Šimunič

Model of longitudinal contractions and transverse deformations in skeletal muscles

DOCTORAL THESIS

Mentor: Proff. Vojko Valenčič, Ph.D.

Ljubljana, 2003

ABSTRACT

In this study we examine different techniques for detection of skeletal muscle properties. The main aim of the study is modelling muscle responses obtained by different methods. Because of the great interest for this field, scientists have developed several measuring methods, but still many issues remain unsolved. Present researches require interdisciplinary of measurements in the field of biomechanics, muscle physiology, system modelling, electrical stimulation and biological system and methods of electro physiology.

Development of computer capacity, technologically modern electronic devices and sensors has in recent years enabled greater technological progress in the field of biomechanical researches. Modern technology has launched more scientific approach of athletes training process as well as rehabilitation process. Therefore many athletes, trainers and physiotherapists incorporate new findings for prevention and rehabilitation of injuries, training dimension and for timing individual's peak performance on the day of competition. Top sport is not the only source, which has increased its demand for developing non-invasive, selective and simple method for monitoring muscle status – the need has expended over other fields, such as medical rehabilitation, diagnosing neuromuscular illnesses and injuries.

A new method called Tensiomyography (TMG) for monitoring skeletal muscle properties was developed at the Faculty of electrical engineering, University of Ljubljana, in Laboratory for biomedical imaging and skeletal muscle biomechanics. Method was evaluated with other well established methods and meets all requirements of top sport field, medicine diagnostics and rehabilitation. TMG method is based on measurements of transverse muscle belly displacement. During muscle contraction its belly enlarges perpendicularly to direction of exerted muscle force. Method's selectiveness is the main advantage of this measuring set-up, however it provides no information on absolute muscle force.

On the basis of results obtained with simultaneous use of TMG and torque measuring method we calculated mathematical models in order to present either similarity or heterogeneity of these results. Standard characteristics of muscle activation elicited by electrical stimulation were measured and interpreted on the basis of results obtained with *in vitro* measurements of toad gastrocnemius. In vitro experiment allowed us to perform measurement on isolated muscle with and without its tendon.

Selective measurements of muscle belly displacement and elbow torque measurements were performed on 15 male subjects. Muscles biceps brachii (BB) and brachioradialis (BR) were selectively stimulated with electrical stimulation. Displacement sensor was placed perpendicularly to the thickest part of the muscle belly. Force transducer was placed on the forearm with known distance away from elbow joint axis. Protocols A and B (defining electrical stimulation) were applied on each muscle. Protocols consisted of twitch and tetanic stimulation. Combining both measuring methods enabled us to monitor activation characteristic, twitch-tetanus ratio, post-tetanic potentiation, torque-length, displacement-length, torque-frequency and displacement-frequency relation.

On the basis of obtained results, models presenting connection between displacement and torque were proposed. In vitro measurements of the toad gastrocnemius were carried out in order to determine the most influential mechanisms, which have impact on muscle responses.

The study revealed that dynamics of muscle belly displacement and muscle joint torque differs due to disturbing parameters, such as: rubbing of surrounding tissue, limited muscle belly enlargement by fascia, joint mechanics, influence of the skin fold and tendons. Measurements on the isolated toad gastrocnemius were used for eliminating the disturbing parameters and tendon's influence on muscle force response was examined. Muscle without its tendon did not show any difference between response dynamics in contrast with muscle-tendon system. Tendon with its capability of storing elastic energy impacts muscle force response.

Method for measurement of muscle belly stiffness in vertical direction was also developed. With this instrument muscle belly passive resistance was detected, which influences muscle belly displacement. With muscle belly stiffness information muscle belly displacement was moderated and thus relative muscle force measurement (with TMG method) was enabled. Absolute muscle force measurement requires additional information on muscle architecture and size measurements.

Ratio between twitch and tetanus amplitude (twitch-tetanus ratio) of muscle displacement measurement was significantly correlated. This conclusion cannot be confirmed with results of torque measurements. Non-significant negative correlation was found between twitch-tetanus ratio and contraction time (Tc) of responses measured with both methods. Results of both methods showed significantly lower twitch-tetanus ratio of BR muscle. The reason could lie in longer tendon and activation pattern. The latter means that firing rate contribution to the maximal muscle response is larger than the contribution of the stimulus amplitude in smaller muscles. We can conclude that not only muscle and its Tc, but also joint angle affects twitch-tetanus ratio measured with both methods. Our findings showed that lower elbow angles increase twitch-tetanus ratio.

In both muscles it was evident that displacement-frequency characteristics depends on elbow angle, which was not the case in torque-frequency characteristics (almost constant). TMG method proved to be more suitable for measuring tetanic responses, especially at lower frequencies, where these responses were not impacted by the forearm persistence. Higher frequencies or higher amplitudes of electrical stimulation cause saturation of muscle belly displacement.

The study also revealed that the increase in response amplitude was not the only contractile parameter to observe in post-tetanic potentiation measurement. Decreases in delay time, contraction time, sustain and half relaxation times of muscle displacement response were significant in both muscles. The same conclusion was drawn for joint torque response. BR muscle has bigger potentiation of response amplitude than BB muscle, which was significantly and positively correlated with percentage of type II fibres. Elbow angle affects the degree of post-tetanic potentiation of muscle belly displacement and also some contractile parameters of torque responses.

On the basis of in vitro TMG measurements, performed on toad isolated gastrocnemius, we built a model in order to demonstrate how the tendon influences the response of muscle force. A neural network was used to show how the responses of belly displacement and muscle force to random pulse-train are connected. Firstly the neural network was subjected to a learning process, which happened to be inappropriate in case of responses of the same muscle in different toads. This indicates a very complex connection between both responses.

Comparison of both responses (belly displacement and muscle force) in isolated toad gastrocnemius muscle revealed that contraction time and half relaxation time in force response are significantly shorter. The same comparison was made for belly displacement and torque in human BB and BR muscles, where again shorter contraction time and half relaxation time in torque response were observed with even higher statistical significance.
In order to study muscle belly metric properties during contraction and relaxation of toad gastrocnemius, a geometrical model was used. During the process of contraction observed muscle is thickened and shortened, which causes the tendon to stretch. Founded on muscle force measurements we calculated tendon’s passive transient function, which differs for the process of contraction and relaxation.

Responses of muscles with a short Tc are presented with curves, which are very specific in the shape of their peak. Modelling fast- (type II) and slow-twitch (type I) muscle fibres enabled to explain these peak-shapes. For the purpose of modelling superposition method was used, relationship between the intracellular calcium concentration and isolated fibre force was adopted from literature and linear relationship between the cause (muscle fibre longitudinal contraction) and the consequence (muscle fibre transverse contraction) was adopted. After model parameters were optimised we compared measured transverse muscle belly force and longitudinal muscle force to modelled contraction process. Different transient functions were calculated for longitudinal and transverse contraction – connective tissue damping coefficient was from 2.2 to 6.5 times greater in longitudinal direction.

Final conclusions: TMG method is suitable for measuring time parameters of muscle contraction and relaxation, especially contraction time. With a simple upgrade it can be used for measuring relative force exerted during muscle contraction. With TMG method muscle activation can be monitored selectively, precisely and with low variability. Completing it with simultaneous force or torque measurements it offers wide range of muscle contraction research possibilities.

INDEX

1. Force exerted by skeletal muscle

1.1.1. Skeletal muscle origo and insertio

Skeletal muscle origo and insertio, joined in the word tendon, are in function of transforming the muscle belly contraction force onto the skeleton and thus enabling the joints to move. The importance of tendon function was researched by numerous scientists (Alexander, 1988; Zajac III, 1989). Tendons consist mainly of collagen, a substance without contractile ability, which categorizes them into a group of passive muscle elements. Their function is attaching muscle to the skeleton, transforming muscle force to the skeleton and storing elastic energy. When assessing skeletal muscles' properties, we must always consider also tendon properties, since they strongly influence skeletal muscle functioning.

Tendons vary in their length, thickness and the way of being attached to the skeleton. Beside collagen (86 %) they comprise elastic, actin, fibronectin, proteoglycans, water and fibroblasts. Collagen is a fibrous protein, mechanically very stable. Its fibres are organized longitudinally and parallelly – for optimal transformation of greater muscular forces. The amount of elastic energy, stored in the tendon, is dependent on its length and is thus bigger in longer tendons (Biewener, 1998). When comparing two tendons, first comprising more parallel fibres than the second, then the force used for the same elongation is greater in case of the first tendon (Fig 2.2).

Tendon elastic properties have been studied *in vitro* (Viidik, 1973; Butler et al., 1978; Ker, 1992), still it is not clear to what extent these results can be applied to *in vivo* physiological conditions. *In vitro* experiments are performed using pincers for attaching the tendons to the sensor, which causes the tendons to stretch irregularly (Ker, 1992) and thus reducing the objectivity. Maganaris and Paul (2000), and Maganaris (2002) have presented a ultrasonic measuring method for *in vivo* monitoring tendon contractile properties, which enabled them to reveal that *in vivo* conditions lead to sliding the muscle-tendon complex along surrounding tissue, which results in two things: longitudinal non-homogeneous tendon stretch and hysteresis of elongation and shortening with respect to the force, which is independent of burden the muscle-tendon complex is subjected to.

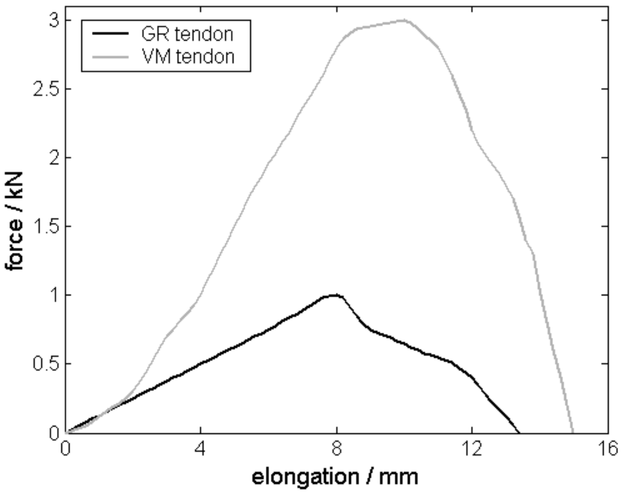

Figure 1.1: Relation between the force (load) and elongation of m. vastus medialis (VM) and m. gracilis (GR) tendon, (Noyes, 1977; Noyes et al., 1984). The force needed for the tendon elongation of 8 mm was in case of VM 2.8 kN and in case of GR 1 kN.

In mammals tendons are stretched (during muscle contraction) from 2 to 5 % (Ker et al., 1988; Zajac III, 1989; Maganaris and Paul, 2000), while the connective tissue (called aponeurosis – it connects the tendon with the muscle belly) is stretched to the same extent (Rack in Westbury, 1984) or even about 10 % more (Huijing and Ettema, 1988/1989, Lieber et al., 1991).

1.1.2. Generating skeletal muscle contraction force

When myosin heads slide along actin this results in shortening of the sarcomere for as long as action potentials are present on the sarcolemma, other wise the shortening is terminated by the H band. The force at both endings of the sarcomere (Z band) is dependent on the number of overlapping heads of actin and myosin within a sarcomere. The overlapping is minor within the stretched sarcomere but increases with its shortening and in the end with further shortening again diminishes – the reason is the geometrical limitation of the shortening, despite the presence of action potentials on the sarcolemma (Fig 3.3, next chapter).

When sarcomere, the smallest contractile element, is contracting and thus shortening it exerts the tension at both endings. In the myofibril the sarcomeres are bounded parallel. The twitch contraction of a single sarcomere results in the twitch contraction of the whole myofibril i.e. the multiple of twitch contractions of a single sarcomere. Force at the endings of a single myofibril equals the force at the endings of a single sarcomere, while the force at the endings of muscle fibre equals the sum of forces in all myofibrils within the same fibre.

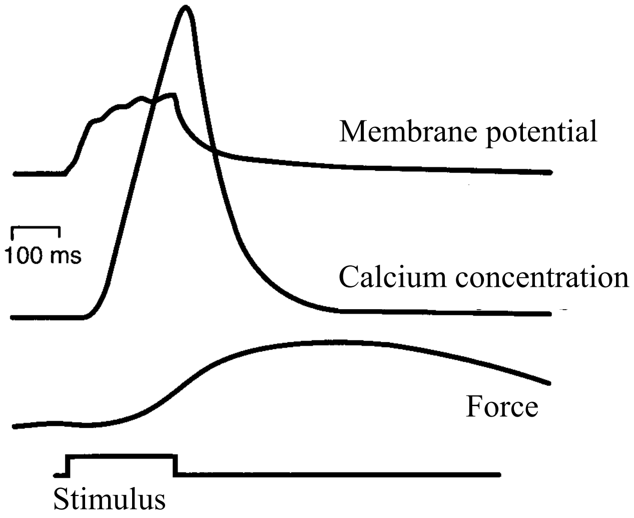

Figure 1.2: Electrical pulse depolarises the muscle membrane, causes an increase in intracellular calcium concentration as well as the force exerted by the muscle fibre.

A unit, which comprises the cell body and dendrites of a motor neuron, the multiple branches of its axon and the muscle fibres that it innervates, is called a motor unit (MU). MU is the smallest functional unit of the nervous-controlled muscular activity. Muscle fibres of the same MU equal regarding their histological classification and are distributed within the muscle in such a manner that two neighbouring fibres cannot be comprised within the same MU. Action potential on the appurtenant axon causes fibres of the same MU to contract on the principle "all or nothing". The number of muscle fibres comprised in the same MU (innervation ratio) is task dependent – for example, facial (eye) muscles are performing very rapid and precise movements, their innervation ratio is small (10 – 100), leg muscles on the other hand, perform more forceful movements, their innervation ratio is therefore bigger – a few thousand muscle fibres.

The activation pattern (MU recruitment order) in voluntary contraction depends on the force to be exerted. Firstly, small and mainly slow-contracting MUs are activated, with increasing force additional – bigger and mainly fast MUs are activated (Henneman, 1980). This force increases on two principles: with additional MU activation (MU recruitment) or with increasing frequency of action potentials (firing rate), the latter contributing to gradual increase of contraction force. The isometric force – MU recruitment relationship is sigmoid (Bigland and Lippold, 1954b) and depends on the contraction speed of MU (Botterman et al., 1986).

During contraction and relaxation of larger muscles, such as m. biceps brachii (BB), the MU recruitment is constantly present, increasing the firing rate only takes over in exerting the maximal force. In case of smaller muscles, such as m. first dorsal intersseous, the case is just the opposite. Already 30 % of maximal muscle force is enough to activate the whole population of MU in the muscle, further increasing of muscle force is due to increasing the firing rate (Kukulka and Clamann, 1981; De Luca et al., 1996). Marsden et al. (1983) presented an instant rise in firing rate at the beginning of contraction, later it stabilises at lower frequency. This is a sort of preventive step against getting fatigued too soon.

Muscle	**Maximal firing rate / Hz**
m. first dorsal interosseus	35 - 40
m. extensor indicis	35
m. tibilais anterior	33
m. adductor digiti minimi	25 - 35
m. adductor pollicis	25 - 30
m. deltoideus	29
m. biceps brachii	20 - 25
m. soleus	11

Table 1.1: Maximal firing rates for different muscles (Bellemare et al., 1983; De Luca et al., 1982; Freund et al., 1975; Monster and Chan, 1977; Tanji and Kato, 1973; Van Cutsem et al., 1997).

Firing rate for exerting minimal muscle force is ranging between 5 and 7 Hz (Kudina and Alekseeva, 1992a; Spiegel et al., 1996). For exerting 35 % of maximal muscle force the MUs with lower recruitment threshold require higher firing rate than the MUs with higher recruitment threshold (Tanji and Kata, 1973; Monster and Chan, 1977). In case of exerting maximal muscle force the findings part. On one hand the same pattern as in exerting 35 % of maximal muscle force was established (Gydikov and Kosarov, 1974; Monster and Chan, 1977), and on the other hand just the opposite (Kamen et al., 1995). For different muscles different maximal values for firing rates have been reported (Table 1.1).

The release of calcium from the sarcoplasmic reticulum and the increase of intracellular calcium concentration are considered the beginning of cross bridges cycle. On the prepared human muscle fibre a sigmoid relationship was presented between calcium concentration and muscle fibre contraction force (Greger and Windhorst, 1996). A study, which involved type I muscle fibre in rat soleus revealed that maximal calcium concentration and maximal force were detected 21 and 151 ms after the electrical stimulus, respectively. Half relaxation time of calcium concentration and force was 126 ms and 305 ms, respectively. In the fast-contracting fibre of rat extensor digitorum longus, maximal calcium concentration was detected 14 ms and maximal force 28 ms after the electrical stimulus. Half relaxation time of calcium concentration and force was 49 ms and 19 ms, respectively (Wetzel and Gros, 1998).

Muscle force is not only dependent on the number of muscle fibres, level of activation and firing rate, but also on geometrical scheme of the muscle, which is presented in the next chapter.

2. Measuring muscle force

2.1. Measuring muscle force – method review

Appropriate measuring methods are required in order to study skeletal muscles properties (optimal muscle length – joint angle, activation pattern) *in vivo* and to be able to perform non-invasive comparisons of different muscles or same muscles of different subjects. Moreover, a method, which would enable measurement of the absolute force exerted by a single muscle hasn't yet been presented – the only methods known are either invasive or non-selective. In most cases absolute muscle force is inferred from modelling on the basis of more or less known anthropometrical data. Still such estimation cannot be used with an individual subject, just because of its individuality (usually far from average).

Two out of several measuring methods for skeletal muscles assessment were used for the purpose of the research work presented in this thesis. In the following chapters both methods are presented in sense of their historical background, research results in field of muscle force measurement, their advantages and disadvantages over other methods, which also offer an explanation why these methods were chosen.

2.1.1. Electromyography

Electromyography (EMG) is a method for detecting muscle's electrical activity (action potentials) during its contraction. The process of depolarisation and action potentials (AP) propagation along the muscle fibre can be detected with bipolar electrodes (separately placed) and one reference electrode placed above the electrically still muscle (ground electrode). The measurement procedure consists of two steps. Firstly, the voltage (potential difference) between the signal detected by each electrode and the ground electrode is determined. Secondly, the difference between the voltage measured by each electrode is calculated and amplified by the device and the output is a voltage-time signal referred to as an EMG. With respect to sensors application two kinds of EMG method applications are in use: surface EMG (sEMG – non-invasive) and intramuscular EMG (iEMG – invasive). Both of them provide results in time domain. EMG response is evaluated with several parameters, the most important being as follows: mean and median frequency of power density spectrum (MPF and MdPF) and the amplitude of integrated EMG (Knaflitz et al., 1990; Merletti et al., 1990 and 1994).

EMG response to voluntary contraction is a sum of APs on muscle fibres. EMG response to electrically evoked contraction results in 1) a singe M-wave when stimulated with a single stimulus and in 2) sequence of M-waves when stimulated with pulse train. The iEMG method is applied using a needle as an EMG detection electrode, inserted directly into the measured muscle and detects electrical activity directly on MUs. The amplitude of iEMG response depends on the location of the detection electrode (DE) insertion and is at some levels of activation linearly related to the force of contraction, regardless of the spot of detection electrode insertion (Onishi et al., 2000; Komi and Buskirk, 1970; Oberg et al., 1992).

sEMG and iEMG power spectrum is used for studying muscle fatigue (Lindström et al., 1970; Merletti et al., 1991), muscle fibre composition (Hagberg et al., 1987) and recruitment order (Bernardi et al., 1996; Bilodeau et al., 1994 and 1995; Moritani and Muro, 1987; Sanchez et al., 1993).
Preliminary studies revealed linear relationship between the amplitude of integrated sEMG and contraction force (Lippold, 1952; Lawrence and De Luca, 1983; Milner-Brown, 1975) and between MPF of sEMG and contraction force (Gerdle et al., 1994; Bilodeau et al., 1990). In case of relationship between MPF or MdPF and torque, studies revealed opposite results: positive (Gerdle et al., 1991; Gerdle and Karlsson, 1994), negative (Komi and Viitsalo, 1976) as well as independent (Komi and Viitsalo, 1976; Nanthavanu et al., 1989) correlation was presented. The most probable ground for these dispersing results would be the way of calculating both MPF and MdPF, differences between measured muscles as well as subjects and their gender, electrodes size and setting up, skin fold and the way of correlating the torque and both frequency dependent parameters (Karlsson and Gerdle, 2000).

Correlation between contraction force and amplitude of integrated sEMG was greater when measurements were performed under isometric conditions (Bigland and Lippold, 1954a; Lawrence and De Luca, 1983) and lesser when performed under non-isometric conditions (Calver and Chapman, 1977; Milner-Brown and Stein, 1975). Hasan and Enoka (1985) presented as follows: in case of muscles BB and BR for the case of extended and flexed elbow the exerted force is greater than for the elbow flexion between those extreme positions, where the exerted force remains constant. This means that the shorter the muscle moment arm the greater the force required.

Kupa et al. (1995) established that MPF and AP conduction velocity are in connection with the muscle fibre type as well as its cross-section for the *in vitro* conditions. Fast-contracting fibres feature higher MPF than the slow-contracting ones. Fibres with larger cross-sectional area feature higher MPF and greater AP conduction velocity.

Electrical stimulation is used in order to reduce subjects affecting the measuring result. The M-wave is result of summed APs of muscle fibres underneath the EMG detection electrode. Bilodeau et al. (2002) presented a positive correlation between the MPF of the EMG power spectrum and the torque during voluntary contraction and a negative correlation between the MPF of the M-wave and the torque during electrically evoked twitch. So far, the explanation of this finding remains unknown.

Frequency spectrum of the EMG response is influenced also by muscle fibre composition. Higher percentage or larger cross-sectional area of fast-contracting muscle fibres results in higher MPF or MdPF (Gerdle et al., 1988, 1991 and 2000; Mannion et al., 1998; Wretling et al., 1987). This means that the reason for the simultaneous increase of the MPF or MdPF (of the EMG) and torque lies in recruitment of larger MUs.

The shape of the MPF and MdPF (of the M-wave) is influenced by the muscle fibre length (Lindström et al., 1970; Bazzy et al., 1986; Inbar et al., 1987; Okada, 1987; Dimitrova et al., 1991) and position of the sEMG detection electrode (Dimitrova et al., 2001; Roy et al., 1986; Lateva et al., 1993; Dimitrov and Dimitrova, 1998; Farina et al., 2001 and 2002). This sets a limitation to monitoring dynamic muscle contractions, under non-isometric conditions.
Maximal voluntary contraction (MVC) is an often-researched phenomenon. However, such a contraction cannot be single-muscle-targeted. To gain information on single muscle, the EMG method can be used (Masuda et al., 1996; Merletti et al., 1990, Sanchez et al., 1993), still only the APs of the fibres directly underneath the sEMG detection electrode will be detected, the same holds for the APs of the fibres near the iEMG detection electrode. For the same reason the EMG method cannot be used for comparing muscle force for different subjects or different muscles. Detecting MVC with the EMG method raises a question on subjectiveness and technical difficulties affecting the repeatability of the method (Baratta et al., 1998). Parameters MPF and MdPF of the EMG can be used for monitoring relative muscle force only at the absence of fatigue. For in fatigued muscle values of both parameters diminish (Kadefors et al., 1968; Kogi and Hakamada, 1962), and the form of the power density spectrum alters (Kupa et al., 1995). Sica and McComas (1971) showed that changes due to muscle fatigue are dependent also on muscle fibres composition.

Merletti et al. (1995) found out that the EMG power-spectrum based parameters are less variable than parameters defined in time domain. Measurement of AP conduction velocity proved to be the most variable one. The shape of the M-wave proved even less variable, but it should be taken into consideration, that this shape varies for each muscle and depends on the position of stimulation and detection electrodes.

Variability coefficient (VC) for EMG parameters on few-day-basis (up to 18 %) and on one-day-basis is considered too big to perform a quality interpretation of measured data (Merletti et al., 1995), yet can be diminished applying certain measures. One of them is to teach the subjects how to cooperate in a measurement protocol as shown by Gabriel (2002), who managed to diminish the VC as well as the mean direct component of the EMG signal from 55 to 40 % for the muscle BB and from 52 to 40 % for the muscle BR. Numerous preliminary studies revealed that subjects attempting to perform a MVC only reach from 70 to 90 % of the reachable MVC (Baratta et al., 1998; Corcos et al., 1993; Darling and Cooke, 1987; Gabriel, 2000) which enters a subjective variability into results of all measuring methods. Erfanian et al. (1998) suggested a model of muscle force prediction (on the basis of EMG results recalibration) in order to diminish the VC on the few-day-basis.

The main source of the EMG method variability is the so called system-noise – the noise caused by amplifiers, interfaces, cards for data acquisition, AD converters, connecting cables, grid voltage, monitors and other electronic components. The signal-to-noise ratio is considered the most sensitive indicator, especially for the EMG recordings of contractions below 25 % MVC (Cinderby et al., 1996; Hagg, 1992). Baratta (1998) presented the algorithm for subtracting the system-noise from EMG recording (in both time and frequency domain), which increased the signal-to-noise ratio.

2.1.2. Measuring torque and muscle force

A method for measuring muscle contraction force is an invasive one in case of inserting the force sensor directly into the muscle tendon or in case of *in vitro* measurements, where the muscle tendon is attached to the force detector. Also available are the optical force detectors, but are only to be used with protocols featuring resolution (< 1 μg). They enable detection of both active and passive force exerted by a single muscle fibre or a single MU (Fearn et al., 1993; Canaday and Fay, 1976; Glerum and Van Mastrigt, 1990). In case of *in vivo* measurements we often measure the torque about a joint and together from so called moment arm modelling (modelling the joint and muscle architecture) we infer on contraction force.

Torque about the joint equals vector product of muscle force and moment arm. Muscle arm is the distance end to end between the joint axis and the muscle insertio. Measured torque is affected by two parameters – muscle force and muscle moment arm. Further, muscle force is dependent on muscle length, moment arm is dependent on joint angle. Moment arm reaches its minimum when the joint is flexed or extended to its outermost position. An et al. (1981) showed that in these positions the moment arm of the elbow was two times smaller (for all major flexor muscles) than at the angle of 1.75 rad.

Muscle moment arm transforms the muscle force into the joint moment and thus plays an important role in joint flexibility (Hogan, 1990). In the relaxed state the angle of pull is small, still it can change with respect to joint angle. For the following elbow flexor muscles BB, BR and brachialis, the angles of pull are 1.4, 0.4 and 1.2 rad, respectively (elbow angle: 1.57 rad) (An et al., 1984b).

So far no correlation between anthropometrical data and moment arm definition has been presented. Amis et al. (1979), An et al. (1981), Gerbeaux et al. (1996) and Murray et al. (1995) attempted to evaluate the length of moment arm for elbow extensor and elbow flexor muscles, but have not reached any consensus regarding their results and also could not find any reasonable explanation for it. Gerbeaux et al. (1996) normalized the moment arm length according to the length of the bone ulna, while An et al. (1981) performed normalization according to physiological cross-section area (PCSA). Murray et al. (2002) reported the correlation between the longer TB moment arm and the bone ulna. He reported no correlation between other hand bones and muscle moment arm lengths.

Muscle force is dependent on the length of its belly (Gordon et al., 1966), its speed (Hill, 1938), moment arm, which defines the length of muscle-tendon complex (An et al., 1984a), the speed of the muscle-tendon complex during the joint rotation (Delp and Loan, 1995) and its composition, which influences the amplitude as well as the speed of the torque, exerted during the muscle contraction (Buchtal and Schmalbruch, 1990; Clarkson et al., 1981; Desmedt and Godaux, 1978; Rice et al., 1988; Thorstensson et al., 1976).

For subjective reasons, such as subject's motivation, figure, coactivation of synergist muscles (contributing to the torque about the observed joint), coactivation of antagonist muscles (contributing the negative torque about the observed joint; Maganaris et al., 1998c) as well as for technical reasons, such as limb fixation and joint axis positioning, the repeatability of applied measuring method is diminished. In order to eliminate some of the abovementioned factors Farina et al. (1999) suggested two ways of limb fixation for the purpose of force measurement (MVC). However, no significant improvement of the method's repeatability was achieved.

On the contrary to voluntarily evoked contraction, the electrically evoked one leads to more selective results of torque measurements. In order to measure the entire force exerted by electrically evoked contraction, the pulse train has to consist of at least 10 pulses. One electrical pulse only is not sufficient to transfer the entire muscle force through series elastic element (SE) onto the bone (Kawakami and Lieber, 2000) and thus the measured torque does not correspond to exerted one (Hoyle, 1983). Thomas et al. (1999) showed that the series of 5 to 7 stimuli is required for exerted muscle force to reach its maximum and to equal the tetanic force – only under such conditions sufficient volume of calcium is released from sarkoplasmic reticulum (SR). Allen et al. (1989) reported maximal force was achieved with pulse train of larger number of pulses.

Multiple usage of electrically evoked torque measuring method was shown by Day et al. (2002), who performed measurements on patients suffering from periodical paralysis. They claimed that in clinical environment it is more suitable to measure torque exerted by electrically stimulated muscles, since the affected muscles are often to weak to exert a measurable torque.

Intramuscular force measurement is selective, but invasive measuring method (Fowler et al., 1993; Herzog and Leonard, 1991; Komi, 1990; Maton et al., 1987), which allows force to be measured only at one end of the muscle. It should be made notable, that in case of multiple activated muscle heads attached to the same tendon, measuring muscle force at the other end of the muscle would not necessarily provide the same result (Huijing and Baan, 2001). For *in vitro* conditions measured force is the same, regardless of the sensor location.

To be able to model force exerted by a single muscle following has to be taken into account: response of the observed muscle (which has to be identified using non-selective response) and anthropometrical data for observed muscle.

2.1.3. Mechanomyography

The tendon tension is not the only mechanical parameter of muscular activity. During isometric contraction the exerted force is in connection with the thickening of muscle fibres. Muscle belly enlargement is also a mechanical response, which occurs together with exerting contraction force, but is not directly connected with it (Zhang et al., 1996). Already in 1665 Grimaldi F.M. perceived the sound of contracting muscles during clenching the fist. In 1810 Vollaston W.H. connected muscle sound with its contraction and also measured the frequencies, which proved to range from

14 to 36 Hz. The same results were gained in later years when measurements were performed using modern measuring instruments.

For the purpose of clinical environment mechanical response (mechanomyogram – MMG) was compared to electrical activity of measured muscle (EMG). By calculating the ratio between both amplitudes they distinguished between healthy and affected muscles (Barry et al., 1990). The synchronous increase of EMG response and decrease of MMG response indicated the atrophy of observed muscle. Coefficient that refers to electrical and mechanical activity is of great clinical importance, especially for better understanding and treatment of pathologies, such as pain in patella region.

Muscle belly dynamic enlargement (Barry, 1992; Barry et al., 1992; Orizio et al., 1996 and 1997) and vibration (Wakeling and Nigg, 2001) have only a few times been a subject to mechanical contractile properties research. In order to stress the mechanical origin of measured responses regardless of the sensor type (Orizio, 1993), such responses have been named *mechanomyogram* (MMG), which is the name for a group of measuring method previously known as *vibromyogram* (Zhang et al., 1992), *muscle sound* (Orizio et al., 1989; Oster and Jaffe, 1980), *acoustic myogram* (Barry et al., 1985), *soundmyogram* (Orizio and Veicsteinas, 1992) also *phonomyogram* (Maton et al.in ostali, 1990) – all the names reflecting the sensor used.

The MMG method enables observations of mechanical or sound vibrations of a contracting muscle with the accelerometer or microphone, attached to the skin over the observed muscle (Orizio, 1993; Wollaston, 1980). Vibrations are the result of muscle belly displacement, MUs activating in their resonance frequency (Barry, 1987; Frangioni, 1987) and oxygen flow, which appears as a result of over dimensioned muscle fibres (Orizio, 1993). It is widely accepted, that the MMG method can be well used for measuring the firing rate and synchronization of MUs as well as the firing rate (Yoshitake and Moritani, 1999; Dalton and Stokes, 1993; Keidel and Keidel, 1989; Maton et al., 1990). Akataki et al. (2001) presented the MMG method as suitable for monitoring muscle activation and detailed monitoring contraction force, above all it enables easier data collection and its processing.

Many studies revealed correlation between muscle force and MMG amplitude up to 80 % MVC (Esposito et al., 1996; Matheson et al., 1997; Maton et al., 1990; Orizio et al., 1989; Smith and Stokes, 1993; Zwarts and Keidel, 1991), for forces exceeding 80 % MVC reported results disperse. Maton et al. (1990), Smith and Stokes (1993) and Zwarts and Keidel (1991) reported the increase of MMG amplitude and interpreted it as a result of MU recruitment (Maton et al., 1990; Stokes and Dalton, 1991). On the contrary, Esposito et al. (1996), Matheson et al. (1997) and Orizio et al. (1989) reported the decrease of MMG amplitude, explaining it with fusion of APs at high frequencies and high muscle tonus (Esposito et al., 1996; Matheson et al., 1997; Orizio et al., 1989, 1993 and 1996).

Myosin heads sliding along actin under isometric conditions causes shortening of contractile element (CE) and thus causes the tension in tendons. Considering the non-changing muscle volume during contraction, muscle diameter is during shortening increased (Baskin and Paolini, 1967). Muscle belly transverse displacement is monitored with MMG method using the laser displacement sensor on the surface of the muscle (Orizio et al., 1999, 2000). The measurement however is affected by lateral displacement due to irregular muscle fibre activation, changes of muscle dimensions and muscle resonance frequency (Barry, 1987; Barry and Cole, 1990; Orizio et al., 1989, 1996). In frequency domain the relation between muscle force and MMG response reveals that muscle force is damped mainly by SE, while muscle belly displacement measured by MMG is mainly damped by parallel elastic element (PE) (Orizio et al., 2000). Orizio et al. (2000) presented correlation between MMG frequency spectrum (sensor type: laser displacement sensor) and muscle force on isolated cat gastrocnemius. Previously, using the same measuring procedure, they demonstrated muscle belly displacement to be quadratic-dependent from force exerted by isolated muscle (cat gastrocnemius), which was explained using different mechanical models for both phenomena. Similar relationship was established by Barry et al. (1985) and Maton et al. (1990) on human m. BB, when they compared firstly the root mean square (RMS) of MMG and the weight the subject was lifting during isometric contraction, and secondly when they compared the RMS of MMG and muscle force.

It has been shown that MMG parameters MPF and MdPF depend on muscle fibre composition or contractile properties (Kouzaki et al., 1999; Orizio, 1993; Petitjean et al., 1998) and the sensor used (Maton et al., 1990). The MMG response is influenced by muscle tonus, the number of recruited MUs, body vibration, surrounding tissue density and elasticity, temperature, reflection and refraction when the sound traverses different tissues (Dalton and Stokes, 1993; Orizio, 1993). Orizio et al. (1993) showed that the MMG response is changed also due to other muscles' coactivation. Wee and Ashley (1990) reported difficulties on separating MMG responses, because of coactivation of synergist muscles and the antagonist muscle. Some but not all factors are welcome for their impact on the MMG response. It has been demonstrated that the collected data are of low amplitudes, the signal-to-noise ratio is small, therefore very precise and thus expensive measuring equipment, impedance-adjusting sensor and cable, and applying certain filtration methods is required (Wong, 2001; Orizio, 2002; Schure, 1970).

Ebersole et al. (1999) reported the MMG response to be dependent on the MU recruitment order, muscle tonus and intramuscular pressure. Suter and Herzog (1997) observed muscle inhibition and claimed that MU recruitment order is changing with knee angle. Intensified muscle tonus diminishes the MMG response amplitude – that occurs due to increased number of restored cross bridges in muscle fibres, which than oscillate with lower amplitude. Increased intramuscular pressure diminishes the MMG response amplitude as well. Sejersted et al. (1984) showed that with increasing muscle force also the intramuscular pressure increases and so the measurement error of MMG method increases with increasing muscle force.

2.1.4. Measuring intramuscular pressure

In the state of inactiveness the intramuscular pressure (IP) only changes due to the capillary blood flow (Aukland in Reed, 1993), while during contraction muscle fibre walls prevent the liquids from flowing through and the IP increases. During isometric contraction muscle fibre dynamics is intensified (Hargens et al., 1982; Parker et al., 1982) and consecutively also the blood flow inside the muscle, which is increased up to 20 times in order to provide enough oxygen and wash away the waste cell material (Van Donkelaar et al., 2001). IP is varying according to Laplace law the equation 2.1:

$$IMP = P_o + n \cdot \Delta h \frac{s}{r}$$ **Equation 2.1**

In the equation 2.1 P_o stands for the initial intramuscular pressure (Pa) while resting, n indicates the number of muscle fibre concentric layers, Δh is the thickness of the individual layer (m), s indicates the muscle fibre tension (Pa) and r – radius of muscle fibre curvature (m), (Sejersted et al., 1984).

The method is based on inserting the pressure sensor through the catheter into the muscle belly (invasive procedure). Measuring results are in form of IP response in time domain and are influenced by the muscle fibre tension, sensor penetration (depth and angle), muscle architecture (muscle fibre curvature and pennation angle), position of subject and measured muscle and in case of *in vitro* conditions also the muscle preparation (Sejersted and Hargens, 1995; Korner et al., 1984).

The amplitude of IP response is directly connected to isometric and isokinetic muscle force (Mazella, 1954; Sadamoto et al., 1983; Sejersted et al., 1984), however the slope coefficient varies for measuring the same muscle as well as measuring different muscles (Sejersted et al., 1984; Jensen, 1991). Parker et al. (1984) showed the IP to be, on the contrary to EMG, independent of muscle fatigue.

2.1.5. Tensiomyography

Tensiomyography (TMG) is measuring method used for monitoring transverse muscle belly displacement under isometric conditions. It was developed in the Laboratory for bioelectromagnetics (LBM) at the Faculty of Electrical engineering, University of Ljubljana, Slovenia. The displacement sensor is positioned perpendicularly to the tangential plane on the largest area above the muscle belly. The muscle belly displacement (enlargement) during contraction is observed and monitored. Valenčič and Knez (1997) demonstrated that TMG method provides valuable data on measured muscle's contractile properties. The main distinction between the TMG and the MMG method (application using laser displacement sensor) is in creating the initial pressure on the surface of the measured muscle (TMG method) and thus increasing both: the signal-to-noise ratio and method's sensitivity. Measuring result is presented in form of TMG response in time domain (Valenčič, 1990).

TMG method enables observation of muscle belly deformation dynamics and has quite a few similarities to MMG method as well as the IP measuring method. TMG method has been evaluated histochemically with high positive correlation (r = 0.93) between the percentage of type I muscle fibres and contraction time for nine selected skeletal muscles (Dahmane et al., 2000). Linear relationship between the amplitudes of transverse and longitudinal twitch torque of m. tibialis anterior has been reported (Knez et al., 1994; Kogovšek, 1991; Burger et al., 1997). Kerševan (2002) demonstrated linear and sigmoid relationship between the amplitudes of the transverse twitch (TMG) and M-wave (EMG).

In my previous research work regarding standardization of the TMG method (Šimunič Master's thesis, 2001) I have shown that the variability coefficient (VC) for TMG measurements within one day can be retained below 5 %, if the standardized measuring equipment is used and standardized measuring conditions are assured. Variability of measuring point selection was tested with multi channel displacement sensor on five muscles. The error caused by the incorrect selection of measuring point (within the ellipsoidal area with its centre in the optimal measuring point, of ± 5 cm length and of ± 2 cm width) remains below 5 % (Šimunič et al., 2002).

2.1.6. Biomedical visualisation

Muscle volume is known as the optimal muscle force predictor (Fukunaga et al., 2001). Muscle force is linearly dependent on the PCSA, which is calculated as a quotient between muscle volume and average length of muscle fibres. Fukunaga et al. (2001) claimed muscle volume to be the most important evaluator of muscle force, regardless of the muscle physical strength. So far, no related studies have been published, which enters some doubt into the relevance of the abovementioned study.

Already in 1836 Weber managed to calculate power of plantar flexor muscles on the basis of the maximal weight subjects could lift and on the basis of muscle anthropometry taken from cadavers. In the following years anthropometrical data of measured muscles were collected under *in vivo* conditions using the *ultrasonic* method (Ikai and Fukunaga, 1968 and 1970). Beside PCSA (Fukunaga et al., 1996; Narici et al., 1996), muscle force was inferred also from anatomical cross-sectional area (Narici et al., 1989; Kanehisa, 1996). Kawakami et al., 1995 and Riley et al., 2000 showed that even though having the same PCSA two different muscles could not exert the same force.

Maximal muscle force normalized according to muscle size is the actual muscle strength, being in most cases the input datum for muscle models and is therefore expected to be measured as accurately as possible. Calculating or adopting the PCSA from literature requires a certain degree of precaution, for some anthropometrical data are collected in resting muscle, some in cadavers. Such anthropometrical data do not correspond to those collected under *in vivo* conditions (Maganaris et al., 1998a, 1998b in 1999). When setting up an *in vivo* experiment measured muscle is shortened (Friederich and Brand, 1990; Yamaguchi et al., 1990) therefore the PCSA in cadavers is smaller than the actual one (Gatton et al., 1999).

2.2. *Measuring relative muscle force*

In this chapter a review of measuring methods and findings in field of measuring muscle force is given. Every measuring method has its advantages as well as disadvantages, the latter often presenting an unavoidable obstacle. Further, for each method six protocols for measuring relative muscle force are presented: defining force-length relation, defining force-speed relation, measuring acute muscle fatigue, measuring lateral symmetry (collateral muscles), measuring post-tetanic potentiation and defining the twitch-tetanus ratio. For every method variability estimation is given, which was the basis for the selection of methods – for the purpose of this thesis tensiomyographic and torque measuring method have been chosen and investigated in detail.

EMG method (sEMG and iEMG)

- Force-length relation and force speed relation: with respect to the measured muscle, position of the sEMG sensor varies up to 1 cm. (Farina et al., 2001; Rainoldi et al., 2000). This is a result of changing the joint angle and so the muscle fibre population directly under the detection electrode does not remain the same, which increases the method's variability. This problem is eliminated when the intramuscular EMG is applied – but it at the same time prevents the use on daily basis (invasiveness). When monitoring voluntary contraction, variability is diminished by non-selective contraction, motivation, coactivation, sports training etc.
- Acute muscle fatigue is indicated by decreased parameters MPF and MdPFi (Merletti et al., 1990 in 1991; Lindstrom et al., 1970). In case of at least 10 % decrease, these differences can be detected (Akataki et al., 1999).
- The positioning of detection electrode (sEMG) itself makes measuring lateral symmetry too variable.
- Post-tetanic potentiation can be measured if it is a result of intensified MU activation and thus increased amplitude of sEMG response.
- Ratio between the M-wave amplitude and the amplitude of M-wave series does not represent the twitch-tetanus ratio. Observing them in frequency domain proved the ratio to be dependent on the length of stimulation pulse-train. We believe that twitch-tetanus ratio cannot be measured using the EMG method.
- Akataki et al. (1999) evaluated the VC of sEMG and reported inter-experimental variability of 10 % and 25 % variability for measurements on daily basis. Merletti et al. (1995) reported 18 % variability of measurements on daily basis and concluded this variability to be too high to perform quality interpretation of measured results. They suggested to rather pay regard to frequency parameters for their lower variability. The main source of the EMG method variability is the so-called system-noise. The signal-to-noise ratio is considered the most sensitive indicator, especially for the EMG recordings of contractions below 25 % MVC.

Torque and intramuscular force measurement

- Force-length (or torque-length) relation and force-speed (or torque-speed) relation: intramuscular measurement means invasive measurement of both characteristics and requires the approval by the committee of ethics plus it cannot be applied daily. Torque measurement enables non-selective measurements of both characteristics for voluntarily contracting group of muscles. Selective measurements can be performed if contractions are evoked electrically, but attention is required with defining the number of stimuli. For getting a representative response and relevant force-length relation, pulse-train must comprise at least 10 stimuli (Kawakami and Lieber, 2000; Thomas et al., 1999; Allen et al., 1989). At the same time we have to assure isometric conditions, otherwise the limb torque has to be taken into account.
- Both methods proved to be suitable for detecting muscle fatigue: measured force of fatigued muscle is diminished, in case of longitudinal twitch both – duration and half relaxation time are prolonged.
- With voluntary contraction force exerted by collateral groups of muscles can be non-selectively compared. To high variability of electrically evoked contractions prevents lateral symmetry to be measured.
- Both methods proved to be suitable for measuring post-tetanic potentiation, which is presented in following chapters.
- Twitch-tetanus ratio can successively be measured using the intramuscular technique. In case of torque measurement results are affected by observed limb's torque. This influence increases when stimulating frequency is lower than 10 Hz.
- In general variability of both methods is quite high and gets too high when measurements are performed outdoor. Coactivation of synergist and antagonist muscles, subject's motivation, limb fixation, position of joint axis, non-isometric conditions during force-length relation measurement, small signal-to-noise ratio in week contractions – all these factors contribute to higher variability.

MMG

- Non-linear relationship between average direct component of MMG and contraction force has been shown by many researchers (Barry et al., 1990; Keidel and Keidel, 1989; Maton et al., 1990; Orizio et al., 1989 and 1999). Besides, it has not yet been defined how factors such as: contraction type, angular velocity, level of activation (Madeline, 2001) and muscle tonus (Dalton and Stokes, 1993; Orizio, 1989) affect this relationship. To a certain degree the MMG method is suitable for measuring force-length relation, still additional research work has to be done – which is not the case for measuring force-speed relation, where the MMG method is useless.
- Since the MMG response reflects the level of activation for type I and type II muscle fibres, muscle fatigue can be monitored.
- Muscle tonus is the main obstacle in measuring lateral symmetry. Beside that, asymmetrical poise, thickness of subcutaneous tissue, PE and SE mechanics affect the MMG response as well. In order to measure lateral symmetry additional measurements and method calibration are required.
- MMG method is suitable for measuring post-tetanic potentiation.

- MMG method is suitable for measuring twitch-tetanus ratio.
- Akataki et al. (1999) reported 10 % variability for voluntary contractions performed during the day and 25 % for measurements on daily basis.

TMG

- The force-speed relation cannot be measured for TMG method is applied under isometric conditions (Valenčič, 1990). In this thesis force-length relation is discussed in detail.
- Since TMG response reflects the level of MU activation (Kerševan, 2002), measuring muscle fatigue is possible. In fatigued muscle time parameters of both longitudinal and transverse twitch (measured using TMG method) occur: response and relaxation time are prolonged, contraction time is shorter, amplitude decreases (Praprotnik, 1999).
- Because of initial pressure TMG based time parameters are independent of muscle tonus, positioning the displacement sensor enters variability below 5 % (Šimunič, 2001). TMG method is suitable for measuring lateral symmetry.
- Preliminary studies revealed that for "faster" muscles TMG response is potentiated more intensively than for "slow" muscles (Šimunič, 2001) which is in accordance with data presented in literature, indicating that type II fibres exert higher potentiation (Gordon et al., 1990; Lev-Tov et al., 1988). Defining post-tetanic potentiation more exactly is the purpose of this thesis.
- Defining twitch-tetanus ratio more exactly is also one of the aims of this thesis.
- Variability has been investigated by Šimunič (2001) and proved to remain less than 5 %.

Measuring the intramuscular pressure

- IP is in no connection with contraction type, contraction speed and muscle length, except for muscles of extreme length where the IP is smaller in case of maximal shortening of measured muscle (Ballard et al., 1994). IP is linearly dependent on isometric as well as isokinetic force (Mazella, 1954; Sadamoto et al., 1983; Sejersted et al., 1984), however even for repeated measurements the slope coefficient is variable (Sejersted et al., 1984; Jensen, 1991). Method for measuring the IP we can be applied in case of measuring both characteristics, but its invasiveness has to be taken into account.
- Parkerja et al. (1984) reported no connection between the IP and muscle fatigue.
- According to previous findings by Sejersted et al. (1984), Jensen (1991) and Sejersted and Hargens, (1995) stating that slope coefficient of linear IP-force relation is variable even for repeated measurements (on the same muscle) and depends on measured muscle position and sensor penetration (depth and angle) we believe lateral symmetry cannot be properly measured.
- Post-tetanic potentiation can be measured properly, since measured IP reflects the increased level of activation (Parker et al., 1984; Sejersted et al., 1984)
- Method for measuring IP is suitable for measuring twitch-tetanus ratio.
- Since measuring IP depends on sensor type, penetration location and depth, muscle geometrical properties and measurement protocol its variability can increase up to 300 % (Sejersted et al., 1984; Jensen, 1991; Nakhostine et al., 1993).

Biomedical visualisation

- Muscle volume and PCSA are reported as the most important evaluation of muscle force (Edgerton et al., 1990; Fukunaga et al., 1996 and 2001; Narici et al., 1996). The Magnetic Resonance Imaging (MRI) is already in use for monitoring muscle activation, tendon elongation and muscle contraction (Fleckenstein and Shellock, 1991), however quality interpretation is rendered impossible due to low resolution. Studies on similar basis are carried out using the ultrasonic measuring method (Maganaris, 2002; Ikai and Fukunaga, 1968 and 1970), which enables the real time monitoring of muscle contraction. Expensive measuring equipment and time consuming protocol as well as interpretation are the main disadvantages of these methods.
- Muscle fatigue is determined with following MRI detectable parameters: pH value in muscle fibres, muscle temperature and concentration of oxygen in blood (Yue et al., 1994; Richardson et al., 1998).
- Post-tetanic potentiation is determined with MRI detectable parameters as follows: MU activation, shortening and thickening of muscle belly.
- In case of MRI twitch occurs to fast to be monitored, which is not the case when performing the ultrasonic measurement. Twitch-tetanus ratio is calculated with complex algorithms.
- If data processing includes anthropometrical data collected during measuring procedure, variability only depends on precision of data collection and data processing.

2.3. Measuring muscle stiffness

Muscle tonus is with EMG method detected as constant involuntary tetanic pre-activation. However, this activation is very low and signal-to-noise ratio is small, therefore measuring this activation with EMG method is inappropriate, namely, we cannot distinguish between the signal and the noise. Along with muscle tonus go some other occurrences such as: micro injuries, muscle fatigue, etc. Therefore the expression *stiffness* instead of tonus will be used. Already in 1898 Sherrington demonstrated a so-called stretch reflex – meaning, that passive muscle stretch leads to appearance of APs in order to shorten the stretched muscle to its original length.

For measuring muscle tonus only a few methods are known beside EMG. On worth mentioning is the *myotonometer* (Neurogenic Technologies®, Inc.), which enables direct measurement of muscle tonus, muscle stiffness, muscle hardness, muscle strength and spasticity (http://www.neurogenic.com). Myotonometric method is non-invasive and is based on measuring muscle softness with pressing on its belly. The greater the resistance with respect to the sensor pressure, the greater the muscle tonus. Myotonometric method was evaluated with a study on spastic subject (Charles et al., 2001), where myotonometer was proved as reliable measuring tool for spastic muscles.

Muscle stiffness is defined as the stiffness of the muscle-tendon complex and is measured as a muscle's passive resistance to stretching. However, actual tendon stiffness is in no connection with actual muscle stiffness (muscle fibres) (Kubo et al., 2001).

3. Materials and methods

3.1. *Sample of participants*

According to the protocol 15 healthy right-handed male subjects were measured. Their personal and anthropometrical data are presented in Table 3.1. One criterion required subjects not to perform any special physical activity with their hands (on daily basis), another (criterion) set limitation for skin fold above the m. BB and m. BR (only up to 7 mm), otherwise it affects TMG measurements. All subjects were acquainted with measuring protocol prior to measurements and all of them successfully performed a warm up in form of learning how to perform MVC.

Subject's code	**AG / years**	**BH / cm**	**BW / kg**	**KG$_{BB}$ / mm**	**KG$_{BR}$ / mm**	**KG$_{TB}$ / mm**	**l$_{\text{upper arm}}$ / cm**	**l$_{\text{forearm}}$ / cm**
UZ	22	181	80	2.5	3	4	36	26
US	27	184	85	2.6	3.5	5	36.5	26.5
TH	30	183	95	5	5	6.8	35	28
MV	26	176	86	6.5	5	7.5	34.5	26
SO	23	187	83	3.7	4	5.3	38	27
GP	22	175	72	3	3.8	3.5	36	26.5
PZ	20	184	90	3.5	4	5	37	26.5
ZJ	19	188	76	4	4	6.4	37	28
AK	20	186	75	4.2	5	6.8	35	26.5
UM	23	181	72	3.5	4	5.5	35.5	28.5
PJ	27	171	78	5	5	13.5	33.5	25
PM	25	179	73	3.1	3.8	6	34	26
MA	24	188	75	4.6	4.2	7.5	38	26.5
MB	28	193	110	5	6.5	10.5	39	29.5
JZ	20	189	76	2.7	2.9	3.8	35.5	29
Mean	23.73	183	81.7	3.93	4.25	6.47	36.03	27.03
± SD	3.35	5.94	10.43	1.13	0.92	2.63	1.56	1.27

Table 3.1: Anthropometrical and personal data on 15 subjects. AG – subject's age, BH – body height, BW – body weight, KG$_{BB}$ – skin fold over BB belly, KG$_{BR}$ – skin fold over BR belly and KG$_{TB}$ – skin fold over TB belly. Values are presented as means ± SD.

3.2. *Measured muscles*

In order to investigate the connection between TMG method and torque measurement we selected muscles, which do not have many synergist muscles and have in the past been subject of different studies. Three muscles were selected – in human: elbow flexor muscles BB and BR (Figure 3.1) in toad: m. gastrocnemius (GAST) (Figure 3.2). Toad GAST was selected for the purpose of studying geometrical changes during contraction and evaluation of both methods.

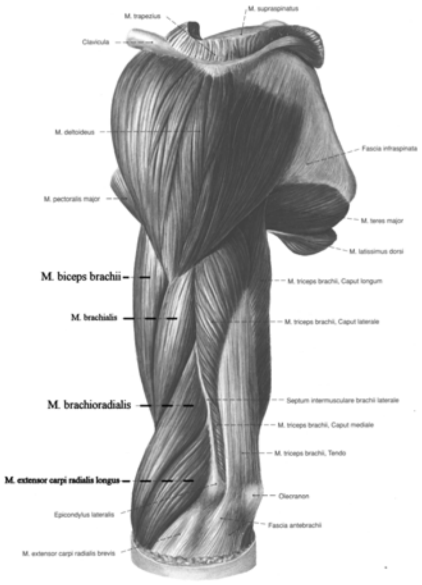

Figure 3.1: Anatomy of upper arm with four marked flexor muscles (adopted from Putz and Pabst, 2001).

Figure 3.2: Toad (Bufo Bufo) gastrocnemius and distal tendon.

M. biceps brachii (Figure 3.1)
Muscle biceps brachii is a double head muscle (one longer and one shorter head), double joint muscle (elbow and shoulder joint), with two origos (longer head – *tuberculum supraglenoidale* and *labrum glenoidale*, shorter head – *apex of proc. coracoideus*) and common distal tendon with two insertia (*tuborisitas radii* and *aponeurosis musculi bicipitis brachii to fascia antebrachii*). M. BB is in function of abductor (longer head), adductor (shorter head), medial rotation plus shoulder joint flexion and elbow flexion plus lateral rotation (*supination*). Muscle fibres are arranged parallelly from origo towards insertio, pennation angle is 0 rad.

M. brachioradialis (Figure 3.1)
Muscle brachioradialis is single head muscle, single joint muscle (elbow joint) with single origo (*margo lateralis humeri, septum intermusculare brachii laterale*) and single insertio (*proc. styloideus radii*). M. BR functions as flexor muscle, enables medial (*pronation*) and lateral rotation of elbow joint. Muscle fibres are arranged parallelly from origo towards insertio, pennation angle is 0 rad.

3.3. *Measurement procedure*

3.3.1. Maximal voluntary contraction

Subjects performed four exercises – in first two they try to perform MVC in second two ballistic MVC (achieving MVC as fast as possible). Only two larger values were chosen. For torque measurements sensor as described in appendix A was used, moment arm was defined prior to measurements. Subject's forearm was lying in a brace with a handle at the end. To prevent the coactivation of wrist flexor muscles, the handle was placed before the wrist. Left hand palm was in supination in order to create the same measuring set-up as in case of electrically evoked contraction.

3.3.2. Measuring electrically evoked torque

Elbow torque was measured with force sensor as described in appendix B, with moment arm of 25.7 cm ± 1.33 cm. Multiplying both results in elbow torque. Sensor was attached just before the wrist, approximately at the end of ulna bone (Figures 3.3. and 3.4.). In order to provide the most effective position for BR and satisfactory for BB, palm was in partial supination. Sensor's output presented input for differential amplifier (appendix E). Amplifier's output was sampled using specific software and the input/output card (appendix F), incorporated in a PC (appendix H). To be able to detect the synchronization signal of 0.2 ms, we had to use sampling frequency of 10 kHz.

Muscle's responses to single pulse and to pulse-train are referred to as *longitudinal twitch* and *longitudinal tetanus*, respectively.

3.3.3. Measuring electrically evoked muscle belly displacement

For muscles BB and BR transverse deformation of their bellies was monitored using TMG method. Measuring point was defined as a point of maximal muscle belly displacement detected with palpation during voluntary elbow flexion. After placing the self-adhesive surface electrodes onto the muscle belly, location of measuring point was checked again using electrical stimulation instead of voluntary contraction. Displacement sensor was positioned perpendicularly to the tangential plane on the largest area above the muscle belly with its tip in measuring point. For BB measuring point was located in the middle of the humerus bone and in the middle sagittal plane of the shorter head (Figure 3.3). For BR measuring point was located at 30 % proximally according to length of ulna bone in the middle sagittal plane of the muscle (Figure 3.4).

Displacement sensor output signals are two digital pulse trains (TTL level), with phase shift with respect to direction of displacement. Pulse trains were sent through counters. Their contents were read through PC parallel interface after 1 kHz sampling. TMG response is displacement of muscle belly in time domain (displacement vs. time).

Figure 3.3: Force sensor, displacement sensor and stimulation electrodes position for measurement on m. BB at elbow angle of 1.75 rad.

Figure 3.4: Force sensor, displacement sensor and stimulation electrodes position for measurement on m. BR at elbow angle of 1.75 rad.

Muscle's responses to single pulse and to pulse-train are referred to as *transverse twitch* and *transverse tetanus* (or transverse tetanic response), respectively.

.

3.3.4. Placing stimulation electrodes

Two pairs of self-adhesive stimulating electrodes (of 50 mm diameter) were used (*AxelGaard, Pals*) for bipolar electrical stimulation. With respect to measuring point cathode was placed 5 cm distally, anode was placed 5 cm proximally (Figures 3.3. and 3.4). Electrodes were stacked on to the muscle prior to measurement and removed after all measurements have been carried out.

3.3.5. Measuring muscle stiffness

For we could not perform stiffness measurements with myotonometer, we have upgraded our displacement sensor with attaching a spacer to its end (Figure 5.5). Spacer served as reference point when measuring the depth of transverse deformation (D_v) of the displacement sensor "into" the measured muscle (Figure 5.6). Muscle stiffness was defined as reciprocal to parameter D_v. The bigger the D_v, the less stiff the muscle. With each subject D_v measurements were performed for both muscles at all angles. D_v measurements were performed on the TMG measuring point. For lower variability measurements were repeated three times, average value was calculated and used in further data processing. Based on investigation of D_v's influence on measuring point we placed the spacer 2.5 cm distant to sensor.

Figure 3.5: Displacement sensor with the spacer.

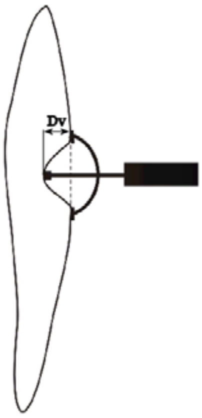

Figure 3.6: Muscle stiffness measuring principle and definition of parameter D_v.

3.3.6. Collecting anthropometrical data

For all three selected muscles (in resting phase and while performing MVC) the circumference of upper arm and forearm was measured with tape measure. For all four elbow angles circumference and skin fold were measured on the measuring point. The length of the humerus bone was measured with tape measure starting at the end of *clavicula*, ending at *epicondylus medialis*. The length of the ulna bone was also measured with tape measure starting at *olecranon*, ending at *proc. styloideus ulnae*. Skin fold was measured with calliper.

3.3.7. Measuring responses of isolated muscle under *in vitro* conditions

In order to perform reliable validation of measuring results from human BB and BR, some measurements on isolated toad GAST were carried out. Muscles were isolated (Figures 3.7 and 3.8) and on proximal end attached to the surface. Measurement set-up is presented in Figure 3.8. Distal end of the muscle (either at the end of muscle belly or at the end of the tendon) was attached to force sensor as shown in appendix C (and so the *muscle* or the *muscle-tendon complex* was observed – Figure 3.7). Prior to either of measuring procedures the same length of muscle belly was assured.

Displacement sensor was placed on the thicker part of the belly (appendix D). Both sensors' outputs were sampled using differential amplifier (appendixs H and E). Protocols A and B were carried out on four GASTs of two toads. *In vitro* measuring results are given in sixth and seventh chapter, where some typical responses of one measured muscle are presented. In order create geometrical model of muscle contraction, photographs of muscle geometry were taken during the measurement.

Figure 3.7: Toad GAST: muscle-tendon complex (a) and muscle only (b). Measurement set-up: displacement sensor position, stimulation electrodes position, joint fixation (on the right), force sensor attachment (on the left).

Figure 3.8: Measuring equipment for *in vitro* measurements on toad GAST.

3.4. Protocols

3.4.1. Preparing subjects for measurement procedure

Prior to measurement procedure each subject performed stretch of elbow flexor muscles, which was followed by procedure of learning how to perform a MVC and ballistic MVC. Each trial was repeated up to five times. After five-minute pause measurement protocol was carried out, beginning with settling subject into adjustable measuring chair (appendix J):
Subject's hip joint was flexed to 1.92 rad (0 rad corresponds to completely extended hip joint), upper arm placed parallel to the body, forearm position was being changed according to the protocol-defined elbow angle. Subject's head was resting on a supporting pad, hip and shoulder joints were fixed in order to assure isometric conditions and prevent any other parts of the body from moving and thus affecting measuring results. Prior to measurement anthropometrical data was collected.

To eliminate the possible repeated-measurement error, we have chosen the elbow joint angle randomly out of four values: 1.75, 1.40, 1.05 and 0.70 rad (0 rad indicates complete extension of elbow joint). For each angle each subject performed MVC and ballistic MVC, the circumference of upper arm and forearm was measured as previously described and stiffness of m. BB and m. BR was measured. Further, protocols A and B were carried out using electrical stimulation.

3.4.2. Protocol A

This protocol involved 0.1 Hz pulse-train with pulses of 1 ms and amplitude increasing from 10 mA up to supramaximal response with increments of 5 mA (Figure 3.9). Contraction threshold was with all subjects above 10 mA, supramaximal amplitude was reached after there was no increase either in transverse or in longitudinal twitch.

For applying electrical pulses electrical stimulator was used, as described in appendix I.

3.4.3. Protocol B

Firstly three single pulses of were applied. Afterwards pulse-trains of 2 sec duration and different frequencies (10, 20, 50 and 100 Hz) were applied (Figure 3.9). Resting period between pulse-trains enabled measured muscle to rest and recover, no fatigue occurred. After a series of pulse-trains again three single pulses of were applied. Pulse width and amplitude remained unchanged: supramaximal amplitude was determined at 50 Hz, pulses of 0.2 ms were used. Stimulation frequency of 100 Hz was used as control-frequency for checking the supramaximal amplitude, while the three lower frequencies were selected on the basis of muscle physiology.

3.5. Data processing

Displacement sensor output is of digital kind and resistant to random noise, therefore it can be automatically processed. Torque measuring results are of analogue kind, including also the noise, which was in case of week contractions quite disturbing. In order to perform automatic processing additional filtering was needed: firstly averaging was applied, further both-way digital low-frequency filter (25 Hz) without phase shift was applied. Butterworth's coefficients (5. order) of the filter used in data processing are presented in Equation 3.1.

$$\begin{aligned} Y_n &= 10^{-6} \cdot (2.34 \cdot X_n + 11.7 \cdot X_{n-1} + 23.41 \cdot X_{n-2} + 23.41 \cdot X_{n-3} + 11.7 \cdot X_{n-4} + 2.34 \cdot X_{n-5} \\ &- (-4.4918 \cdot Y_{n-1} + 8.0941 \cdot Y_{n-2} - 7.3121 \cdot Y_{n-3} + 3.311 \cdot Y_{n-4} - 0.6011 \cdot Y_{n-5}) \end{aligned}$$

Equation 3.1

Synchronization of both responses was performed on the basis of common stimulating signal

For both twitches maximal amplitude was observed and four time parameters were defined (Td, Tc, Ts, and Tr) (Figure 3.10). For tetanic response (protocol B) maximal amplitude was observed and indicated D_{TMG} and D_{torque} or we used a common name $D_{tetanus}$.

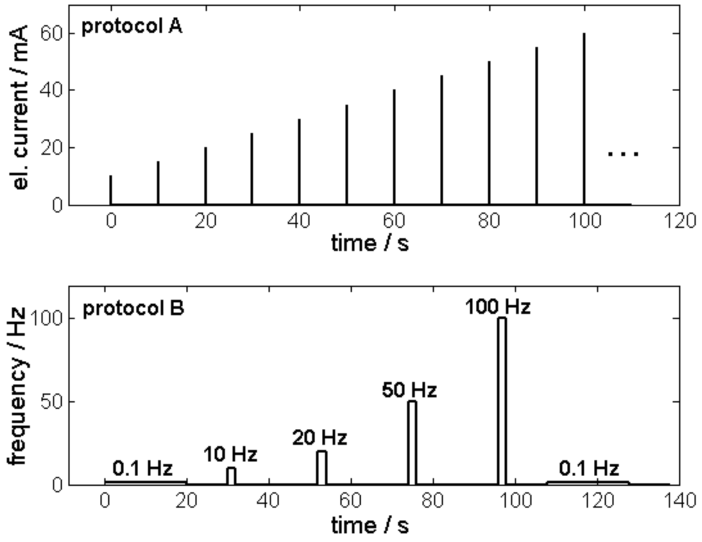

Figure 3.9: Graphical presentation of both measuring protocols. Upper figure illustrates increasing stimulation amplitude (protocol A), lower figure illustrates increasing stimulation frequency and single (control) twitches (protocol B).

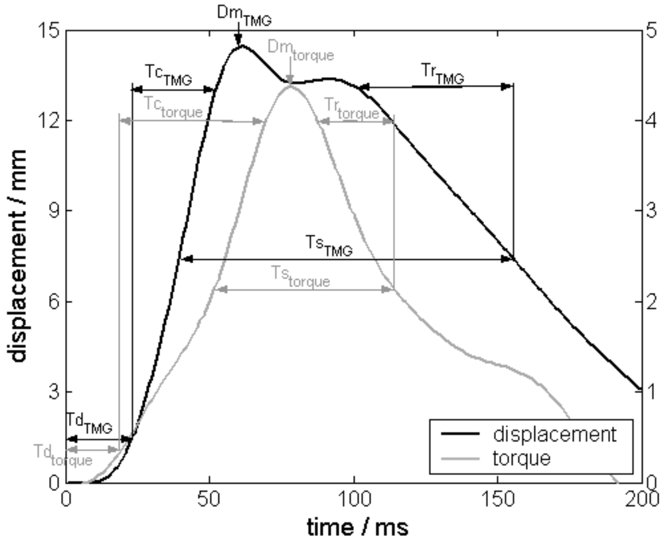

Figure 3.10: Parameter definition is the same for transverse (TMG) and longitudinal (torque) twitch. Maximal twitch amplitude: Dm or D_{twitch}. Delay time (Td): 0 – do 10 % Dm, contraction time (Tc): 10 – 90 % Dm, sustain time (Ts): >50 % Dm and half relaxation time (Tr) 90 – 50 % Dm.

3.6. Statistical analysis

For performing statistical analysis we employed first order statistical methods (average values and standard deviations), methods for testing hypotheses (correlation between observed parameters, variance analysis) and data normalizing for joint processing and presentation of measured data. A level of $p<0.05$ was selected to indicate statistical significance. Matlab 5.3 statistical toolbox (*The MathWorks, Inc.*), statistical functions in Microsoft® Excel 2000 (*Microsoft Corporation*) and some other tools were used.

For the purpose of modelling we used some optimisation methods and Matlab *Simulink* together with Matlab *Neural Network Based System Identification* (*The MathWorks, Inc*).

3.7. Modelling skeletal muscle

3.7.1. Geometrical modelling

For the purpose of geometrical modelling universal muscle shape was used, for there are not two muscles of the same kind (architecture, geometrical properties...). We have chosen geometry of toad GAST, which is a single head muscle with one tendon at each end. Proximal tendon is very short, because the muscle is attached to the bone with aponeurosis and fascia. Distal tendon is approximately 2 cm long and was used for setting up a muscle-tendon complex.

3.7.2. Neural network modelling

Prior to creating a hybrid model of GAST we want to make sure there is a connection between longitudinal and transverse response. For this purpose muscle was stimulated with pseudo random stimulation of 20 sec duration. Pause intervals ranged from 0.05 and 2 sec, frequencies ranged from 0.5 to 20 Hz. TMG response and force were monitored.

Neural network architecture was selected with respect to noise in both responses and with respect to the output of learning procedure. Finally, a second order non-linear system with twice delayed input and output was chosen (Figure 3.11). TMG response was used as the input signal; the output signal was in a form of a modelled muscle force exertion (F). Model architecture was determined with nine neurons for the input and one neuron for the output (Figure 3.11). Learning procedure was performed on a pair of responses muscle belly displacement-muscle force and lasted as long as maximal number of iterations was achieved (300). The efficiency of learning process was tested on three pairs of responses taken from toad GAST.

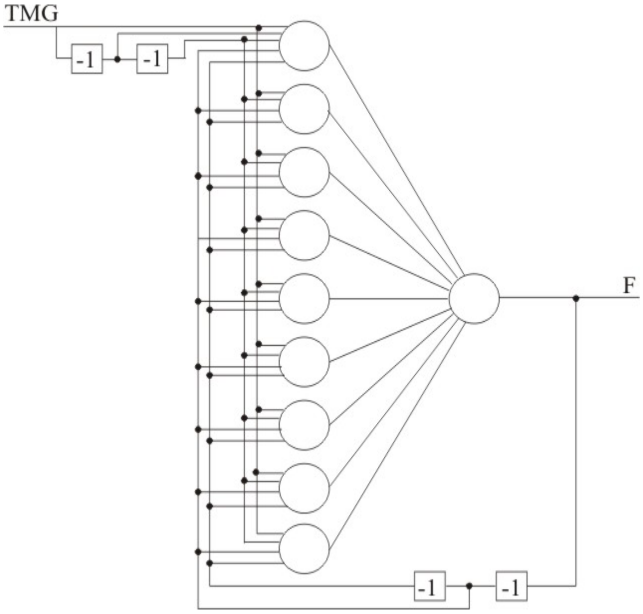

Figure 3.11: Neural network architecture used for force modelling. Input data: muscle belly response, force response. Output data: force response.

3.7.3. Hybrid modelling

Using digital camera we have taken photographs from relaxed and contracted toad GAST during isotonic and isometric contractions. Along with the muscle there was a metric scale, which helped us evaluating the changes in longitudinal and transverse dimensions of muscle belly. Geometrical rotational shape was selected for modelling skeletal muscle. It was dimensioned according to measured muscle volume, which finally lead to relationship between muscle belly thickening and tendon elongation.

Different courses of longitudinal and transverse twitches occur due to hysteresis describing relationship between passive muscle stretch and contraction. For describing this passive characteristic (muscle force-tendon length) mechanical model was used.

For fast contracting muscles a TMG response reaches its maximal value in form of quite sharp peak. In order to give an explanation for that phenomenon we looked for contractile parameters for isolated type I and type II muscle fibres from the literature. We used this data with model in order to find key factors, which cause transformations in transverse and longitudinal direction.

4. Results

4.1. *Determining optimal elbow angle*

At optimal joint angle maximal force is exerted. In this chapter for both muscles (BB and BR) optimal elbow angle is determined and relationship between joint angle and contractile properties is investigated.

4.1.1. MVC and ballistic MVC

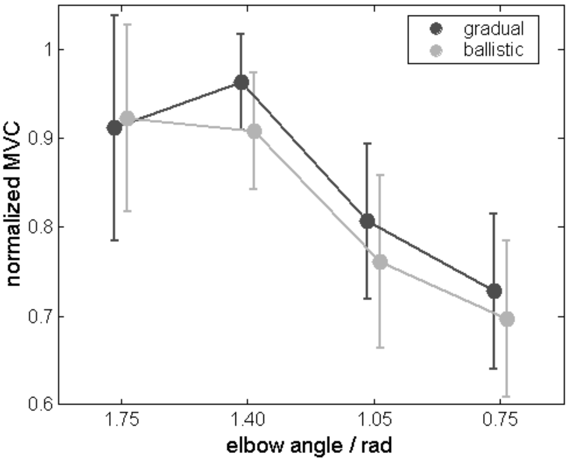

Figure 4.1: Elbow angle dependency of normalized gradual and ballistic MVC (means ± SD).

Using force sensor, placed at a distance of 26.67 cm ± 1.53 cm from elbow joint axis, MVC and ballistic MVC was measured. Measured values for MVC ranged from 53.53 Nm to 120.62 Nm (average MVC 73.27 Nm ± 20.24 Nm) values for ballistic MVC ranged from 37.72 Nm to 108.53 Nm (average ballistic MVC 70.02 Nm ± 16.89 Nm). MVC and ballistic MVC were significantly maximal at angles of 1.75 and 1.4 rad, as shown in Figure 4.1. Subjects, who produced stronger MVC, also produced stronger ballistic MVC, which is confirmed with statistically significant positive correlation.

4.1.2. Transverse and longitudinal twitch

In figure 4.2 protocol A is illustrated with a typical response. It is clearly visible, that transverse twitches reach their maximal value faster than longitudinal twitches. Transverse twitch of muscle belly and longitudinal force twitch of muscles BB and BR were recorded using TMG method and torque measuring method, respectively.

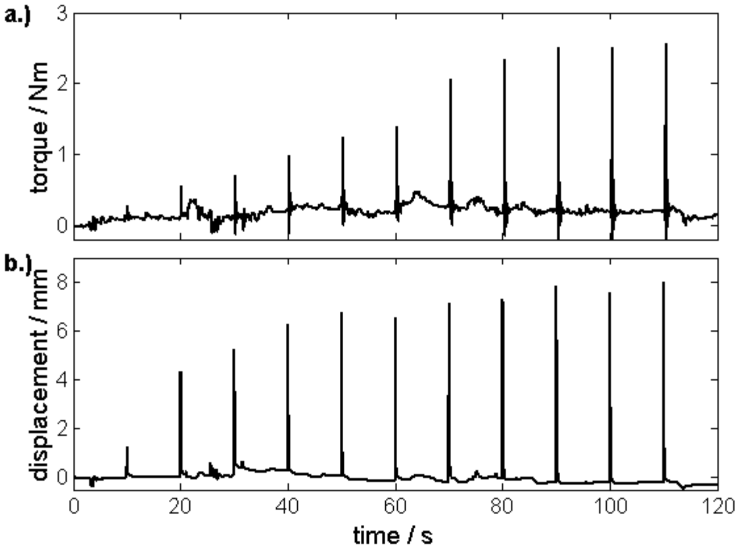

Figure 4.2: Protocol A was applied; Longitudinal (a) and transverse (b) twitches in BR at elbow angle of 1.40 rad are shown.

Dm_{TMG} - Dm_{torque} relation is a non-linear one and is altered with elbow angle for both m. BB and m. BR (Figure 4.3). Coefficients of corresponding models (Equation 4.1) also show the dependence on elbow angle (Table 4.1), where y stands for normalized Dm_{torque} and x stands for normalized Dm_{TMG}. Relation between both amplitudes is exponential with tendency towards linearity at smaller angles. Before processing the series of twitches (Figure 4.2) they were normalized according to their maximal value for each muscle and for each elbow angles separately.

$$y = C_1 \cdot e^{-k_1 \cdot x} + C_2 \cdot e^{-k_2 \cdot x}$$ **Equation 4.1**

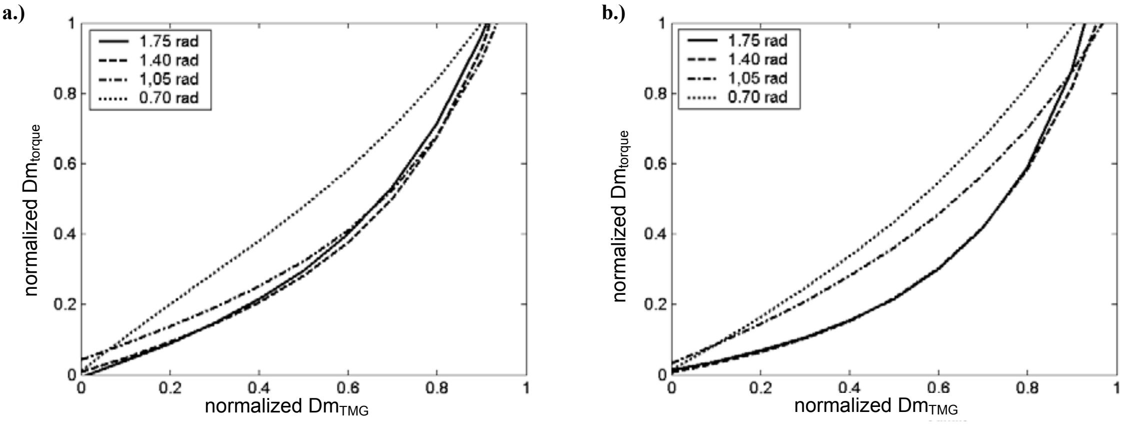

Figure 4.3: Fittings for normalized Dm_{TMG} and Dm_{torque} in BB (a) and BR (b) at different elbow angles.

In Figure 4.3 relationship between normalized Dm_{TMG} and Dm_{torque} is presented. Again it is clearly presented that Dm_{TMG} reaches its maximal value faster than Dm_{torque}. The difference in achieving the maximal value is altered according to the level of activation – this is discussed later on.

When observing TMG twitches (Figure 4.4a) we can see the peak approximately 70 ms after the stimulation pulse. This phenomenon was detected in case of all subjects. In order to investigate this phenomenon the *peak-amplitude* was defined as the difference between Dm_{TMG} and displacement at the time at the end of the peak when the relaxation starts. No significant correlation was found neither between the peak-amplitude and skin fold, nor between peak-amplitude and D_v.

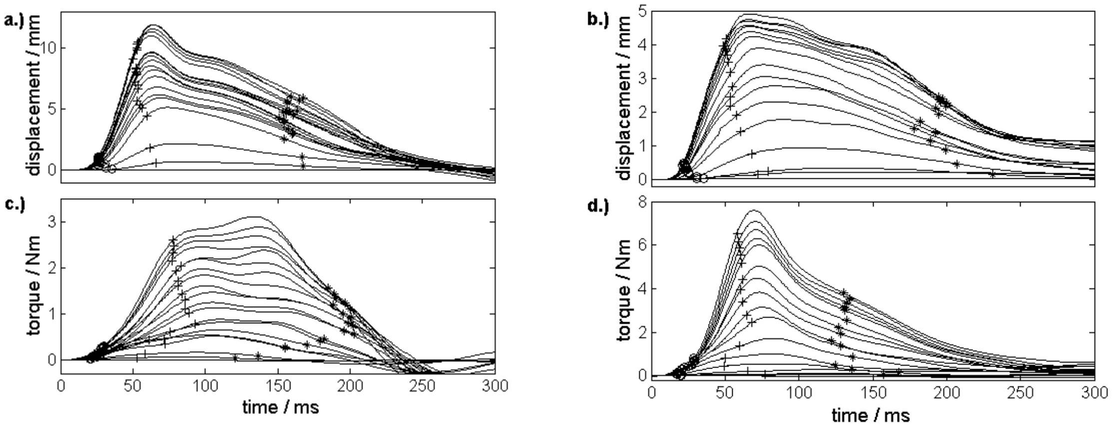

Figure 4.4: Protocol A was applied at elbow angle of 1.40 rad; In figures (a) and (c) typical m. BB displacement and torque responses are shown, figures (b) and (d) show the same for m. BR. Marker “+” indicates 90 % Dm in contraction phase, marker “* “ indicates 50 % Dm in the relaxation phase.

Dependency of normalized time parameters (of twitches recorded with both TMG and torque measuring method) on stimulation amplitude is presented in Figure 4.5. Following conclusions were made:

- With increasing stimulation amplitude Td_{TMG} decreases for both muscles and Td_{torque} decreases only for m. BB;
- With increasing stimulation amplitude Tc_{TMG} for both muscles and Tc_{torque} for m. BB firstly increase, but start decreasing after 50 % supramaximal displacement was achieved. For m. BR parameter Tc_{torque} decreases with increasing stimulation amplitude;
- Ts_{TMG} for m. BB decreases until 60 % supramaximal displacement is achieved; for m. BR this parameter only decreases with increasing stimulation amplitude. For m. BB Ts_{torque} dynamics are opposite to Ts_{TMG}, for m. BR dynamics of Ts_{torque} and Ts_{TMG} are the same;
- Tr_{TMG} and Tr_{torque} decrease until 30 % supramaximal displacement (and torque) is achieved and afterwards increase consistently.

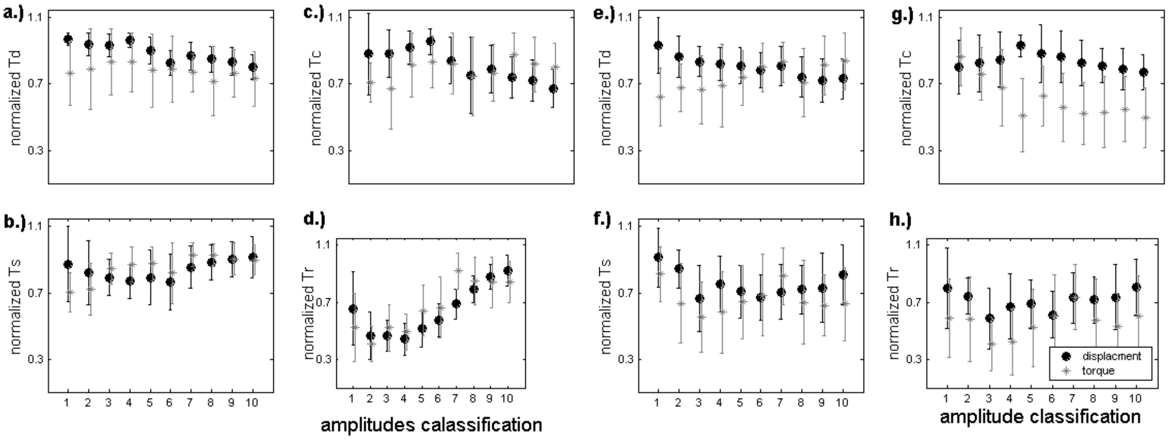

Figure 4.5: Elbow angle: 1.40 rad; Means ± SD of normalized time parameters are presented; Diagrams (a – d) present transverse and longitudinal twitch parameters in m. BB, diagrams (e – h) present transverse and longitudinal twitch parameters in m. BR with respect to supramaximal twitch amplitude. Afterwards, they were classified into 10 classes according to twitch amplitudes: first class – twitch amplitudes between 0 and 10% of supramaximal stimulation, second class – twitch amplitudes ranging from 10 to 20 % and so on, up to 100 %.

Figures 4.6 and 4.7 present dependence of time parameters for supramaximal twitches (both measuring methods) on elbow angle. Each parameter was normalized according to its maximum value (values for all four angles were taken into consideration). In order to compare average values of observed parameters original (not normalized) values were retained. For diminished elbow angle following conclusions were made:

- Muscle BB:
    - Td_{TMG} decreases, Td_{torque} increases; for all four angles Td_{TMG} is significantly smaller than Td_{torque};
    - Tc_{TMG} decreases, Tc_{torque} increases up to 1.05 rad and decreases for the angle of 0.70 rad; for all four angles Tc_{TMG} is significantly smaller than Tc_{torque};
    - Both Ts_{TMG} and Ts_{torque} decrease; for all four angles Ts_{TMG} is (insignificantly) smaller than Ts_{torque};
    - When elbow angle is diminished from 1.75 rad to 1.40 rad Tr_{TMG} increases, and decreases with further angle diminishing; Tr_{torque} decreases consistently; for all four angles Tr_{TMG} is significantly smaller than Tr_{torque}.
- Muscle BR:
    - Except for the angle of 0.70 rad Td_{TMG} remains unchanged; Td_{torque} decreases consistently; for all four angles Td_{TMG} is significantly smaller than Td_{torque};
    - Tc_{TMG} decreases consistently; Tc_{torque} increases at 1.40 rad and further on decreases; for all four angles Tc_{TMG} is significantly smaller than Tc_{torque};
    - Ts_{TMG} decreases consistently; Ts_{torque} increases until the elbow is extended to 1.05 rad and further on decreases; for all four angles Ts_{TMG} is significantly smaller than Ts_{torque};

- Tr_{TMG} and Tr_{torque} both increase at the angle of 1.40 rad and further on decrease; for all four angles Tr_{TMG} is significantly smaller than Tr_{torque}.

When Tc_{TMG} and Tc_{torque} of supramaximal twitches were compared following was concluded: for m. BR both parameters are significantly smaller than for m. BB, which is also the case for all four elbow angles (Table 4.2).

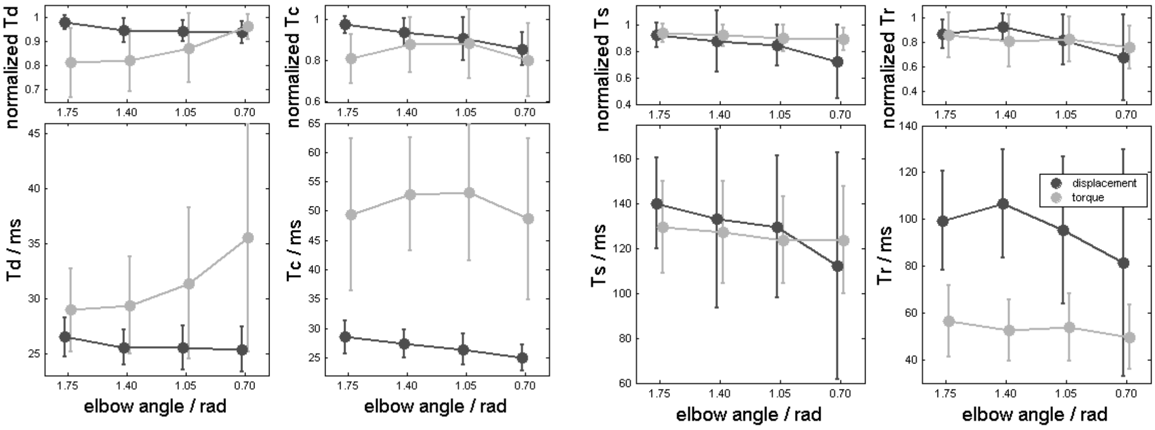

Figure 4.6: Time parameters for supramaximal transverse and longitudinal twitch of m. BB are presented; upper row figures display elbow angle dependency of normalized time parameters, lower row figures display mean values.

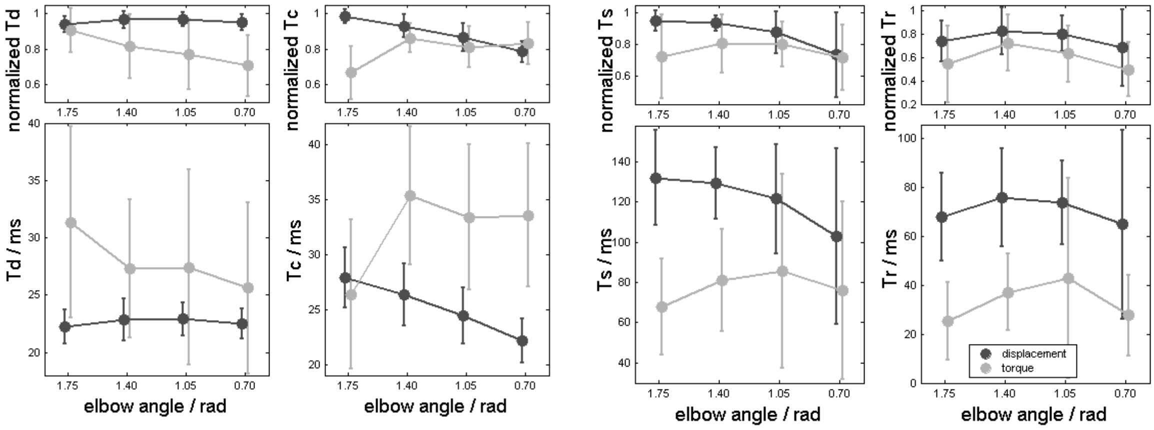

Figure 4.7: Time parameters for supramaximal transverse and longitudinal twitch of m. BR are presented; upper row figures display elbow angle dependency of normalized time parameters, lower row figures display mean values.

Muscle	Tc_{TMG} / ms	Tc_{torque} / ms	Type I muscle fibres / %
BB	26.42 (± 2.63)	53.15 (± 11.61)	[a]50.5 ([b]50)
BR	24.40 (± 2.52)	32.60 (± 6.80)	[a]39.8 ([b]40)

Table 4.1: Mean values (± SD) of Tc_{TMG} and Tc_{torque} and percentage of type I muscle fibres are given for m. BB and m. BR at elbow angle of 1.05 rad. Percentages of type I muscle fibres are adopted from literature ([a] Johnson, Polgar, Weightman in Appleton, 1973; [b] Dahmane, Valenčič, Knez in Eržen, 2000).

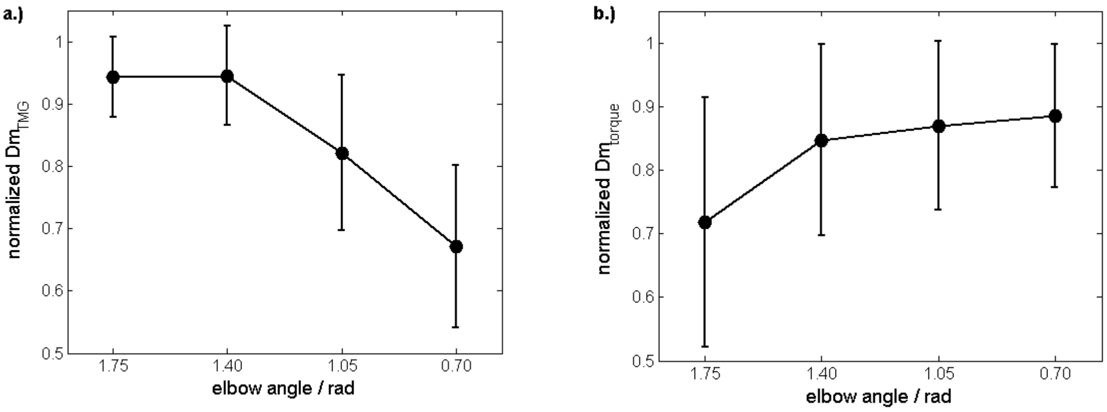

Figure 4.8: Elbow angle dependency of mean normalized (± SD) Dm_{TMG} (a) and Dm_{torque} (b) of supramaximal transverse and longitudinal twitch of m. BB.

Angle dependent characteristics for averaged and normalized parameters Dm_{TMG} and Dm_{torque} of m. BB twitch are dissimilar (Figure 4.8). Both parameters were normalized according to their maximum value (values for all four angles were taken into consideration). For angles at 1.05 and 0.70 rad Dm_{TMG} decreased significantly. Dm_{torque} increases insignificantly when elbow angle is diminished.

Angle dependent characteristics for averaged and normalized parameters Dm_{TMG} and Dm_{torque} of m. BR twitch are dissimilar (Figure 4.9). Parameter Dm_{TMG} decreases significantly when elbow angle is diminished, while Dm_{torque} significantly increases at the angle of 1.40 rad and with further angle diminishing significantly decreases to its original value.

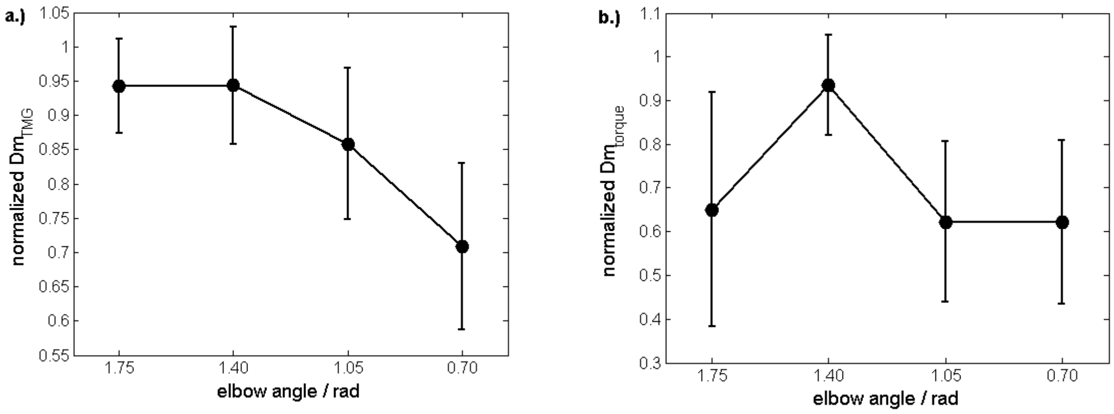

Figure 4.9: Elbow angle dependency of mean normalized (± SD) Dm_{TMG} (a) and Dm_{torque} (b) of supramaximal transverse and longitudinal twitch of m. BR.

4.1.3. Measuring muscle belly stiffness

Preliminary studies (Knez, 2000) revealed Dm_{TMG} to be dependent on the initial pressure when sensor tip is pressed against the skin above the measured muscle. In order to perform statistical evaluation, D_v for each subject was normalized according to its maximal value regardless of the joint angle at which this maximum was measured. Following was noticed: when elbow angle was being decreased, D_v was decreasing, too. This decrease was statistically significant for m. BR and insignificant for m. BB (Figure 4.10).

When parameters Dm_{TMG} and D_v were joined into one parameter, which was then compared for both muscles, positive correlation was calculated (r = 0.53), (Figure 4.11). In case of separate observations no correlation was found, meaning that parameter D_v is not the only one having influence on Dm_{TMG}.

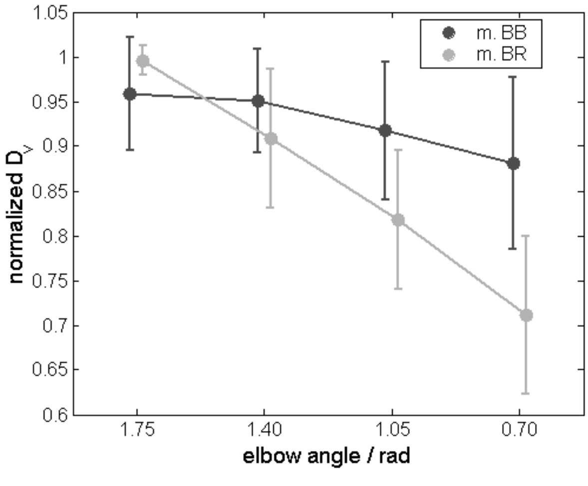

Figure 4.10: Elbow angle dependency of mean normalized (± SD) D_v in both measured muscles.

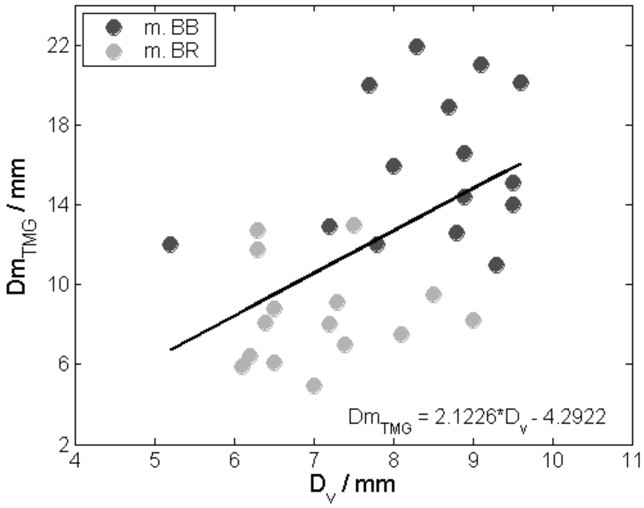

Figure 4.11: Statistically significant correlation between supramaximal Dm_{TMG} and D_v, linear trend. N = 15, measured muscles: m. BB and m. BR, elbow angle: 1.40 rad.

When muscle stiffness was taken into consideration (dividing Dm_{TMG} by D_v), the Dm_{TMG}/D_V-joint angle dependency was calculated and is presented in Figure 4.12. Muscle BB's stiffness does not affect the belly displacement-muscle length characteristic, which is not the case for m. BR, where maximum is reached at the angle of 1.05 rad.

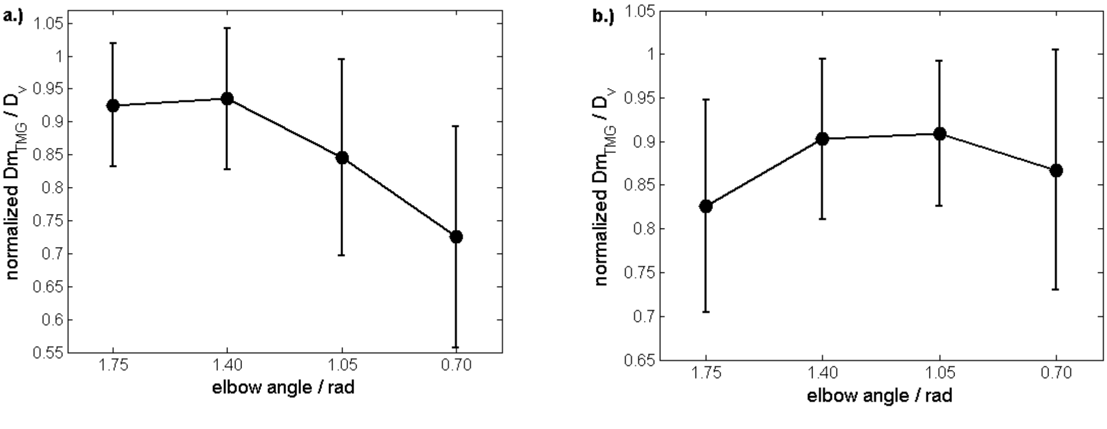

Figure 4.12: Elbow angle dependency of mean (± SD) normalized quotient Dm_{TMG}/D_v for transverse twitch of m. BB (a) and m. BR (b).

4.1.4. Transverse and longitudinal tetanic responses

Results of the B protocol are tetanic responses to 2-second-pulse-trains of different frequencies, preceded and followed by three single control pulses. Figure 4.13 illustrates responses of both measuring methods to B protocol. Following was observed: response amplitude increases with pulse-train frequency, the three twitches at the end of the protocol are bigger than those at the beginning. In Figure 4.14 some tetanic responses as well as control twitches are presented in detail and it is possible to see that responses at 10 and 20 Hz are still unfused.

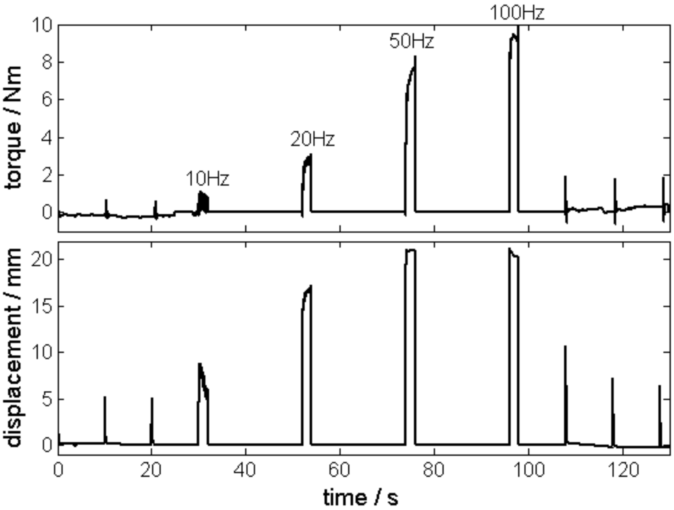

Figure 4.13: Protocol B applied in m. BB at elbow angle of 1.40 rad. Upper figure: torque response, lower figure: TMG response (muscle belly displacement).

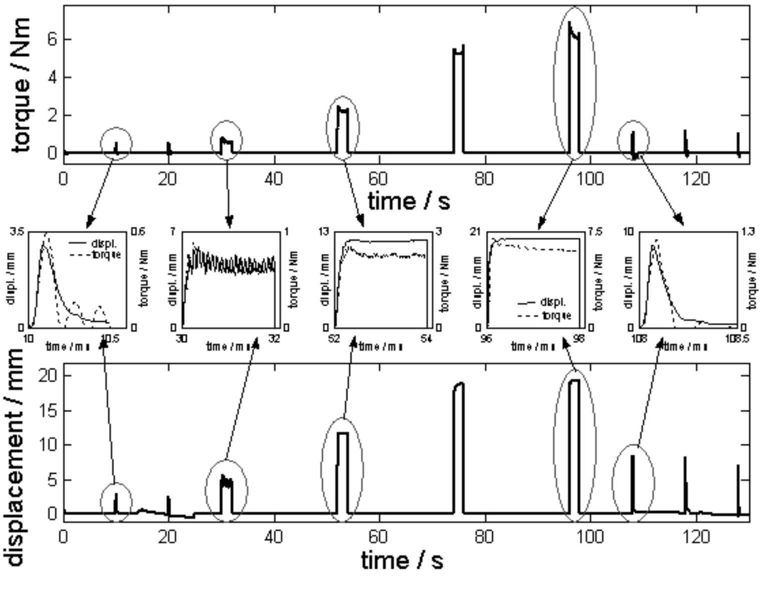

Figure 4.14: Torque response (upper figure) and muscle belly response (lower figure) of m. BR at elbow angle of 1.40 rad. Figures in the middle: detailed presentation of single twitches before and after protocol B as well as tetanic responses of protocol B.

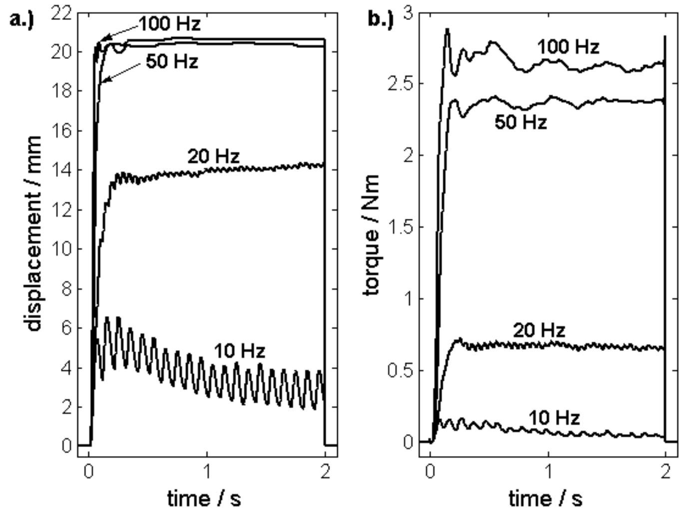

Figure 4.15: Transverse tetanic responses of muscle belly (a) and longitudinal tetanic torque responses (b) of m. BR at elbow angle of 1.75 rad with common time axis (stacked).

In Figure 4.15 time scale for different responses was unified. At 20 Hz we can still see the unfused tetanus, at higher frequencies muscle fibres' contraction and relaxation can no longer follow and response is called the fused tetanus. In Figure 4.15 another typical phenomenon can be observed: saturation of transverse tetanic response, which occurs sooner than in case of longitudinal response.

In Figure 4.16 frequency dependency of following parameters is presented: average normalized values of D_{twitch} and $D_{tetanus}$, control twitches at the beginning of the B protocol and tetanic responses. These characteristics are called: force-frequency, torque-frequency and displacement-frequency characteristic. In Figure 4.16 both muscles and all four angles are comprised. Displacement-frequency characteristic for m. BB: when elbow angle is diminished, slope coefficient of the characteristic diminishes. Torque-frequency characteristic is not joint-angle dependent. Displacement-frequency characteristic for m. BR: when elbow angle is diminished and frequencies of 20 or 50 Hz is applied, amplitude of transverse tetanic response decreases.

Frequency marked as f_h, is the frequency needed for achieving 50 % supramaximal $D_{tetanus}$. When elbow angle is diminished, f_h decreases for both muscles.

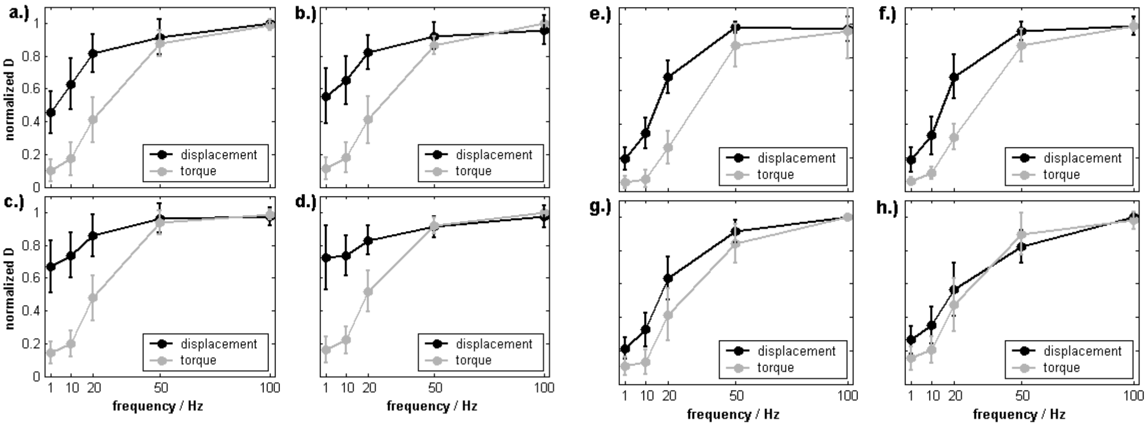

Figure 4.16: Torque-frequency and displacement-frequency characteristics in m. BB (a – d) and m. BR (e – h) at different elbow angles ((a) and (e) – 1.75, (b) and f – 1.40, (c) and (g) – 1.05, (d) and (h) – 0.70 rad). "D" stands for both – D_{twitch} and $D_{tetanus}$.

In Figure 4.17 two characteristics are presented: torque-frequency and displacement-frequency. The differences were quantitatively evaluated with models as described with Equation 4.1. Coefficients of best-fitting models are given in Table 4.3. These coefficients inform us about characteristics' angle dependency. In data processing and presentation of given characteristics only frequencies between 10 and 100 Hz were taken into account. For each subject and each elbow angle measuring results of B protocol were normalized according to their maximal values.

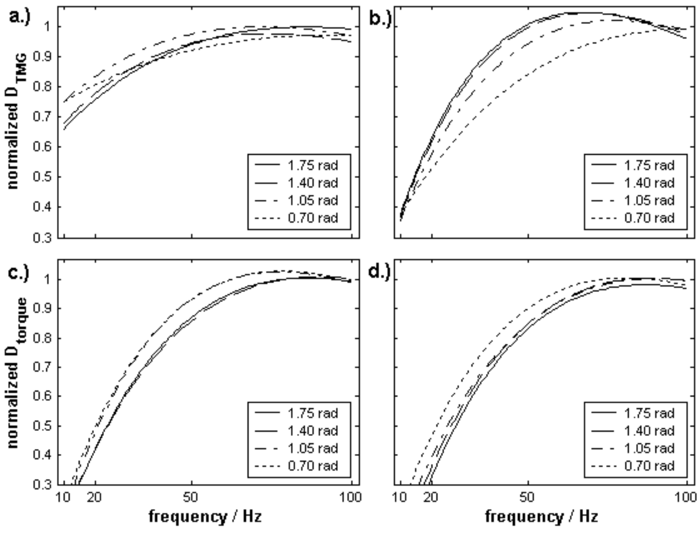

Figure 4.17: Modelled and normalized displacement-frequency (a and b) and torque-frequency (c and d) characteristics are plotted. Characteristics were measured in m. BB (a and c) and m. BR (b and d) at given elbow angles. Model parameters are given in Table 4.3.

Since no correlation between characteristics torque-length and displacement-length for protocol A was calculated (Figures 4.8 and 4.9), we investigated correlation between characteristics describing amplitudes of tetanic responses for protocol B. For all four tetanic responses and for each elbow angle maximal amplitudes D_{TMG} and D_{torque} were selected. Furthermore these amplitudes were normalized according to maximal amplitude of all four angles. We concluded that characteristics of tetanic response amplitudes (Figures 4.18 and 4.19) feature similar dynamics as characteristics of twitch amplitudes (Figures 4.8 and 4.9).

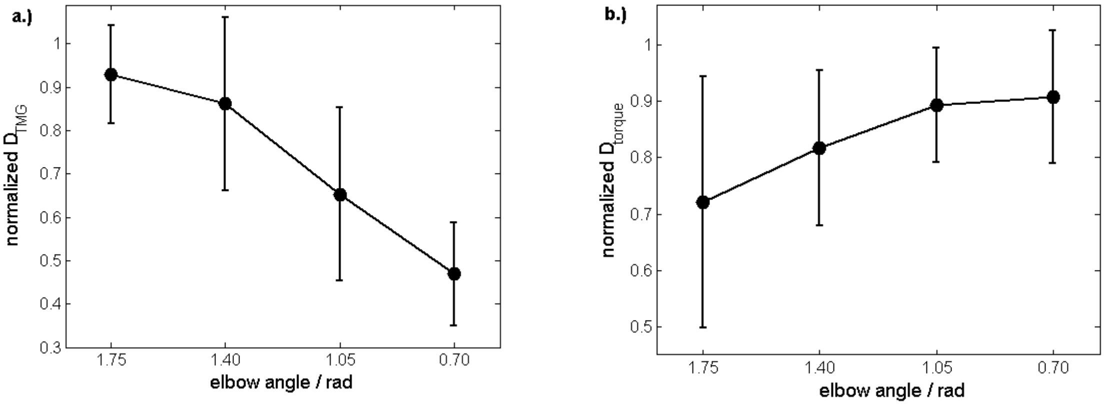

Figure 4.18: Elbow angle dependency of mean (± SD) normalized profiles for D_{TMG} (a) and D_{torque} (b) for transverse and longitudinal tetanic responses of m. BB.

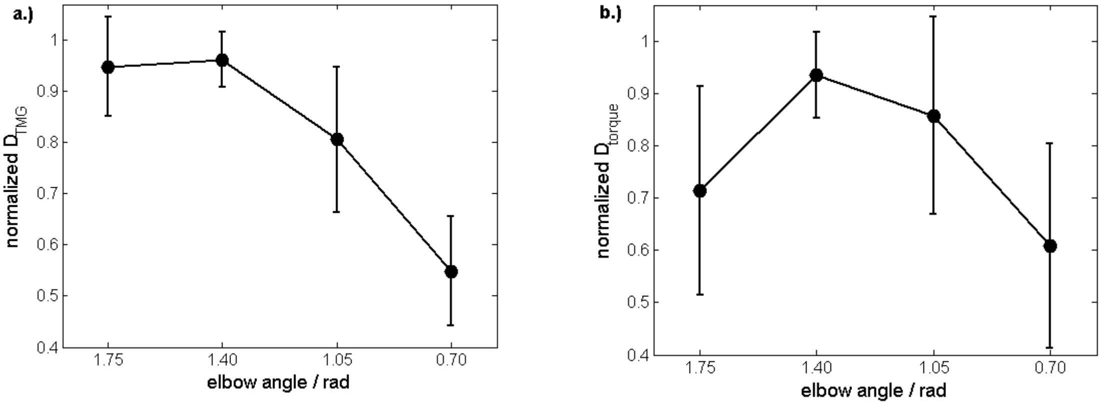

Figure 4.19: Elbow angle dependency of mean (± SD) normalized profiles for D_{TMG} (a) and D_{torque} (b) for transverse and longitudinal tetanic responses of m. BR.

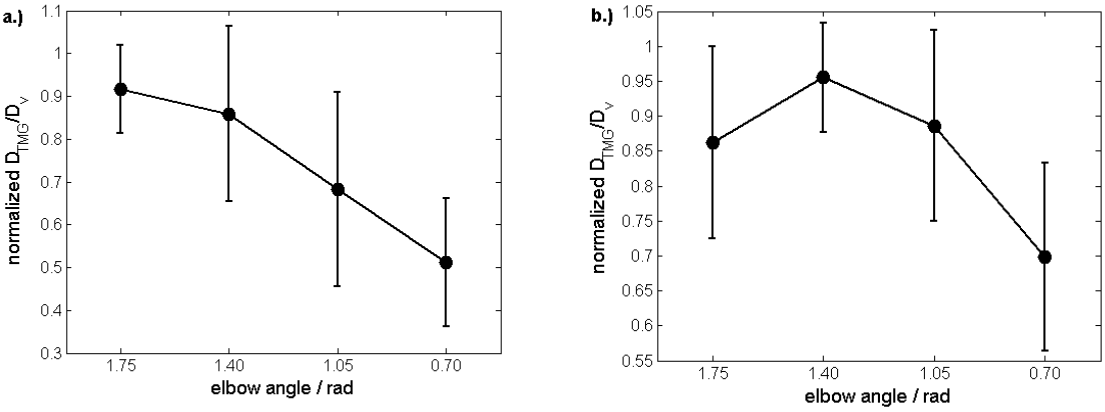

Figure 4.20: Elbow angle dependency of mean (± SD) normalized quotient Dm_{TMG}/D_v for transverse tetanic responses of m. BB (a) and m. BR (b).

As we have for transverse twitches (Figure 4.12), we presented the D_{TMG}/D_V-joint angle relation for transverse tetanic responses as well. Normalization was performed in the same manner as normalization of data presented in Figures 4.18 and 4.19, except for additional division by D_V.

4.2. Twitch-tetanus ratio

Twitch-tetanus ratio is ratio between amplitudes of twitch response and of tetanic response (D_{twitch} - $D_{tetanus}$) and was observed for TMG measurements as well as for torque measurements. This ratio informs us about connective tissue (SE and PE) properties and muscle force exertion, with respect to number of restored cross bridges. For calculating the twitch-tetanus ratio we divided the amplitude of supramaximal twitch (Dm_{twitch}) measured in protocol A by the amplitude of supramaximal tetanic response $Dm_{tetanus}$ measured in protocol B. The quotient is called the amplitudes ratio.

When compared to m. BB, m. BR amplitudes ratio is smaller for displacement as well as for torque, (Figures 4.21 and 4.22). Correlation between both amplitudes (Dm_{twitch} and $Dm_{tetanus}$) was statistically significant only for muscle belly displacement (not for torque) of m. BB at all four angles (Figure 4.21 and Table 4.4). For m. BR this correlation was also positive, but insignificant (Tables 4.4 and 4.5).

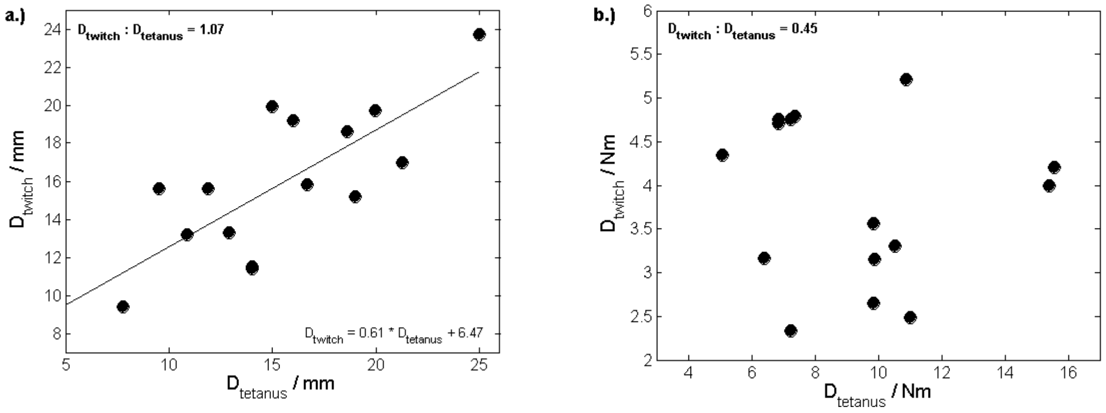

Figure 4.21: D_{twitch}-$D_{tetanus}$ ratio for displacement measurement (a) and torque measurement (b) in m. BB is presented. D_{twitch}-$D_{tetanus}$ ratio for displacement measurement expresses statistically significant linear trend (equation is printed in the lower right corner of the figure on the left). In the upper left corners mean values for D_{twitch}-$D_{tetanus}$ ratio are printed.

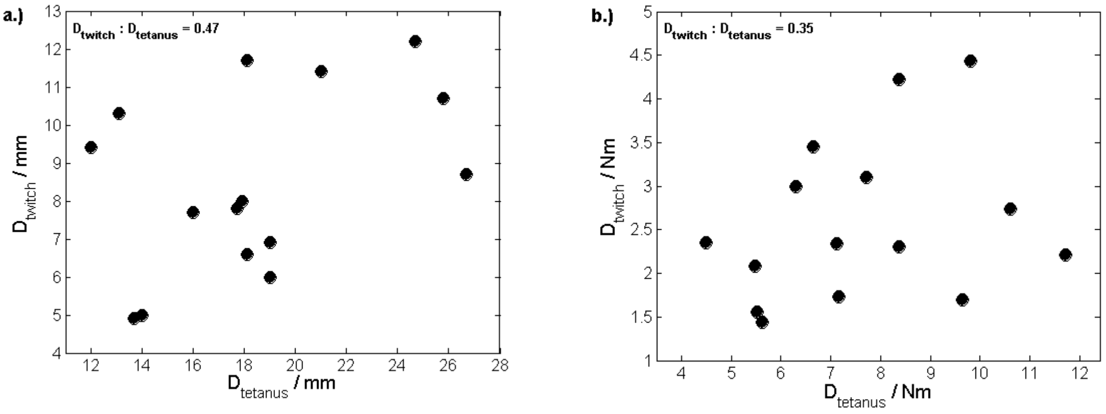

Figure 4.22: D_{twitch}-$D_{tetanus}$ ratio for displacement measurement (a) and torque measurement (b) in m. BR is presented. In the upper left corners mean values for D_{twitch}-$D_{tetanus}$ ratio are printed.

Muscle	Angle / rad	D_{twitch}-$D_{tetanus}$ ratio (± SD)	r
BB	1.75	1.07 ± 0.30	0.63^*
	1.40	1.21 ± 0.39	0.57^*
	1.05	1.45 ± 0.58	0.54^*
	0.70	1.61 ± 0.59	0.67^*
BR	1.75	0.47 ± 0.15	0.46
	1.40	0.47 ± 0.13	0.47
	1.05	0.52 ± 0.16	0.50
	0.70	0.64 ± 0.21	0.50

Tabela 4.1: Elbow angle dependency of D_{twitch}-$D_{tetanus}$ ratio for m. BB and m. BR belly displacement is given. For both amplitudes correlation coefficient (r) and statistical significance (*) based on Student (n–2) statistical test were calculated.

Muscle	Angle / rad	D_{twitch}-$D_{tetanus}$ ratio (± SD)	r
BB	**1.75**	0.45 ± 0.23	0.05
	1.40	0.52 ± 0.23	0.16
	1.05	0.50 ± 0.27	0.33
	0.70	0.51 ± 0.25	-0.05
BR	**1.75**	0.35 ± 0.17	0.16
	1.40	0.47 ± 0.24	-0.08
	1.05	0.35 ± 0.19	0.26
	0.70	0.52 ± 0.33	0.13

Table 4.3: Elbow angle dependency of D_{twitch}-$D_{tetanus}$ ratio for m. BB and m. BR torque response is given. For both amplitudes correlation coefficient (r) and statistical significance (*) based on Student (n–2) statistical test were calculated.

When only protocol B was investigated, Dm_{twitch} was supramaximal amplitude of one twitch out of three (prior to tetanic stimulation), $Dm_{tetanus}$ remained supramaximal amplitude of tetanic response. For this purpose the quotient is indicated $Dm_{twitchB1}$ - $D_{tetanus}$. For this ratio following findings are presented: for diminishing joint angle ratio $Dm_{twitchB1}$ - $D_{tetanus}$ increases for both muscles and for both methods (Tables 4.4 and 4.5). Correlation between both amplitudes ($Dm_{twitchB1}$ and $Dm_{tetanus}$) was statistically significant only for muscle belly displacement (not for torque) for both muscles at both angles (Table 4.4). No correlation in case of torque measurement was calculated (Table 4.5). In figures 4.23 and 4.24 these correlations are presented. When elbow is extended from 1.70 rad to 0.70 rad $Dm_{twitchB1}$ - $D_{tetanus}$ ratio increases for 70 % (m. BB) and 42 % (m. BR) for displacement measurements. In case of torque measurements this ratio increases for 60 % (m. BB) and 200 % (m. BR).

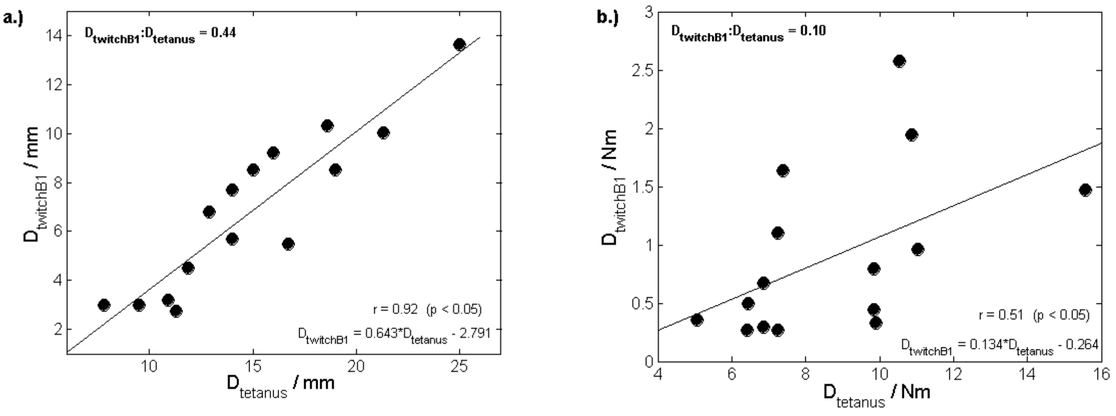

Figure 4.23: $D_{twitchB1}$-$D_{tetanus}$ ratio for displacement measurement (a) and torque measurement (b) in m. BB is presented. Both characteristics expresses statistically significant linear trend (equation is printed in the lower right corner of the figures). In the upper left corners mean values for $D_{twitchB1}$-$D_{tetanus}$ ratio are printed.

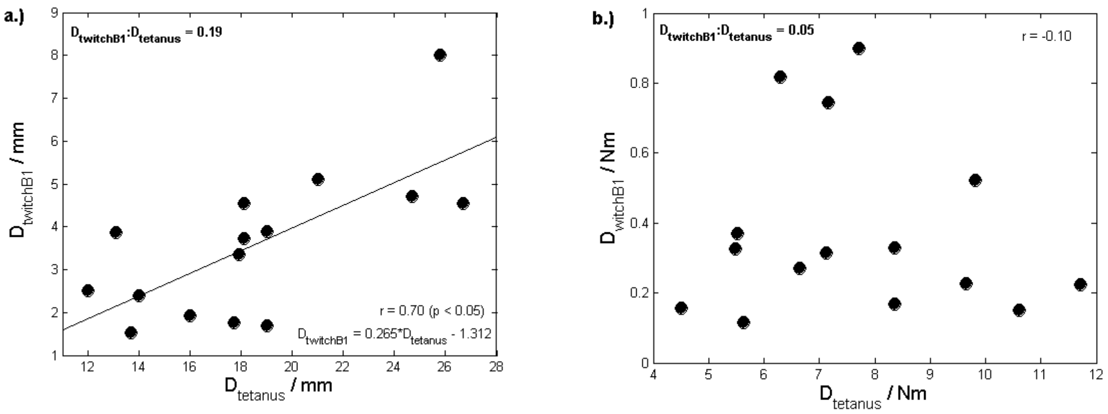

Figure 4.24: $D_{twitchB1}$-$D_{tetanus}$ ratio for displacement measurement (a) and torque measurement (b) in m. BR is presented. D_{twitch}-$D_{tetanus}$ ratio for displacement measurement expresses statistically significant linear trend (equation is printed in the lower right corner of the figure on the left). In the upper left corners mean values for D_{twitch}-$D_{tetanus}$ ratio are printed.

For torque measurements (both muscles, all angles) statistically significant correlation between $Dm_{twitchB1}$-$Dm_{tetanus}$ ratio and $Dm_{twitchB1}$ was calculated. The same correlation was calculated for displacement measurements and it proved statistically significant for m. BR at all angles and for m. BR at only one angle of 1.70 rad. Graphs in Figure 4.25 demonstrate typical dependencies for m. BR. One more relation is noticeable: muscles with smaller $Dm_{twitchB1}$ of transverse and longitudinal twitch present also smaller $Dm_{twitchB1}$-$Dm_{tetanus}$ ratio.

Muscle	Angle / rad	$D_{twitchB1}$-$D_{tetanus}$ ratio (± SD*)*	r
BB	**1.75**	0.44 ± 0.11	0.92^*
	1.40	0.55 ± 0.16	0.82^*
	1.05	0.65 ± 0.16	0.87^*
	0.70	0.75 ± 0.24	0.70^*
BR	**1.75**	0.19 ± 0.07	0.70^*
	1.40	0.19 ± 0.07	0.63^*
	1.05	0.21 ± 0.06	0.79^*
	0.70	0.27 ± 0.08	0.76^*

Table 4.4: Elbow angle dependency of $D_{twitchB1}$-$D_{tetanus}$ ratio for m. BB and m. BR belly displacement is given. For both amplitudes correlation coefficient (r) and statistical significance (*) based on Student (n-2) statistical test were calculated.

Muscle	Angle / rad	$D_{twitchB1}$-$D_{tetanus}$ ratio (± SD)	r
BB	**1.75**	0.10 ± 0.07	0.51^*
	1.40	0.11 ± 0.07	0.24
	1.05	0.14 ± 0.07	0.25
	0.70	0.16 ± 0.08	0.27
BR	**1.75**	0.05 ± 0.04	-0.10
	1.40	0.06 ± 0.02	0.61^*
	1.05	0.11 ± 0.05	0.32
	0.70	0.15 ± 0.07	0.49

Table 4.5: Elbow angle dependency of $D_{twitchB1}$-$D_{tetanus}$ ratio for m. BB and m. BR torque response is given. For both amplitudes correlation coefficient (r) and statistical significance (*) based on Student (n-2) statistical test were calculated.

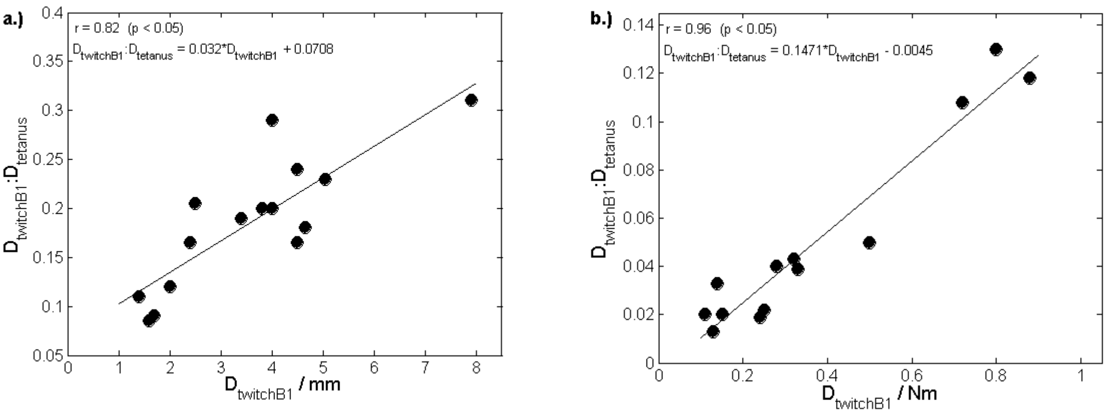

Figure 4.25: $D_{twitchB1}$-$D_{tetanus}$ ratio and $D_{twitchB1}$ dependency is presented. Measurements of transverse (a) and longitudinal (b) twitch of m. BR were carried out at elbow angle of 1.75 rad.

In Figure 4.26 relations between amplitudes and parameter Tc for both measuring methods are presented. No statistically significant correlation was calculated. Positive correlation between $D_{tetanus}$ and Tc was calculated at all angles and for transverse and longitudinal response. Negative correlation between $Dm_{twitchB1}$-$Dm_{tetanus}$ ratio and Tc was calculated for both transverse and longitudinal response.

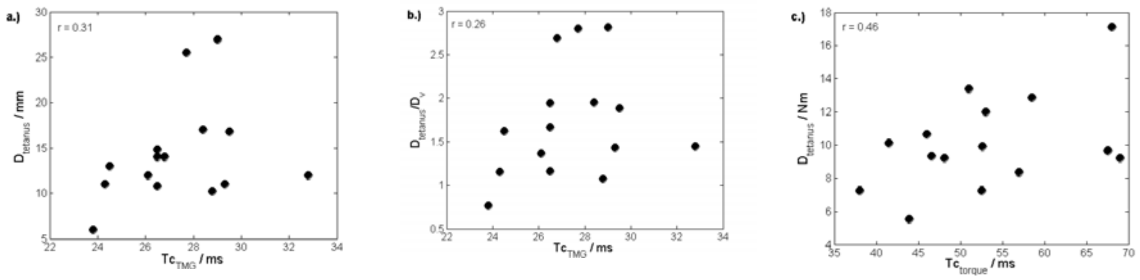

Figure 4.26: $D_{tetanus}$- Tc_{TMG} dependency for transverse tetanic response of m. BB is presented in figure (a). Normalized $D_{tetanus}$- Tc_{TMG} dependency for transverse tetanic response of m. BB is presented in figure (b). In figure (c) $D_{tetanus}$- Tc_{torque} dependency for longitudinal tetanic response of m. BB is presented. Elbow angle: 1.40 rad.

4.3. Post-tetanic potentiation

After first and second series of twitches in protocol B was compared, differences were observed, which indicate post-tetanic potentiation of responses (Figure 4.27).

Coefficient indicating intensity of post-tetanic potentiation was calculated as quotient between amplitude of the twitch *after* protocol B ($D_{twitchB2}$) and amplitude of the twitch *before* protocol B ($D_{twitchB1}$).

Parameters of transverse twitches before and after protocol B differed significantly: time parameters significantly decreased, amplitude significantly increased for both muscles and at all angles. In case of torque measurements, differences of time parameters show similar trend, but are not statistically significant (Table 4.6). Amplitudes of longitudinal twitches before and after protocol B differ significantly for both muscles and at all angles.

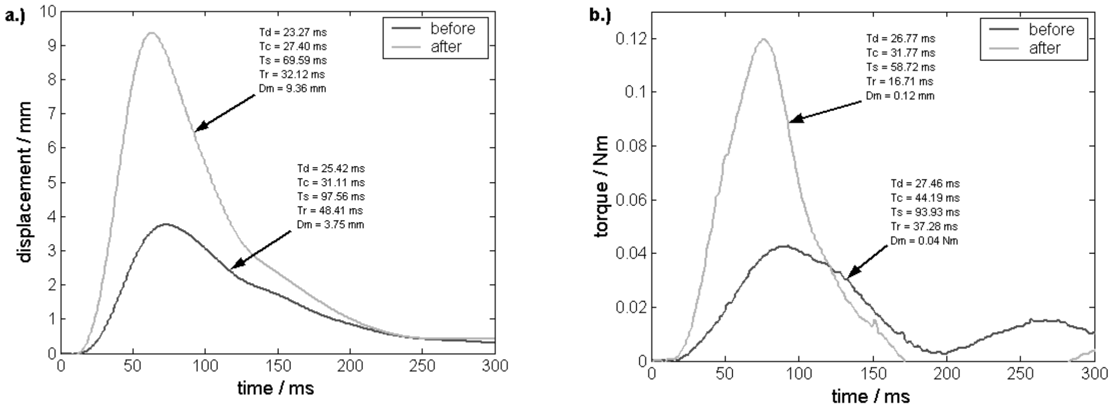

Figure 4.27: Figures show potentiation of transverse (a) and longitudinal (b) twitch of m. BR at elbow angle of 1.75 rad. Post-tetanic potentiation affected twitch amplitude as well as twitch time parameters, which are printed on both figures.

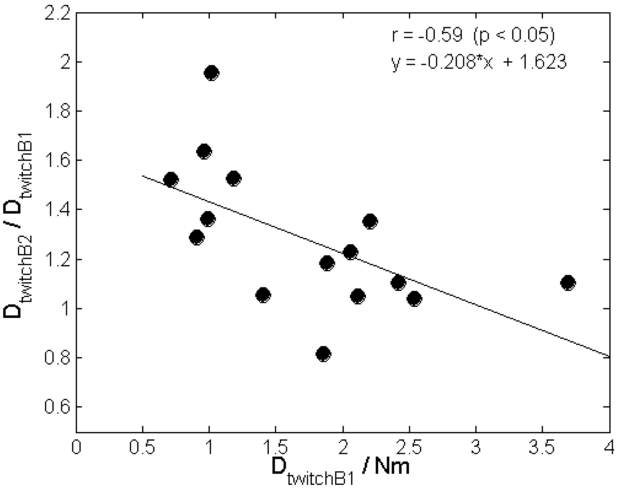

Figure 4.28: Coefficient of amplitude potentiation ($D_{twitchB2}/D_{twitchB1}$) in longitudinal twitch is plotted against amplitude of longitudinal twitch of m. BB before protocol B, at elbow angle of 0.70 rad. Linear trend of the model is shown and correlation coefficient is given.

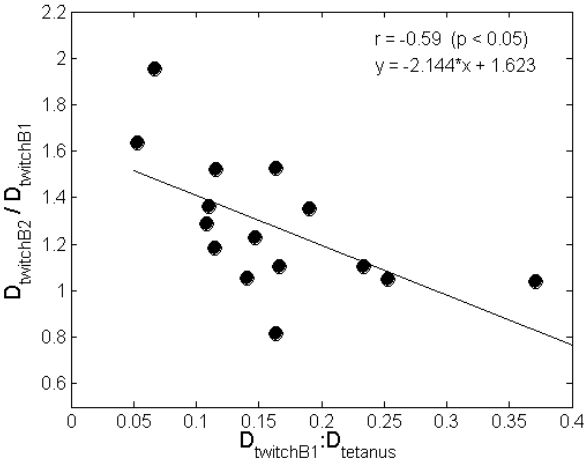

Figure 4.29: Potentiation ($D_{twitchB2}/D_{twitchB1}$) of longitudinal twitch amplitude is plotted against $D_{twitchB1}$-$D_{tetanus}$ ratio. Torque measurements were carried out in m. BB at elbow angle of 0.70 rad. Linear trend of the model is shown and correlation coefficient is given.

For muscle BR twitches before and after protocol B (at all angles) following was observed: statistically significant increase in Dm_{TMG}, Dm_{torque}, Ts_{torque} in Tr_{torque} statistically significant decrease in Tc_{TMG} as well as Tc_{torque}.

For both m. BB and m. BR more statistically significant changes were observed:

- Potentiation of Ts_{TMG} and Tr_{TMG} is in m. BR higher than in m. BB (at 1.40 rad);
- Potentiation of Ts_{TMG}, Tr_{TMG} in Td_{torque} is in m. BR lower than in m. BB (at 0.70 rad).

Comparison of twitch and tetanic responses of protocol B revealed more intensive amplitude potentiation for muscles of smaller $D_{twitchB1}$-$D_{tetanus}$ (Figure 4.29) ratio and smaller $D_{twitchB1}$ (Figure 4.28). In Table 4.7 comparison of potentiation coefficients and amplitudes of transverse and longitudinal twitches before protocol B are given. Comparison is statistically evaluated (Table 4.7).

Muscle	Response	Angle / rad	Normalized Td	Normalized Tc	Normalized Ts	Normalized Tr	Normalized Dm
BB	Displacement	1.75	0.88 (± 0.06)*	0.79 (± 0.18)*	0.70 (± 0.14)*	0.74 (± 0.23)*	1.35 (± 0.33)*
		1.40	0.87 (± 0.07)*	0.81 (± 0.10)*	0.74 (± 0.14)*	0.78 (± 0.27)*	1.30 (± 0.26)*
		1.05	0.87 (± 0.06)*	0.86 (± 0.11)*	0.64 (± 0.21)*	0.63 (± 0.32)*	1.06 (± 0.05)*
		0.70	0.85 (± 0.06)*	0.88 (± 0.11)*	0.55 (± 0.18)*	0.46 (± 0.27)*	1.21 (± 0.21)*
	Torque	1.75	0.89 (± 0.13)*	0.82 (± 0.23)*	0.91 (± 0.13)*	1.12 (± 0.62)	1.71 (± 0.78)*
		1.40	0.96 (± 0.09)	0.88 (± 0.28)*	0.90 (± 0.11)*	1.07 (± 0.53)	1.34 (± 0.36)*
		1.05	0.95 (± 0.10)*	0.88 (± 0.19)*	0.94 (± 0.15)	1.25 (± 0.41)*	1.24 (± 0.33)*
		0.70	0.92 (± 0.07)*	0.88 (± 0.32)*	0.98 (± 0.16)	1.11 (± 0.25)	1.28 (± 0.29)*
BR	Displacement	1.75	0.87 (± 0.10)*	0.84 (± 0.08)*	0.59 (± 0.18)*	0.58 (± 0.22)*	2.23 (± 0.73)*
		1.40	0.87 (± 0.10)*	0.83 (± 0.07)*	0.57 (± 0.12)*	0.55 (± 0.25)*	2.60 (± 0.67)*
		1.05	0.88 (± 0.12)*	0.87 (± 0.06)*	0.61 (± 0.08)*	0.61 (± 0.22)*	2.49 (± 0.38)*
		0.70	0.87 (± 0.13)*	0.89 (± 0.06)*	0.67 (± 0.12)*	0.70 (± 0.21)*	2.27 (± 0.49)*
	Torque	1.75	1.01 (± 0.18)	0.94 (± 0.36)	0.82 (± 0.22)*	0.85 (± 0.45)*	3.43 (± 2.05)*
		1.40	1.01 (± 0.13)	0.99 (± 0.18)	0.79 (± 0.13)*	0.83 (± 0.41)*	2.89 (± 1.10)*
		1.05	0.99 (± 0.07)	0.96 (± 0.16)	0.82 (± 0.13)*	0.76 (± 0.21)*	2.38 (± 0.80)*
		0.70	1.01 (± 0.10)	0.88 (± 0.12)*	0.83 (± 0.17)*	0.83 (± 0.41)*	1.80 (± 0.53)*

Table 4.6: Mean normalized coefficients (± SD) of post-tetanically potentiated parameters. Statistically significant changes are marked with “*”.

Muscle	Angle / rad	Correlation between coefficient of longitudinal twitch amplitude potentiation and $D_{twitchB1}$ of measured torque	Correlation between coefficient of transverse twitch amplitude potentiation and $D_{twitchB1}$ of measured displacement
BB	1.75	-0.51*	-0.57*
	1.40	-0.55*	-0.08
	1.05	-0.65*	0.43
	0.70	-0.59*	-0.42
BR	1.75	-0.57*	-0.44
	1.40	-0.50*	-0.55*
	1.05	-0.56*	-0.47
	0.70	-0.40	-0.61*

Table 4.7: Correlations between coefficients of amplitude potentiation and amplitudes of control twitches B1 were calculated. Calculations were performed for transverse and longitudinal twitches, for both muscles and at all selected elbow angles. Statistically significant correlations are marked with “*”.

In Table 4.8 relationships between potentiation coefficients and $D_{witchB1}$-$D_{tetanus}$ ratio are presented and statistically evaluated (for both measuring methods – TMG and torque).

Muscle	Angle / rad	Correlation between coefficient of longitudinal twitch amplitude potentiation and $D_{twitchB1}$-$D_{tetanus}$ ratio of torque response	Correlation between coefficient of transverse twitch amplitude potentiation and $D_{twitchB1}$-$D_{tetanus}$ ratio of measured displacement
BB	**1.75**	-0.51^{*}	-0.64^{*}
	1.40	-0.55^{*}	-0.47
	1.05	-0.51^{*}	0.03
	0.70	-0.59^{*}	-0.33
BR	**1.75**	-0.66^{*}	-0.52^{*}
	1.40	-0.74^{*}	-0.46
	1.05	-0.47	-0.62^{*}
	0.70	-0.65^{*}	-0.63^{*}

Table 4.8: Correlations between coefficients of amplitude potentiation and $D_{twitchB1}$-$D_{tetanus}$ ratios were calculated. Calculations were performed for transverse and longitudinal twitches, for both muscles and at all selected elbow angles. Statistically significant correlations are marked with "*".

4.4. Skeletal muscle modelling

For the purpose of modelling transverse thickening-longitudinal twitch relation results of *in vitro* measurements were employed (measurements on toad GAST). On the basis on neural network firstly, a simple model of responses to random stimulation was created. Further on, geometrical muscle belly deformations during contraction and relaxation were measured and mathematical function for describing muscle geometry was created. This geometrical model was used as a basis for upgrade with modelling muscle's mechanical properties.

4.4.1. Neural network modelling

We used neural network to model belly displacement-muscle force relationship. Input: transverse tetanic response and delayed longitudinal tetanic response; output: modelled longitudinal tetanic response (Figure 3.11). Neural network learning process was already described (chapter 3.7.2.) and is presented in Figure 4.30a. After the learning process was completed, a test response was fitted 85 % (Figure 4.30a). The efficiency of learning process was tested on three pairs of responses taken from toad GAST (Figures 6.30b, c and d), model fitting was 7, 45 and 33 %.

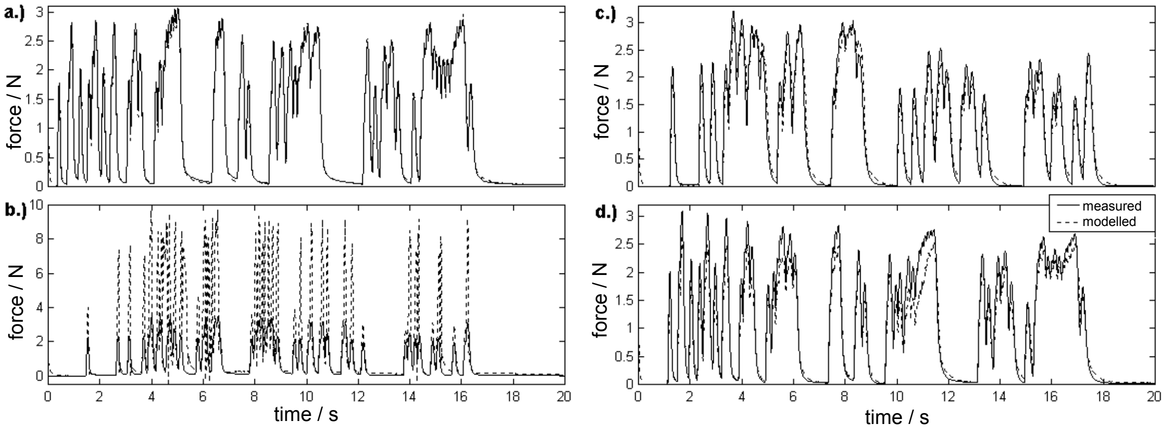

Figure 4.30: Output of neural network learning process, which was carried out on basis of measured transverse and longitudinal tetanic response (a). Three additional pairs of responses were used to verify the rules of neural network (b, c in d).

4.4.2. Geometrical model

Digital camera was used to make recordings of the isolated muscle in resting phase and during isometric contraction and thus tendon elongation, longitudinal contraction and transverse thickening was visualised (Figure 4.31). Muscle was contracted with direct stimulation in form of 3-second-pulse-train.

In order to define geometrical changes of GAST belly during contraction we have used rotational ellipsoid, whose outer contour is defined with parabola (Equation 4.2), where y stands for thickness, x for length, o for half-thickness and c half-length of muscle belly. When parabola is rotated around x axis, a geometrical body – ellipsoid is created. In order to choose the most appropriate parabola we entered our measuring results (dimensions of contracted muscle belly) and checked whether the volume of the ellipsoid corresponded to muscle volume ($V = 4\ cm^3$) (Figure 4.31). After our parabola was weighted with exponence α, the volume of the body corresponded to muscle volume. The value for α was calculated from volume according to Equation 4.3. During isometric and isotonic contraction the value for α was 0.55 and 0.8, respectively. Figure 4.32 presents two-dimensional elliptical shape of a muscle belly for resting and contracting phase.

Isolated muscle was contracted also isotonically, but only for the purpose of model verification. Verification provided acceptable results on model fitting.

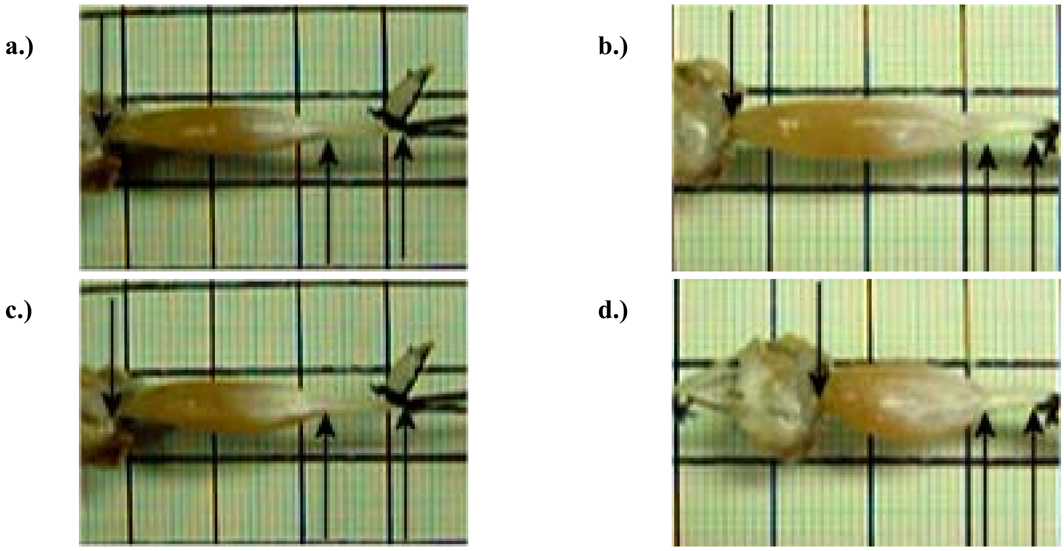

Figure 4.31: Photographs (a) and (c) show relaxed and isometrically contracted toad GAST, respectively. Photographs (b) and (d) show relaxed and isotonically contracted toad GAST, respectively. Arrows indicate positions of markers used for monitoring the changes in muscle and tendon lengths (Table 4.9).

Type of contraction	**Muscle belly length / mm**		**Tendon length / mm**		**Muscle belly width / mm**	
	Relaxed	Contracted	Relaxed	Contracted	Relaxed	Contracted
Isometric	26.25	24	9.5	10.5	5.5	6
Isotonic	26	17.25	5	5.25	6	8.25

Table 4.9: Changes of muscle belly length and width, and tendon length in toad GAST during isometric and isotonic contraction.

$$y = \left(o \cdot \left(1 - \left(\frac{x}{c} \right)^2 \right) \right)^{\alpha} \qquad \textbf{Equation 4.2}$$

$$V = \pi \int_{-c}^{c} y^2 dx \qquad \textbf{Equation 4.3}$$

According to a presumption that muscle belly during contraction thickens in vertical and horizontal direction equally, we can conclude that in case of longitudinal shortening times *m*, muscle belly is thickened times $\sqrt{m}$. In this case muscle belly cross-section is circle-shaped, which makes this presumption acceptable for this study. The same presumption can be employed for ellipse-shaped cross-section.

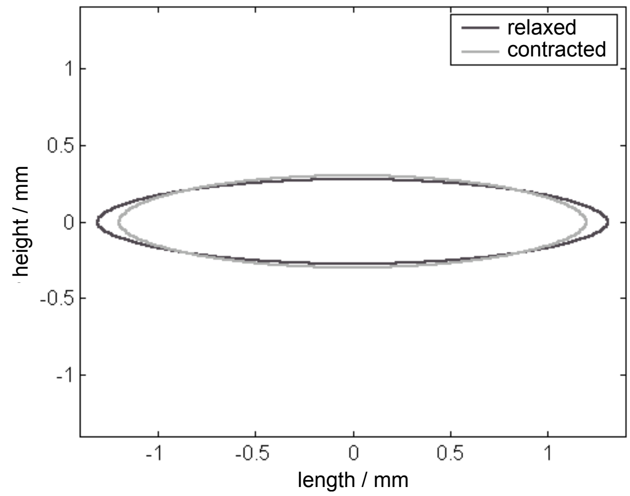

Figure 4.32: Two-dimensional geometrical model of relaxed and isometrically contracted toad GAST belly. GAST belly shortening occurred due to elongation of tendons and aponeurosis.

4.4.3. Mechanical model

When creating the mechanical part of the hybrid model, we included tendon as the most elastic component of our system. For this purpose we performed *in vitro* measurements of transverse and longitudinal twitch with and without distal tendon (Figure 3.7) on toad GAST. In Figure 4.33b we can see a non-hysteretic relationship between transverse and longitudinal twitch. For the muscle-tendon complex tendon's influence over muscle force is noticeable (Figure 4.33c) in form of hysteresis (Figure 4.33d).

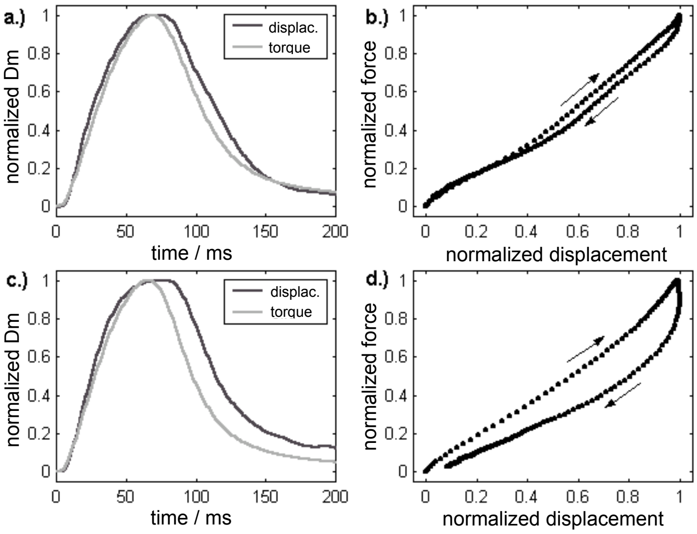

Figure 4.33: Figures (a) and (c) show normalized transverse and longitudinal twitch of toad GAST without and with tendon attached to it, respectively. Figures (d) and (b) show hysteretic and non-hysteretic twitch dynamics (force, displacement) for muscle-tendon complex and muscle with its tendon removed.

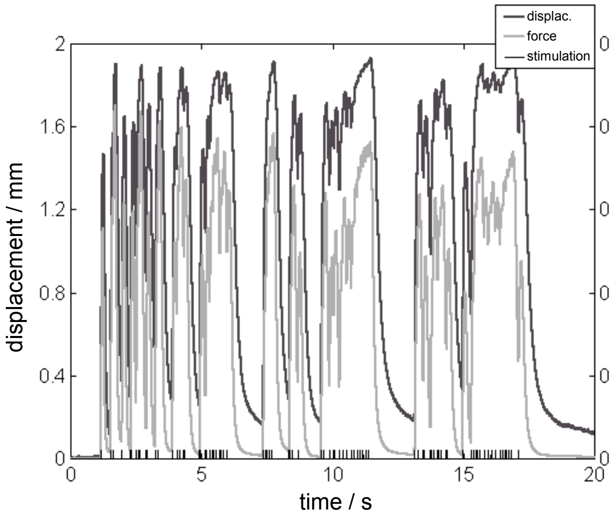

Figure 4.34: Transverse and tetanic response of muscle-tendon complex to random pulse-train.

Afterwards, transverse and longitudinal tetanic responses to random pulse-train were processed in frequency domain (Figure 4.34). Data processing revealed the same frequency spectrum and no shift (zero phase). Similar results were obtained when muscle and muscle-tendon complex were compared. Further, the same responses were processed in time-domain: when both groups of responses (transverse and longitudinal) were plotted in the same graph hysteresis was more obvious for the muscle –tendon complex (Figure 4.35b) than for the muscle only (Figure 4.35b).

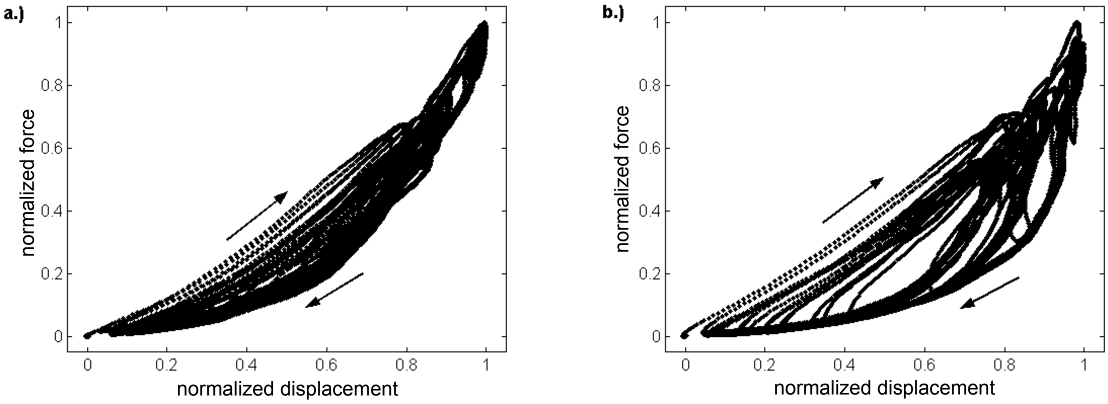

Figure 4.35: Figures (a) – muscle without tendon and (b) – muscle tendon complex show how tendon affects relation between transverse and longitudinal tetanic response of toad GAST to random pulse-train.

To interpret muscle force dynamics, especially during its relaxation, we investigated the course of passive characteristics force-tendon length. Muscle tendon is not the only element influencing muscle contractile properties with its passive properties, but is definitely is the largest SE. When compared to SE, PE is often considered negligible; therefore in various derivations of Hill's model its influence is often disregarded.

Our basis was measured transverse twitch (D_y). Elastic components elongation (in time domain) was gained from geometrical model (D_x, Equation 4.4). Further, mechanical model was used to create passive characteristics for muscle and muscle-tendon complex, separately for the phase of contraction and phase of relaxation (Figure 4.36).

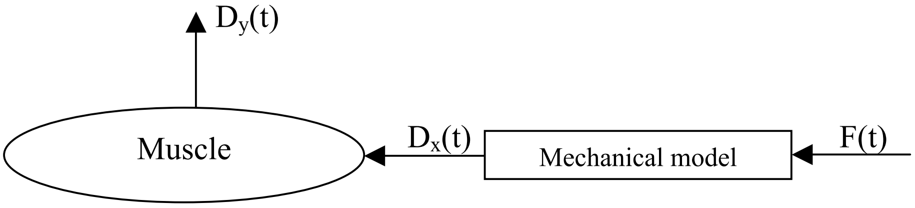

Figure 4.36: Hybrid modelling approach: fusion of data on muscle belly geometry and mechanical model of elastic tissue.

$$D_x(t)=\frac{D_y(t)}{\sqrt{m}} \qquad \textbf{Equation 4.4}$$

$$F_1(D_x(t))=A_1 \cdot e^{b_1 D_x(t)}; \qquad 0 < t \le t_{\max(D_x)} \qquad \textbf{Equation 4.5}$$

$$F_2(D_x(t))=A_2 \cdot e^{b_2 D_x(t)}; \qquad t_{\max(D_x)} < t \le length(t) \qquad \textbf{Equation 4.6}$$

Following observation was made: the course of the passive characteristic force-tendon differs for both systems: in case of muscle-tendon complex relaxation phase differs from contraction phase; in case of muscle without tendon, characteristics for contraction and relaxation phase are similar (Figure 4.37).

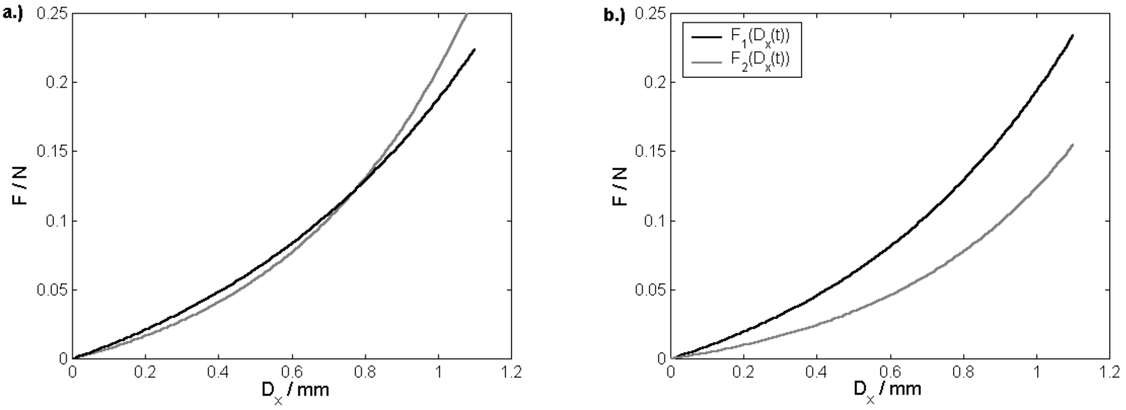

Figure 4.36: Passive connective tissue characteristic for muscle with (b) and without (a) tendon. Characteristics were acquired through mechanical model (Equations 4.5 and 4.6). Values of coefficients (A_i, b_i) for elongation and shortening of connective tissue in muscle with removed tendon are (0.0714, 1.2892) and (0.0346, 1.9530), respectively. For muscle-tendon complex the coefficients values for elongation are (0.0560, 1.4939) and for shortening (0.0212, 1.9217).

4.4.4. Modelling responses of type I and type II muscle fibres

The peak of transverse twitch response is more pointed in muscles with shorter Tc_{TMG} (Figure 3.10). This can be explained using separate models for type I and type II muscle fibres on the presumption that all muscle fibres of the same type exert the same twitch response. This presumption is most probable for fibres comprised in the same muscle.

The scheme presented in Figure 4.38 shows a model for summation of modelled twitches (type I and type II fibres), which is in longitudinal direction transferred to the skeleton (over the tendon) and in transverse direction to muscle belly displacement force.

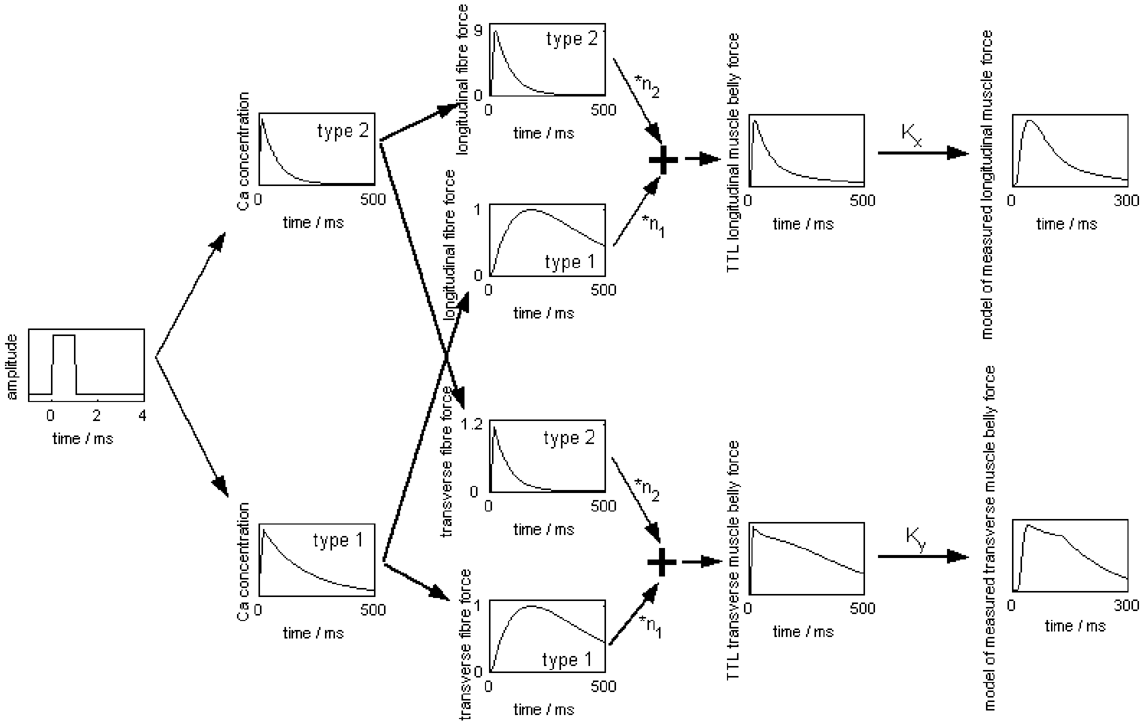

Figure 4.37: Model of connection between longitudinally measured force and transversely measured displacement of human muscle belly.

In order to follow muscle belly displacement properly, displacement sensor comprises a so-called "recurrent spring", which pushes the sensor tip against the skin above the measured muscle. When measured transverse displacement is multiplied by elasticity coefficient of the aforementioned spring it is in linear connection with transverse muscle belly displacement force. Selectively measured calcium concentration and longitudinal force exerted by isolated fibres were taken from the literature (Wetzel and Gros, 1998). Longitudinal twitch of type II muscle fibre starts increasing later, at higher calcium concentration and its amplitude is up to nine times higher than in longitudinal twitch of type I fibres (Wetzel and Gros, 1998; Sica and McComas, 1971).

With respect to their shortening and on the presumption they are cylindriform and of the same length, type I and type II isolated fibres thicken quadratically and proportionally. Type II fibres diameter is 5 – 20 % larger (in this thesis a 20 % larger diameter was taken into account) (Knez, 2000; Johnson et al., 1973). Von Donkelaar et al. (1999) claimed that there is a linear relationship between muscle belly thickening and its shortening. For the purpose of this thesis we presupposed equal dynamics but different amplitudes of transverse and longitudinal twitch of isolated muscle fibre.

Further, transverse and longitudinal twitches of both types of isolated fibres were multiplied by respective percentage for each fibre type comprised in measured muscle (n_1, n_2). Thus the entire muscle belly force was calculated. In the end, we were interested in damping coefficient of the connective tissue, for it affects both muscle fibre type responses. Parameter Tc was minimized with an optimisation procedure, which resulted also in coefficient ratio: damping coefficient –

damping in transverse plus longitudinal direction. Optimisation procedure was reapplied on ten sets of transverse and longitudinal twitches. The calculated values for K_x were from 2.2 to 6.5 times bigger than for K_y (mean ± SD: 4.6 ± 3.2), of course, depending on subject and measured muscle. We interpreted this result as follows: damping coefficient for a transient function (of measured transverse (longitudinal) force and modelled transverse (longitudinal) force) differs significantly for transverse and longitudinal direction, especially at higher frequencies.

5. Discussion

In this chapter our experimental and modelling results are discussed in connection with already published ones.

5.1. Optimal contraction angle

Characteristics describing force-length and torque-length relation in human have already been measured using different methods, on the contrary to muscle belly displacement-length characteristics, which has not been investigated until now. These characteristics were measured using torque measurements (Hasan and Enoka, 1985; Hutchins et al., 1993; Kasprisin and Grabiner, 2000), intramuscular force measurements in muscle tendon (Komi, 1990; Fowler et al., 1993), muscle modelling (Uchiyama et al., 1998; Bennet et al., 1994; Huijing, 1998; Chang et al., 1999) and were used for making inferences on optimal muscle length. Measurements were performed in voluntarily (Kasprisin and Grabiner, 2000; Hasan and Enoka, 1985; Chang et al., 1999) and electrically evoked contractions (Day et al., 2000; Thomas et al., 1999).

This chapter is divided in following sections: firstly, torque-muscle length characteristic is introduced, elbow flexor muscles were contracted voluntarily; in second and third section measuring results of electrically evoked contractions in two elbow flexor muscles are presented and in the fourth section results of *in vitro* measurements are discussed.

5.1.1. Torque-muscle length characteristic in voluntary contraction

MVC and ballistic MVC were measured at elbow angles of 1.75, 1.40, 1.05 and 0.70 rad. Our observations were in accordance with already published results and were as follows: elbow flexor muscles exerted maximal torque during ballistic MVC at the angle of 1.40 and 1.75 rad (Figure 4.1). Performing both – increasing MVC and ballistic MVC enabled elimination and evaluation of body movement and coactivation of not measured muscles. Both contraction patterns were significantly correlated ($r = 0.95$), which proved that MVC was performed correctly.

Chang et al. (1999) reported that force-length characteristics for different elbow flexor muscles differ significantly (Table 5.1). Muscles BB and brachialis dominate at larger angles, m. BR at smaller elbow angles. The reason is in PCSA: PCSA of BB is 3.1 times bigger and of brachialis 4.7 times bigger than PCSA of BR, therefore they are able to exert greater force (Table 5.2).

Muscle	Normalized muscle force		Optimal angle / rad
	2.09 rad	0.26 rad	
m. BB	0.9	0.21	1.88
m. BR	0.65	0.22	1.71
m. brachialis	0	0.82	0.85

Tabela 5.1: Force-length characteristic for three elbow flexor muscles (Chang et al., 1999). Given are the values of normalized force at two elbow angles and the optimal elbow angle.

Muscle	[a]Muscle length / cm	[a]Fibre length / cm	[a]CSA / cm^2	[b]PCSA/ cm^2	[c]Moment arm / cm	[d]Distance to joint axis / cm	
						Proximal	Distal
BB	24.0	17.8	5.8	4.6	4.8	28.2	4.8
BR	23.7	14.7	2.0	1.5	5.6	5.5	22.2
m. brachialis	20.1	14.4	7.4	7.0	3.3	13.5	3.5

Tabela 5.2: Anthropometrical data on three elbow flexor muscles ([a] Enoka, 2002; [b] An et al., 1981; [c] Uchiyama et al., 1998; [d] Faszczewski et al., 1994). In m. BB moment arm is maximal at 1.75 rad, in m. BR and m. brachialis moment arms are maximal at 1.92 rad. When elbow angle is diminished from 1.75 to 0.70 rad, lengths of m. BB, m. BR and m. brachialis increase for 5, 5.5 and 3.5 cm, respectively (Uchiyama et al., 1998).

Koo et al. (2002) reports big difficulties with measuring optimal muscle length under *in vivo* conditions and wide dispersion of results published so far. Koo himself performed simultaneous *in vivo* measurements of torque and EMG in elbow joint and showed that in the rising part of force-length characteristic m. BB's relative force ranges from 10 to 100 % (longer head) and from 40 to 100 % (shorter head). For m. BR relative force ranges from 55 do 100 %, which was confirmed by Murray et al. (2000). Koo et al. (2002) used a model to calculate the optimal lengths of m. BB and m. BR, which are for both muscles at the angle of 1.40 rad. Such deviations probably result from using the unreliable EMG method (Koo et al., 2002) and performing measurements on cadavers (Murray et al., 2000), which proved inappropriate in researches of this kind.

5.1.2. Torque-muscle length characteristic in electrically evoked contraction

Torque measurements, carried out on m. BB and m. BR revealed following contractile properties – length dependency: during diminishing elbow angle amplitudes of longitudinal twitch and tetanic response of m. BB were increasing (Figures 4.8 and 4.18), while amplitudes of m. BR reached their maximum at the angle of 1.40 rad (Figures 4.9 and 4.19). These measuring results are in accordance with results taken from the literature, however they differ from theory dealing with relation between joint angle and optimal muscle length.

The selective force-length characteristic of electrically evoked contraction has been often investigated (Marsh et al., 1981; Sale et al., 1982), still no statistically significant results were reported. Marsh et al. (1981) and Sale et al. (1982) applied torque-measuring method about ankle joint and made certain inferences on contractile properties of tibialis anterior and gastrocnemius medialis, but paid no attention to the level of activation.

Our findings, showing that the amplitude of longitudinal twitch increases with muscle elongation, are again in accordance with findings taken from literature (Mela et al., 2001; Rack and Westbury 1969; Maginaris, 2001; Hanchard et al., 1998). Some of them explain these findings with differences in muscle activation (Mela et al., 2001; Maginaris, 2001), others with additional SE elongation, which is bigger in stretched muscle (Rack and Westbury, 1969; Brown and Loeb, *in press*). The increase in duration and relaxation of longitudinal twitch is also discussed (Brown and Loeb, *in press*). Studies on elongated isolated muscles revealed the increase of relaxation time and increase of longitudinal twitch amplitude as well as longitudinal tetanic response amplitude. Morgan (1985) used prepared muscle to explain the longitudinal twitch amplitude increase in muscles, of lengths bigger than their optimal length – the reason was supposed to be the non-uniform distribution of sarcomere lengths within muscle fibres. Huijing (1999) and Trotter (1993) claim this could not be the case for *in vivo* measurements, for then muscle force is transferred via fascia.

To identify isometric forces of individual elbow flexor muscles Kasprisin and Grabiner (2000) suggested the use of muscle activation - namely, they noticed significant activation changes in m. BB and insignificant changes in m. BR. Muscle activation can be well described also with alteration of longitudinal twitch time parameters, which was employed it this thesis. Parameters Td and Tc of longitudinal twitch were significantly longer than those of transverse twitch, however no correlation was found. Parameters Ts and Tr of transverse as well as longitudinal twitch are significantly correlated, for similar courses of both muscles' characteristics (Figures 4.6 and 4.7).

For m. BR our measurements revealed shorter Tc of longitudinal as well as transverse twitch for m. BR, which is in accordance with our previous investigation (Dahmane et al., 2000), where Tc_{TMG} for m. BB and m. BR was compared and statistically significant correlation between Tc and percentage of type I muscle fibres was demonstrated.

Electrically evoked contraction cannot be compared to voluntary one. The former employs constant frequency stimulation (Botterman and Cope, 1988), while the latter occurs at altering frequencies. Usually, voluntary contraction is accompanied by coactivation of synergist muscles, which affects tendon compliance – also the tendons of observed muscles.

5.1.3. Displacement-contraction duration characteristic in electrically evoked contraction

Muscle belly displacement measurements, carried out on m. BB and m. BR revealed following dependency: during diminishing elbow angle amplitudes of transverse twitch and tetanic response were decreasing, with their maximums at angles of 1.75 and 1.40 rad (Figures 4.8, 4.9, 4.18 and 4.19), for m. BB transverse twitch time parameters decreased and for m. BR transverse twitch parameters Td in Tr remained unchanged (Figures 4.6 and 4.7).

The amplitude of transverse twitch is affected by several factors such as: level of muscle activity (Figures 4.2, 4.4 and 5.3), muscle geometry (its size, MU distribution, pennation angle, SE, PE) and undesirable disturbances (muscle belly lateral movements and body movements, which are added to measured muscle belly displacement). Quite many of these factors can be eliminated if supramaximal electrical stimulation is applied and elbow and shoulder are properly fixated. It can be presupposed that during the stretch phase muscle volume, CE homogeneity and pennation angle remain unchanged. Passive force of connective tissues changes with muscle length and can therefore not be neglected.

Measuring muscle belly stiffness:

Muscle belly stiffness in transverse direction was defined with amplitude of transverse twitch and amplitude of muscle belly tetanic response. We manufactured a stiffness-measure, which was used for the purpose of this thesis. Kubo et al. (2001) showed that under *in vivo* conditions muscle belly longitudinal stiffness and tendon elasticity are not connected. He further reported non-dependence between the stiffness of muscle-tendon complex and tendon elasticity, meaning that tendon anthropometrical data (length and thickness) do not indicate muscle belly stiffness.

Additional relations were revealed in this study: muscle belly stiffness proved to be dependent on joint angle (Figure 4.11); m. BR stiffness is significantly higher than that of m. BB (Figure 4.10). This could be the effect of m. BR's less elastic muscle belly and smaller CSA. The influence of joint angle on muscle belly stiffness is considerably bigger for m. BR than for m. BB (Figure 4.11).

Measured muscle belly stiffness was used with creating displacement-length characteristic, which informed us about dependency of Dm_{TMG}/D_v quotient on elbow angle. Aforementioned quotient for transverse twitch reached its maximum at the angles of 1.75 and 1.40 rad for m. BB, and 1.05 rad for m. BR (Figure 4.12). For tetanic responses quotient maximum was reached at 1.75 rad for m. BB and 1.40 rad for m. BR (Figure 4.20).

5.1.4. Defining the optimal length for isolated toad gastrocnemius

In Figure 5.1 force-length and displacement-length characteristics are plotted for transverse and longitudinal measurements. Noticeable differences (opposite course) are presented in Figure 5.1b for muscle with removed tendon. These findings were used for interpretation of measured results in human twitch and tetanic responses: m. BB's tendon is shorter and less elastic than m. BR's tendon, therefore force-length and displacement-length characteristics are of opposite course (Figures 4.8 and 4.18). In case of m. BR, which has a longer and more elastic tendon, the course of both characteristics is the same as in Figure 5.1a (Figures 4.9 and 4.19).

In human transverse twitch parameter Tc is shorter and parameters Ts and Tr are longer than in longitudinal twitch (Figures 4.6 and 4.7). Same results were obtained from isolated toad GAST (Figure 5.2).

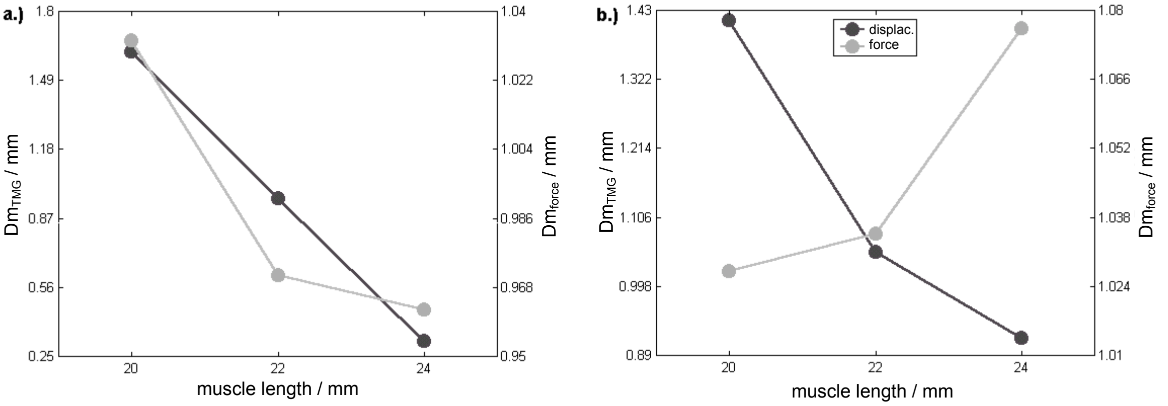

Figure 5.1: Twitch-amplitude characteristics for muscle-tendon complex (a) and muscle with removed tendon (b) in toad GAST.

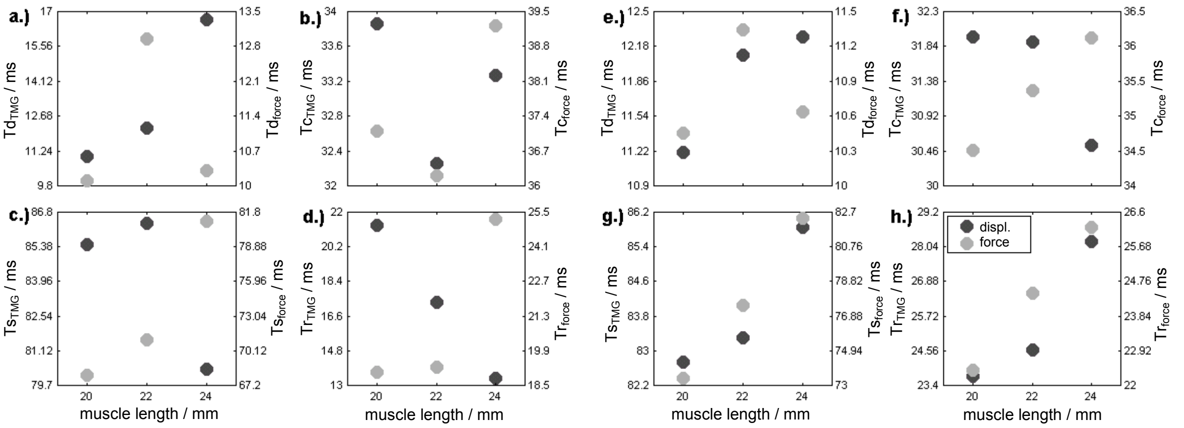

Figure 5.2: Muscle length dependency of time parameters for transverse and longitudinal twitches in toad GAST. Figures (a – d) present muscle-tendon complex, while figures (e – h) present time parameters for twitches of muscle only (without tendon). Muscle length was changed within its physiological limits. For the purpose of measurements synchronisation passive force measurements were performed.

5.2. *Muscle twitch-activation level dependence*

In vivo measurements and comparison between muscle belly transverse displacement and longitudinally measured torque have not yet been carried out. Orizio et al. (1999) performed *in vitro* measurements on isolated cat’s GAST and carried out belly displacement measurements with laser displacement sensor. Still he reported on many factors affecting the measurement negatively (exacting sensor placing affecting also variability of choosing the measuring point…).

Other advantages of muscle belly displacement measuring method over torque measuring method have already been mentioned (Chapter 2).

With transverse twitch measurement we also measure geometrical changes of muscle belly, but at the same time some disturbing factors have to be taken into account (especially with small muscles): non-homogeneous distribution of contractile elements, muscle fibre length, sarcomere activity and fascia properties (longitudinal direction). From transverse twitch we gain information on muscle activation, useful for better understanding and modelling (muscle activation).

5.2.1. Connection between amplitudes of transverse and longitudinal twitch

For transverse and longitudinal twitch relation between Dm_{TMG} and Dm_{torque} is exponential and a function of elbow angle, except for the smallest angle where muscle length was maximal and relation was linear.

Transverse twitch has a lower contraction threshold and reaches its maximum in a shorter time than longitudinal twitch. Dm_{torque} / Dm_{TMG} dependency is presented in Figure 4.3 and can be divided into two sections: larger alteration of Dm_{TMG} in the first section, alteration of Dm_{torque} in the second section. Such pattern was noticeable in elongation-tension characteristic of elastic tissue ("*toe region*"). While muscle belly displacement reaches its saturation, longitudinal tension (with increasing stimulation) can still increase.

Measuring transverse and longitudinal twitches of toad GAST:
Isolated GAST was stretched to its maximal functional length (2.2 cm) and measured, which resulted in linear relationship between amplitude of longitudinal twitch (Dm_{force}) and transverse twitch (Dm_{TMG}) (Figure 5.3). Orizio et al. (1999) have presented exponential relationship between both amplitudes in cat gastrocnemius, but have not given any data on muscle length.

5.2.2. Time parameters of transverse and longitudinal twitches

Transverse and longitudinal twitches have been classified according to the stimulating amplitude, which helped providing data on muscle contractile properties with respect to increase of stimulation amplitude (Figure 4.5). For both muscles parameters Td and Tc differed for transverse and longitudinal twitches, just the opposite of Ts and Tr. This means there must be a different filtration system applied to the process of transformation chemistry within the contracting muscle into measured mechanical movements.

Measured Tc_{TMG} of transverse twitch for both muscles (Figure 4.5) is in accordance with theory of non-homogeneous type II muscle fibre distribution, which states that there is a higher density on the surface of the muscle (Elder et al., 1982; Lexell et al., 1983). We presume that electrical stimulation of threshold amplitude only innervates the superficial neurons, and further, they activate superficial MUs. The increasing stimulation amplitude, the deeper MUs activation, until supramaximal amplitude is applied. This pattern was investigated by Dahmane et al. (*in press*) on nine human muscles with TMG measurements and histochemistry: in every muscle Tc at 5 % supramaximal amplitude was significantly shorter than Tc at 50 % supramaximal amplitude of transverse twitch.

For torque measurements Tc_{torque} (longitudinal twitch) is prolonged for every increase in amplitude (figure 4.5). The reason is probably MU recruitment order – during electrical stimulation, firstly larger and faster MUs are activated and later the slower ones. Savelberg (2000) used Huxley's model (Maenhout et al., 2000) to show that Tc of muscles with 40 to 60 % type I muscle fibres (includes m. BB and m. BR) increases when activation of longitudinal twitches is increased.

Parameters Ts_{TMG} and Ts_{torque} in human express similar pattern (Figure 4.5) as Ts_{force} of *in vitro* twitches in toad GAST (Figure 5.4). The same goes for Tr_{TMG} and Tr_{torque} in human compared to Tr_{TMG} and Tr_{force} in toad GAST. When stimulation amplitude was increased, parameters Tr_{torque} and Tr_{force} of longitudinal twitch in human (Figure 4.5) and in toad, respectively, initially decreased, which is in accordance with findings from Savelberg (2000). Gonyea et al. (1981) are ones of the few who demonstrated statistically significant correlation between parameter Tr_{force} of isometric longitudinal twitch (in isolated wrist flexor muscles in the cat) and percentage of type I muscle fibres (in the same muscles). This indicates not only response amplitude and Tc but also Tr is to be taken into account when dealing with MU or muscle classification.

Measuring responses of isolated toad GAST:

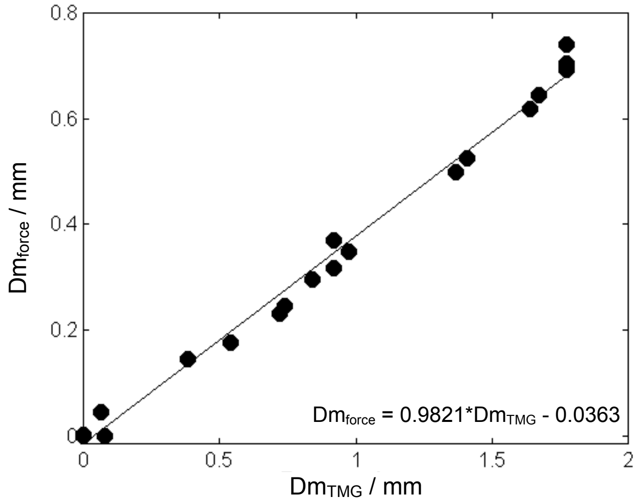

Figure 5.3: Linear model of relation between transverse twitch amplitude and longitudinal twitch amplitude in toad GAST is shown in this figure: while Dm_{TMG} already reached its supramaximal value, Dm_{force} is still increasing.

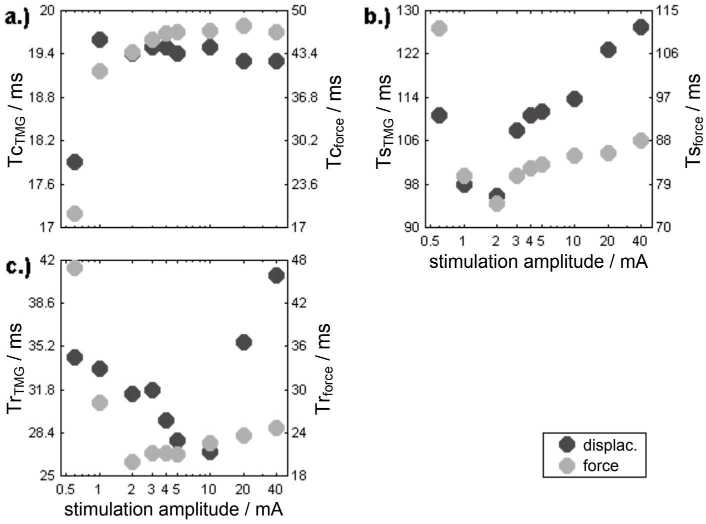

Figure 5.4: Figures show stimulation amplitude dependency of parameters Tc (a), Ts (b) and Tr (c) for transverse and longitudinal twitch of toad GAST.

To evaluate our measuring results we wanted to compare them with results from literature, but we did not manage to find any similar studies. Therefore we performed the experiment under *in vitro* conditions on toad GAST and it revealed similar characteristics (Figure 5.4). Parameter Tc_{TMG} was maximal at minimal stimulation amplitudes, with increasing stimulation amplitude he increased and then decreased again. Similar pattern was observed for parameter Tc_{force}, only without the final decrease (at supramaximal stimulation amplitude).

5.2.3. Properties of muscle belly transverse twitch

Even though displacement sensor is positioned selectively on muscle belly, synergist muscles coactivation is detected to a smaller extent than with force sensor placed non-selectively on the forearm. We presume that the increase of m. BB longitudinal twitch, which occurs 50 ms after maximal response is reached (Figure 4.4), is a result of m. brachialis coactivation. This is the case when stimulation amplitude is in the range of supramaximal muscle activation.

Peak of transverse twitches was often very distinctive (Figure 3.10), which was not the case with longitudinal twitches. The cause remains unexplained, but is discussed later.

Prior to performing measurements regarding this thesis we:
- Assured us that displacement sensor stays attached to the skin throughout the entire measurement (no rebounding), in order to obtain relevant measuring results.
- Verified frequency relations: transverse and longitudinal twitch are limited upwards by 10 Hz, which is more than four times less than sensor's frequency.
- Investigated the influence of skin fold, for it lies just between the sensor and measured muscle. No correlation between skin fold and peak of the response or transverse muscle stiffness was found. The only correlation ($r = -0.41$) was found between the peak amplitude and Tc_{TMG} in BR, which indicates that muscles with shorter Tc_{TMG} exert higher peak amplitude.

5.3. Influence of the tendon on responses of isolated toad GAST

Figure 5.2 shows time parameters of transverse and longitudinal twitches in one out of 4 toad GAST, for all measured results showed similar trends. From this it is evident that tendon properties have great impact on muscle contractile properties. Due to only 4 available preparations, no statistical analysis was performed.

When comparing muscle with removed tendon to muscle-tendon complex we noticed that Tc for transverse and longitudinal twitches was longer for muscle-tendon complex, meaning tendon hinders its contraction; Tr and Ts for transverse and longitudinal twitches were shorter for muscle-tendon complex, meaning that accumulated elastic energy (in tendon during contraction) is released during relaxation phase (Figure 4.33).

Huijing and Been (2001) reported a difference in results of *in vitro* and *in vivo* measurements – mostly for the difference in forces at the proximal and distal muscle endings, which equals zero for *in vitro* measurements and even 23 % for *in vivo* measurements. Still generalization of *in vitro* findings is possible, but great precaution is required.

Van Eijden et al. (2002), Yemm and Nordstrum (1974) and Weijs et al. (1989), demonstrated hysteresis for passive muscle force and muscle length during *in vivo* stretch and contracting the muscle-tendon complex in animals. Hysteresis indicates that not entire accumulated energy is released during relaxation phase, to certain amount it is transformed into heat. Same conclusions were made based on our measurements of active muscle contraction (Figures 4.33 and 4.35).

Every tendon elongation results in accumulation of elastic energy. Elongation can occur either during voluntarily or electrically evoked muscle contraction. During maximal tetanic force Loren and Lieber (1995) reported wrist tendons elongation of 2.46 %.

5.4. How responses depend on stimulating frequency

Force-frequency or torque-frequency characteristic informs us about one of the basic input-output relation in MUs. It describes relation between amplitudes of tetanic responses and frequency of respective stimulation and at the same time identifies transformation of nervous system output (APs) into mechanical responses of MUs. From this point of view the force-frequency characteristic is of greater importance than MU contraction velocity.

The literature survey did not provide any information on how muscle length affects displacement-frequency characteristic. Even torque-frequency characteristic was examined very rarely – the reason might be difficult measurements of tetanic responses. More research work was done in muscle fibre, where the impact of certain parameters on force-frequency characteristic was investigated.

5.4.1. Torque-frequency characteristic in human

We demonstrated angle dependency of torque-frequency characteristic (Figures 4.16 and 4.17) for elbow joint and elbow flexor muscles. The estimated f_h diminishes when elbow angle is diminished (holds for BB and BR). Parameter f_h is used for MU classification: one group of MUs had longer Tc and Tr of longitudinal twitch force and lower f_h (Kernell et al., 1975; Botterman et al., 1986). Our measuring results indicated similar findings. M. BB comprising bigger percentage of type I muscle fibres has lower f_h and longer Tc_{TMG}, Tc_{torque}, Tr_{TMG} in Tr_{torque} (Figures 4.6, 4.7, 4.16, Table 4.2).

Force-frequency characteristic can shifts either towards lower frequencies (potentiation) or towards higher frequencies (fatigued muscle).

As already mentioned, it has not been often investigated how muscle length affects force-frequency characteristic. A shift towards lower frequencies was reported after the muscle was elongated (Huijing, 1998; Mela et al., 2001). This means that values for optimal muscle length increase with lower stimulation frequencies. Explanation is based on contractile element properties dependency of muscle length (Stephenson and Wendt, 1984) and is in accordance with researches in animals (Balnave and Allen, 1996; Stephenson and Williams, 1982; Rack and Westbury, 1969). Marsh et al. (1981) explained this shift on tibialis anterior for it has a rather long tendon and thus many SE. Mela et al. (2001) disagreed and claimed longer tendons should cause just the opposite. Our measuring results are accordant to findings by Mela et al., for the same shift of torque-length was noticed, even though m. BR's tendon is quite longer than m. BB's (Figure 4.16).

In voluntary contraction firstly a doublet is fired (second one delayed from 5 to 15 ms), then after a short interval further APs follow (Bawa and Calancie, 1983; Desmedt and Godaux, 1977; Kudina and Alekseeva, 1992b). In animal experiments it was shown that such combination maximizes the integral of force response in time domain (Burke et al., 1976; Zajac III and Young, 1980a and 1980b). Thomas et al. (1999) presented the amplitude of the longitudinal doublet twitch to be 3.5 times bigger than the usual longitudinal twitch amplitude, which presents 48 % of supramaximal longitudinal twitch amplitude. However, no information on stimulation amplitude was given.

Our measuring results are as follows: mean amplitude of longitudinal twitch of m. BB equals 5.82 Nm ± 1.30 Nm and in m. BR 4.61 Nm ± 1.68 Nm. Both amplitudes were summed up and so presented 14.23 % of the MVC amplitude. The same was performed for tetanic longitudinal twitches, amplitudes equalled 12.91 Nm ± 4.19 Nm in m. BB and 10.77 Nm ± 3.02 Nm in m. BR. Both amplitudes were again summed up, compared to MVC amplitude and presented 32.18 % of the MVC amplitude. Similar findings were reported by Bűlow et al. (1995); they performed non-selective stimulation of muscle group quadriceps femoris and the longitudinal twitch amplitude presented 15 % of MVC amplitude.

5.4.2. Displacement-frequency characteristic in human

Displacement-frequency characteristic for m. BB and m. BR proved to be significantly dependent on elbow joint (Figures 4.16 and 4.17). When elbow angle was diminished the amplitude of transverse twitch and tetanic responses of m. BB significantly increased for lower stimulation frequencies. Changes in parameter f_h could not be detected, since transverse twitch of m. BB exceeded 50 % of supramaximal transverse tetanic amplitude. In m. BR the estimated f_h increased with diminished elbow angle, presumably because of m. BR comprising larger SE than m. BB.

5.4.3. Force-frequency and displacement-frequency characteristic in toad isolated muscle

Figures 5.5 and 5.6 illustrate force-frequency and displacement-frequency characteristic for both complexes – muscle-tendon, muscle without tendon. Beside the difference in amplitudes, no other differences were noticed. Amplitude of transverse tetanic responses was higher for muscle without tendon. Amplitude of longitudinal tetanic responses was higher for muscle-tendon complex. Similar observations were made for the control twitch at the end of the protocol (Table 5.3). This again indicates the difference in transverse and longitudinal twitch mechanics. Characteristics dependence on muscle length was not studied.

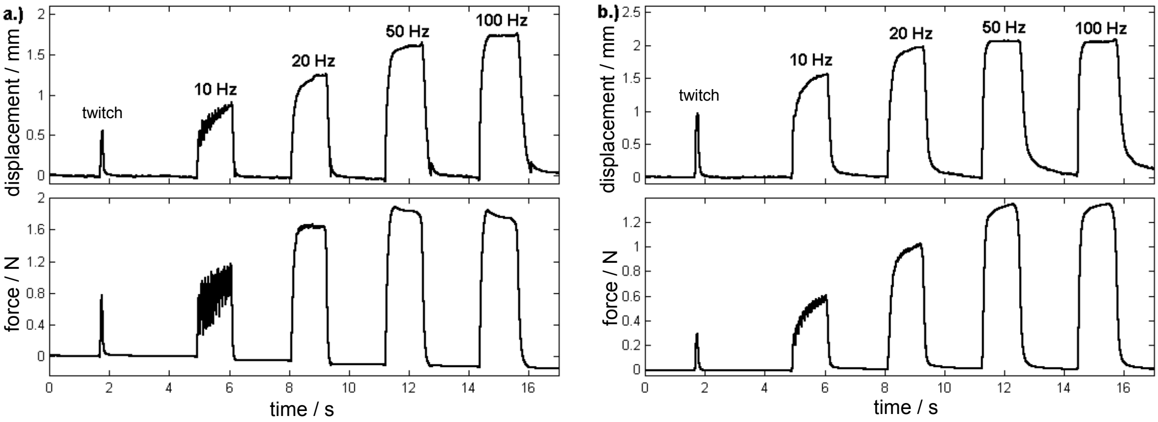

Figure 5.5: Transverse and longitudinal twitch- and tetanic responses of toad GAST to short pulse-trains. Responses of muscle-tendon complex are presented on the left (a), while on the right side responses of muscle without tendon are presented (b).

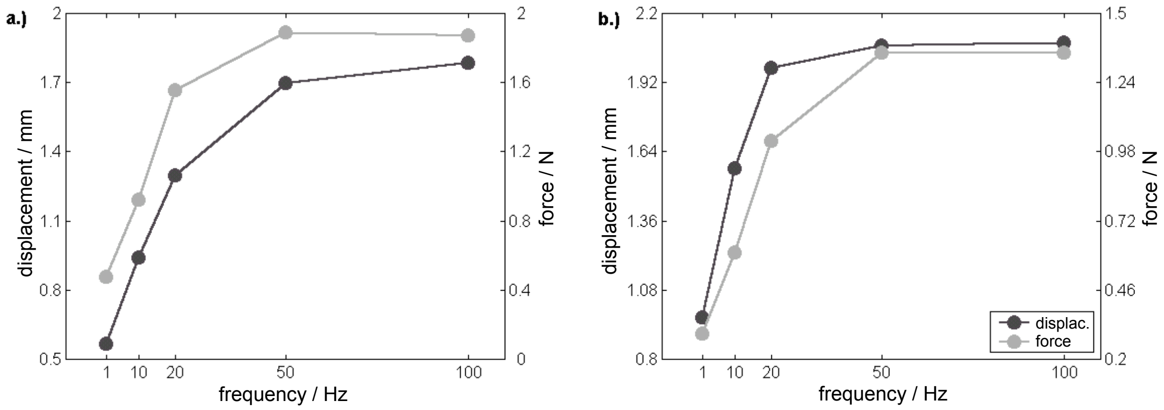

Figure 5.6: Force-frequency and displacement-frequency characteristics for toad GAST with- (a) and without tendon (b).

5.4.4. Tetanic responses properties

Between Tc of longitudinal twitch and amplitude of supramaximal longitudinal tetanic response either in m. BB or in m. BR no correlation was found. The same was reported by Sica and McComas (1971) on extensor hallucis brevis in human.

When stimulation frequency was increased from 10 to 20 Hz the peak-to-peak amplitude decreased in unfused transverse as well as longitudinal tetanic response (Figure 4.16). This observation is in accordance with observations in cat gastrocnemius by Orizio et al. (1999 in 2000).

In vitro measurements in toad GAST revealed higher amplitude of transverse and longitudinal tetanic response for the muscle-tendon complex (f= 10 Hz, Figure 5.5). The reason probably lies in tendon releasing its elastic energy and thus accelerating the relaxation process.

Pulse-train stimulation of isolated muscle increases or accelerates its fatigue (Table 5.3) – all time parameters of control longitudinal twitch are prolonged, as do parameters Tr_{TMG} and Ts_{TMG} of control transverse twitch, which indicates that transverse relaxation is more sensitive to fatigue. Similar conclusions are made if we analyse Figure 6.36a more in detail. When compared to single pulse stimulation, tetanic stimulation much sooner pumps out muscle energy stores and thus in Figure 4.34b no hysteresis typical of tendon or fatigued muscle is noticeable.

Amplitudes of control (transverse and longitudinal, in m. BB and in m. BR) tetanic responses at 100 Hz were higher than those of tetanic responses at 50 Hz (Figure 4.16). It means we did not apply supramaximal stimulation, but were quite close. Applying supramaximal stimulation was rather difficult, for some subjects felt a certain level of pain and so a bit lower amplitudes were applied.

5.5. Twitch-tetanus ratio

The abovementioned ratio for longitudinal measurements was suggested to present a measure for muscle activation (Brown and Loeb, 1998). High correlation between innervation ratio and MU maximal tetanic force was presented (Bodine et al., 1987; Kanda and Hashizume, 1992; Zepetnek et al., 1992) and is used for estimation of innervation ratio. Statistically significant positive correlation between MU size and twitch-tetanus ratio in longitudinal direction was calculated also by Bewick et al. (1993).

Measuring twitch-tetanus ratio in torque responses is difficult because of the torque exerted by the limb, which affects longitudinal tetanic responses. This problem can be eliminated with increasing the stimulation frequency.

So far presented twitch-tetanus ratio measurements were performed with force or torque measurements, but revealed dispersive results: Thomas (1997) presented ratio of 0.09 (in human), but did not offer any criterions for choosing stimulation amplitude; Fuglevand et al. (1999) presented a ratio of 0.36 (longitudinal responses in human), similar results were presented also by Burke et al., 1973; Lev-Tov, 1988), who performed measurements in animal muscles. Desmedt (1967), Burke (1967) and Slomić et al. (1968) presented a ratio ranging between 0.1 and 1 (longitudinal responses in human).

We intended to find a reason for these dispersive results and finally concluded that twitch-tetanus depends on measured muscle, subject and most of all on stimulation frequency.

Firstly twitch-tetanus ratio was defined as D_{twitch}-$D_{tetanus}$ amplitude ratio. D_{twitch} are the amplitudes of transverse and longitudinal twitch obtained from protocol A. $D_{tetanus}$ are the amplitudes of transverse and longitudinal tetanic response obtained from protocol B.

Secondly twitch-tetanus ratio was defined as $D_{twitchB1}$-$D_{tetanus}$ amplitude ratio. $D_{twitchB1}$ are amplitudes of transverse or longitudinal twitch measured at the beginning of protocol B. $D_{tetanus}$ are amplitudes of transverse or longitudinal tetanic response measured during protocol B. Stimulation amplitude remained unchanged.

In both studies we perform displacement as well as torque measurements. In a comparative study on toad GAST ratio was defined as amplitude ratio D_{twitch}-$D_{tetanus}$. D_{twitch} are amplitudes of transverse or longitudinal twitch response, $D_{tetanus}$ are amplitudes of transverse or longitudinal tetanic response to the same stimulating frequency.

5.5.1. Twitch-tetanus ratio for supramaximal amplitudes

Firstly D_{twitch}-$D_{tetanus}$ ratio was observed, where D_{twitch} and $D_{tetanus}$ were the supramaximal amplitudes of twitch responses (protocol A) and tetanic responses (protocol B).

Data given in Tables 4.4 and 4.5 illustrate how this ratio increases with increasing muscle length. Similar findings were presented by Mela et al. (2001). This indicates that twitch-tetanus ratio depends on muscle length and can therefore not be considered a constant. This dependence is shown as angle dependent ratio: D_{twitch}-$D_{tetanus}$ ratio for m. BB and m. BR in longitudinal direction is significantly bigger at 0.70 rad than at other angles (Table 4.4).

No explanation has yet been offered why twitch-tetanus ratio differs for different muscles – the ratio for MUs of type II fibres is supposedly greater (Enoka and Fuglevand, 2001). Fuglevand et al. (1999) performed *in vivo* measurements in human and revealed that MU types can be classified on the basis of f_h and twitch-tetanus ratio (torque measurements). Firs MU group: f_h = 9.1 Hz ± 0.5 Hz, twitch-tetanus ratio of 0.36, second MU group: f_h = 15.6 Hz ± 1.1 Hz, ratio of 0.25.

Our displacement measurements revealed following results: D_{twitch}-$D_{tetanus}$ = 0.47 in m. BR, D_{twitch}-$D_{tetanus}$ > 1 in m. BB (Figures 4.21 and 4.22) – meaning that the amplitude of supramaximal transverse twitch exceeds the amplitude of supramaximal transverse tetanic response. This might occur due to different ways of force exertion: larger muscles maximize their force only by additional activation of MU, while smaller muscles use this pattern only until 30 % of their maximal force is exerted, further they increase the firing rate (Kukulka and Clamann, 1981; De Luca et al., 1996). Both research groups classified m. BB large muscle, m. BR was unfortunately not investigated, but has three to four times smaller diameter.

Duchateau and Hainaut (1986) reported connection between potentiation and twitch-tetanus ratio in human; Thomas et al. (1993) showed that the ratio is changed with MU fatigue. Further, twitch-tetanus ratio (force measurements) is lower for muscles with higher potentiation. We obtained similar results: D_{twitch}-$D_{tetanus}$ ratio (for both transverse and longitudinal responses) was significantly lower in m. BR than in m. BB (Figures 4..21 and 4.22) and potentiation (for both transverse and longitudinal responses) was significantly higher in m. BR than in m. BB (Table 4.8). Finally, it can be concluded that twitch-tetanus ratio depends on “history“ of contractions.

5.5.2. Twitch-tetanus ratio for non-supramaximal amplitudes

In this chapter only protocol B was analysed: $D_{twitchB}$-$D_{tetanus}$ ratio includes mean amplitude of tree twitches at the beginning of protocol B ($D_{twitchB}$) and supramaximal amplitude of tetanic response.

Tables 4.6 and 4.7 present $D_{twitchB}$-$D_{tetanus}$ ratio for transverse and longitudinal response, respectively.

Statistically significant correlation between $D_{twitchB}$-$D_{tetanus}$ ratio and $D_{tetanus}$ was calculated for transverse responses of both muscles at all four elbow angles (Table 4.6). For longitudinal responses no significant correlation was calculated (Table 4.7). Statistically significant correlation was also calculated between $D_{twitchB}$-$D_{tetanus}$ ratio and $D_{twitchB}$ for responses in transverse and longitudinal direction of both muscles and at all angles (Figure 4.25). Statistically significant correlation between MUs with lower longitudinal twitch amplitudes and $D_{twitchB}$-$D_{tetanus}$ ratio was calculated also by Thomas et al. (1999).

No correlation was found between transverse or longitudinal tetanic response and contraction time (Tc) (Figure 4.26).

In toad GAST following ratios were calculated: D_{twitch}-$D_{tetanus}$ for transverse responses: 0.31 and for longitudinal responses 0.39.

5.6. Post-tetanic twitch potentiation

Potentiation is a phenomenon where response increases more than expected, regarding previous responses. The degree of potentiation depends on previous muscle activation and was noticed in at least three different forms (Rankin et al., 1988). First is potentiation after certain number of twitches, second after a short pulse train (post-tetanic potentiation) and third kind of potentiation occurs after a few longer pulse-trains. The common occurrence is the increase in amplitude.

Post-tetanic potentiation can be presented also from calcium-sensitivity point of view (Sweeney et al., 1993) but this is in most cases neglected (Mela et al., 2001). Twitch potentiation is in most cases in connection with phosphorus impregnation of myosin heads, which brings them closer to actin and thus increases the possibility of activation even at very low excitation (Sweeney and Stull, 1990). Post-tetanic potentiation does not occur only after a longer resting period, but also during physical activity and depends on the force of previous contraction (Bülow et al., 1993). So it was often noticed after MVC (Belanger et al., 1983; Brown and Loeb (*in press*); Vandervoort et al., 1996) and rarely after electrical stimulation (Mela et al., 2001).

Brown and Loeb (1998) revealed that muscle contraction force is not the only cause for potentiation and suggest research area to expand on other contraction parameters. Only few studies investigating potentiation of response time parameters were found, most of them were engaged in half-relaxation time of force-response (Brown and Loeb, *in press*; Belanger and McComas, 1985; Vandenboom and Houston, 1996; Vandervoort et al., 1983). In our research we were studying potentiation of time parameters in transverse and longitudinal responses. We believe that observing potentiation in transverse twitches is more objective, because longitudinal twitches are affected by elastic properties of connective tissue.

Many studies dealt with amplitude post-tetanic potentiation dependence on muscle length (Mela et al., 2001; Roszek and Huijing, 1997; Yang et al., 1998). However, time parameters potentiation was not investigated. We examined how muscle length affects post-tetanic potentiation of all five TMG-based parameters in transverse and longitudinal twitch. We also compared post-tetanic potentiation of transverse and longitudinal twitch.

5.6.1. Post-tetanic potentiation of twitch amplitude

During muscle elongation we noticed a decrease of Dm_{torque} post-tetanic potentiation in both muscles (Table 4.8), which does not hold for parameter Dm_{TMG}; further, maximal post-tetanic potentiation occurs at the smallest length of BB and in not length-dependent in BR (Table 4.8). Same findings were presented also by Mela et al. (2001): they established that post-tetanic potentiation of longitudinal twitches in human *tibialis anterior* is higher at smaller muscle length and is in entirely stretched muscle hardly noticeable. Same observations were reported also by Roszek and Huijing (1997) as well as Yang et al. (1998).

Moreover, we noticed higher post-tetanic potentiation in muscles with lower transverse or longitudinal twitch amplitudes (Figure 4.28, Table 4.9) and in muscles with lower twitch-tetanus ratio (Figure 4.29, Table 4.10), which was presented also by Thomas et al. (1999), only that he performed measurements on human MUs. We did not find any significant correlation between the degree of Dm potentiation and parameter Tr or Tc of longitudinal MU twitch (neither did Thomas et al., (1999)).

Type II MUs in animals (Gordon et al., 1988 and 1990; Lev-Tov et al., 1988) and in humans (Hamada et al., 2000) exert higher post-tetanic potentiation. Measuring results given in Table 4.8 show significantly higher post-tetanic potentiation in m. BR, which also comprises higher percentage of type II fibres (Johnson et al., 1973). Higher post-tetanic potentiation in BR can be explained also with considering longer tendon, which gets even longer after several contractions. Maganaris (2002) reported tendon elongation (after several contractions) for 32 %. Gordon et al. (1988) studied amplitude potentiation for different muscle fibre types in isolated cat motor units. He observed longitudinal tetanic response to paused pulse-train of 240 sec and noticed as follows:

- Type I muscle fibres: no amplitude potentiation noticed, no fatigue symptoms;
- Type II muscle fibres:
    - Fatigue resistant fibres (FR): amplitude potentiated for 25 %, after 30 sec fatigue symptoms are present, after 240 sec amplitude is decreased to its primary value;
    - Intermediate fibres (FI): amplitude potentiated for 13 %, after 20 sec fatigue symptoms are present, after 240 sec amplitude is decreased to 35% of its primary value;
    - Fast fatiguing fibres (FF): amplitude potentiated for 20 %, after 10 sec fatigue symptoms are present, amplitude is decreased to zero after 180 sec.

5.6.2. Post-tetanic potentiation of twitch time parameters

Beside amplitude we observed potentiation also in time parameters of transverse and longitudinal twitch, which manifested in decreased time parameters. Statistically significant differences are marked in Table 4.8, where smaller coefficients indicate higher potentiation.

Muscle length impact on the degree of post-tetanic potentiation of time parameters is also presented in Table 4.8. The aforementioned impact is different for transverse and longitudinal response potentiation. Mela et al. (2001) reported shorter duration of post-tetanic longitudinal twitches in m. tibialis anterior, independently of ankle angle. We made similar observations in m. BB and m. BR.

Post-tetanic potentiation of longitudinal twitch was at first presented as a result of increased calcium release during contraction (Close, 1972b), however this should further lead to prolonged twitch relaxation (MacIntosh and Gardiner, 1987), which is in opposition to our measuring results and published results from Brown and Loeb (*in press*), Belanger and McComas (1985), Vandenboom and Houston (1996) and Vandervoort et al. (1983), which indicate significantly shorter relaxation time of transverse and longitudinal twitch of both muscles (Figure 4.28 and Table 4.8).

Thomas et al. (1999) presented post-tetanic potentiation of relaxation time in longitudinal MU twitch of 0.71. Our results revealed as follows: Tc_{TMG} potentiation in m. BB equalled 0.83, Tc_{torque} potentiation in m. BB equalled 0.86, Tc_{TMG} potentiation in m. BR equalled 0.86 and Tc_{torque} potentiation in m. BR equalled 0.94. Differences occurred due to different measuring methods: Thomas et al. (1999) applied intramuscular force measurement and selective stimulation of a single MU.

Post-tetanic potentiation of responses in toad gastrocnemius:
Post-tetanic potentiation of contractile parameters was observed during protocol B, measuring results are presented in Table 5.3. In transverse twitch (after protocol B) parameters Td and Tc decreased, parameters Ts and Tr increased. In longitudinal twitch time parameters increased, while the amplitude remains almost unchanged. These results support the hypothesis about the connection between potentiation and muscle fatigue. When stimulated with pulse-train (as in protocol B) isolated muscle is very sensitive to fatigue.

Response	Timing	Td / ms	Tc / ms	Ts / ms	Tr / ms	Dm
Displacement	Before	13.89	35.85	87.95	21.09	1.08 mm
	After	11.86	33.58	139.08	37.97	2.20 mm
Force	Before	13.00	33.65	67.75	19.54	0.91 N
	After	14.22	38.50	96.64	26.00	0.90 N

Tabela 5.3: Contractile parameters for toad GAST transverse and longitudinal twitches measured before and after protocol B.

5.7. *Muscle belly deformation*

Force-length and force-speed characteristics are well known indicators of mechanical functionality; still they describe only one dimension of muscle functioning. In order to study influences of contraction on muscle fibre length, connective tissue length and pennation angle, two-dimensional indicator is required (central muscle sagittal plane) (Gielen, 1998; Otten, 1988).

Zuurbier and Huijing (1993) reported 24 % diminishing of sagittal cross-section area in human m. gastrocnemius medialis during isometric contractions, still methods they used seem unreliable due to not enough surface markers, neglected cross-section curvature and muscle rotation (during contraction).

Van Bavel et al. (1996) took it up by measuring muscle belly thickening in muscle transverse plane during passive stretching. He reported muscle belly as well as aponeurosis thickening of about 6 %.

Scott and Loeb (1995) claimed that during thickening fascia circumference is enlarged, but no results was given. Van Bavel et al. (1998) observed the change of circumference in detail and reported maximal circumference diminishing at tendons and minimal at muscle belly.

Due to curvature in transverse direction, two-dimensional indicator dos not suffice, meaning a three-dimensional indicator is required (Huijing and Ettema, 1988/1989; Scott and Loeb, 1995; Van Bavel, 1996).

Changes in longitudinal dimensions have often been studied. These studies revealed changes in aponeurosis length between 1 and 5 % during isometric contractions (Huijing and Ettema, 1988/1989; Scott and Loeb, 1995). Zuurbier et al. (1994) demonstrated non-homogeneous stretch of distal aponeurosis - stretch of distal part was greater than of proximal part (of distal aponeurosis. Griffiths (1991), Van Bavel et al. (1998) and Van Donkelaar et al. (1999) claimed that during isometric contraction muscle fibre length is diminished by 15 %.

In general changes of longitudinal dimensions are lesser in connective tissue than in muscle fibres, due to lower elasticity of connective tissue. Therefore muscle belly thickening depends on connective tissue elasticity and consecutively on muscle length. This is accordant to our results: transverse twitch amplitudes were significantly higher in m. BB than in m. BR, which has longer and thinner tendon.

Van Donkelaar et al. (1999) reported human gastrocnemius medialis belly thickening of 4.8 % and thickening of its aponeurosis of 6.1 %. During isometric contraction muscle volume remains constant, cross-sectional area of muscle sagittal plane diminishes independently of muscle length, therefore changes in transverse muscle dimensions compensate for its shortening. Relationship between muscle transverse thickening (d_T) and longitudinal shortening (d_L) is linear: ($d_T = -0.98 \cdot d_L - 8.67$).

5.8. Modelling skeletal muscle responses

In previous chapters we presented mathematical models for quantitative description of muscle functioning. They were used to explain and improve understanding of definite mechanisms that influence muscle functioning. Such models are created on the basis of certain simplifications, but still sufficiently describe muscle properties.

5.8.1. Neural network modelling

On the basis of neural network we created a model for modelling relation between transverse muscle belly deformation and longitudinal twitch. We intended to identify the connection between both transverse and longitudinal "deformation" and then verify the model with responses of other muscles.

The network architecture was able to learn the rules of connection between toads GAST belly displacement and force (Figure 4.30a). However, these rules were to specific to be successfully applied, which is evident from fittings presented in Figures 4.30b, c and d.

The abovementioned indicates there probably are many parameters affecting relation between transverse and longitudinal response. Muscle preparation, measuring conditions, sensors positioning – all this has to be carefully prepared, especially in smaller muscles. Relation between both responses depends on muscle architecture, elastic properties of connective tissue and fascias and other geometrical factors such as muscle length and rotation, measuring point etc.

5.8.2. Geometrical modelling

All disadvantages mentioned in chapter 5.8.1 directed us towards other types of models. We selected the toad GAST and created a respective geometrical model. We used this model to identify relation between transverse muscle belly displacement and longitudinal tendon elongation.

We used a mathematical function (Equation 4.2) to describe rotational ellipsoid (Figure 4.32), which was satisfactory in describing muscle geometry. It was dimensioned in order to describe geometrical changes during contraction at the constant muscle volume. Model fitting was verified with isometric as well as isotonic contraction (Table 4.11).

Knez (2000) suggested creating a model on the basis of cylindrical shape, however this shape does not correspond to dynamics of muscle transverse thickening and longitudinal shortening, monitored during contraction.

Our geometrical model revealed linear relationship between transverse thickening and longitudinal shortening of muscle belly, which is in accordance with findings by Van Donkelaar et al. (1999), who monitored muscle belly geometrical changes with high-frequency camera.

5.8.3. Modelling tendon passive characteristic

In toad GAST we observed the longitudinal twitch: for muscle-tendon complex this twitch was of shorter duration and faster relaxation than for the muscle with removed tendon, which resulted in a hysteresis when transverse and longitudinal twitch dynamics were presented in the same (Figures 4.33d and 4.35).

We employed mechanical model to find appropriate transient-function for SE, of which the main part is represented by tendon. Through tendon longitudinal shortening is transformed into measured force response at the tendon ending. Further, SE transient-functions were compared for muscle-tendon complex and muscle without tendon. Comparison revealed that in case of muscle-tendon complex SE transient-function consists of two transient-functions – one representing longitudinal elongation and the other tendon longitudinal shortening (Figure 4.37).

Our findings correspond with findings by Maganaris et al. (2000 in 2002), which obtained similar results with ultrasonic measurements.

The same procedure could have been used for investigating tetanic responses in toad GAST (Figure 4.34), but appearance of potentiation and fatigue, which implement different patterns of responding to electrical stimulation (such as hysteresis as presented in Figure 4.35), helped us decide for modelling twitch response only.

In order to investigate human muscle, a far more complex model would be required to include other mechanical parameters such as joint mechanics, limb torque and own frequency, changes in join axes during contraction, skin fold etc.

5.8.4. Modelling responses of type I and type II muscle fibres

Knez (2000) presented a model of muscle contraction based on calcium input. The model employed type I and type II muscle fibres contractile properties and their combined responses, which was performed by creating separate model for calcium release (from SR) and afterwards type I and type II fibres force exertion.

The peak, typical of twitch responses with short Tc_{TMG}, was explained with modelling transverse force of both muscle fibre types (Figure 4.38). Savelberg (2000) came to same conclusion: peak appears in muscles with higher percentage of fast MUs. In his model he included longitudinal twitches of isolated fibres, but no connective tissue mechanics.

Data on calcium release from SR for type I and type II muscle fibres and data on contractile properties of isolated type I and type II muscle fibres were taken from literature (Wetzel and Gros, 1998; Sica and McComas, 1971). We presupposed the equality of transverse and longitudinal twitch dynamics. This presumption is based on equality of elasticity coefficients in transverse and longitudinal direction in isolated fibre. On the basis of findings by Van Donkelaar et al. (1999) similar presumption was made for damping coefficient in isolated fibre. Van Donkelaar et al. (1999) performed measurements of muscle contraction dynamics and demonstrated linear relationship between changes of longitudinal and transverse muscle belly dimensions.

If muscle fibre is presented with a cylinder of length “l” and radius “p”, then they are related as follows: $\frac{p^2}{p_s^2} = \frac{l_s}{l^2}$. Index “s” stands for contracted fibre (Knez, 2000).

The difference between “p” and “p_S” corresponds with increased muscle belly displacement. For the radii of two fibres “p_1” and “p_2” following can be noted: $\frac{p_1}{p_2} = \frac{p_{1S}}{p_{2S}}$, for this ratio remains unchanged also during contraction. This indicates that irrespective of relaxed or contracted muscle fibres, diameter of type II muscle fibres always remains 20 % bigger than diameter of type I muscle fibres (Knez, 2000; Johnson et al., 1973).

Histochemical analyses on m. BB and m. BR composition have been performed in the past (Johnson et al., 1973; Dahmane et al., 2000) so data on muscle fibre type percentage were taken from literature (Table 4.2).

We created transient-function of connective tissue for transverse and longitudinal direction, which transforms transverse and longitudinal muscle belly twitch into measured transverse and longitudinal twitch of muscle-tendon complex, respectively. Further it was noticed that damping in longitudinal direction affects exerted torque to a much greater extent than damping in transverse direction. In spite of the fact that connective tissue damping coefficient differs for different muscles as well as different subject it can be concluded that damping coefficient in longitudinal direction exceeds that in transverse direction by 2.2 – 6.5 times.

Damping coefficient includes connective tissue damping as well as the entire mechanics of elbow joint. Along with this following question arises: how about the damping or elasticity inside the muscle belly (in transverse and longitudinal direction)? Muscle belly elasticity coefficient in longitudinal direction almost equals tendon elasticity coefficient, which was demonstrated also in toad GAST: during fused tetanus muscle belly was shortened by 8.5 % while tendon was elongated by 10.5. As well as the tendon muscle fibres also comprise collagen – on one hand tendon comprises higher percentage of collagen, on the other hand muscle belly is a wider structure. Comparing transverse and longitudinal twitch of toad GAST did not reveal any significant correlation between transverse and longitudinal damping coefficient neither for connective tissue nor muscle-tendon complex.

Sometimes peak in transverse twitches is not so well defined. The reason might be damping effect of the fascia (for instance in m. tibialis anterior), coactivation of underlying muscle or higher percentage of type I muscle fibres comprised in measured muscle. The peak of longitudinal twitch is usually flattened (or smoothened) by elasticity coefficient and connective tissue damping in longitudinal direction and with sliding against surrounding tissue, so that *in vivo* measurements almost never reveal it.

6. Conclusion

In this thesis transverse and longitudinal twitch and tetanic responses were analysed using tensiomyographic and torque measuring method, respectively. Mathematical models were applied to demonstrate relationship between measuring results obtained by one single method and between measuring results of both methods.

Responses were measured in muscles of different muscle fibre composition, but the same muscle architecture. This enabled us to define influences of separate elements (tendon dimensions, muscle fibre composition, position of muscle insertio and origo) on measured responses.

Finally, conclusions were made on the basis of comparative measurements on isolated muscles. Transverse and longitudinal deformations were modelled with geometrical model; to investigate relation between transverse and longitudinal response mechanical model was used.

Authentic contributions and findings:

- **Determination of optimal muscle length**

Optimal muscle length is defined with respect to stiffness measurement and achieving maximal muscle force. So-far defining optimal muscle length was always accompanied by certain difficulties originating mainly from muscle stiffness. Torque measurement of electrically evoked longitudinal responses enabled optimal length estimation, still measuring results reflect high variability, which makes such estimations unreliable. Therefore, TMG displacement sensor was upgraded in sense of mechanical stiffness detection – it detects stiffness of muscle belly in transverse direction. This upgrade enables us to provide relevant estimations on optimal muscle length.

- **Determination of twitch-tetanus ratio**

Methods that can be applied for measuring mechanical parameters of tetanic responses are either invasive or of high variability. We recorded displacement-frequency and torque-frequency characteristics, analysed their elbow angle dependencies and thus determined twitch-tetanus ratio for both measured muscles – m. biceps brachii and m. brachioradialis. We showed that this ratio depends on both – elbow angle and stimulation amplitude. Tensiomyographic method proved suitable for detecting activation characteristics of muscle contraction; selective sensor positioning (directly on/over muscle belly) classifies this method adequate for detecting tetanic responses, especially to pulse-trains of physiological frequencies.

- **Determination of post-tetanic potentiation**

Because of certain disadvantages of non-invasive methods (when measuring time parameters of muscle contraction), so far only longitudinal twitch amplitude was used for measuring the degree of potentiation. It happened rarely that also half-relaxation time was observed. We showed that the degree of potentiation depends on joint angle and that beside aforementioned amplitude and half-relaxation time there are other time parameters of transverse muscle belly twitch, which indicate the degree of potentiation.

- **Skeletal muscle geometrical model and identification of damping coefficient in connective tissue model**

In order to investigate how transverse muscle belly twitch and longitudinal force twitch are connected the use of geometrical model was suggested. It was defined on the basis of measurements on isolated toad gastrocnemius. Complementing geometrical muscle model with mechanical tendon model resulted in two different passive transient functions – one for tendon elongation and the other for its shortening. Considering this we interpreted the connection between longitudinal twitch of muscle-tendon complex and transverse muscle belly twitch: connective tissue damping coefficient is statistically bigger than coefficient in transverse direction.

7. References

Akataki, K., Mita, K., Itoh, Y. (1999). Repeatability study of mechanomyography in submaximal isometric contractions using coefficient of variation and interclass correlation coefficient. Electrom and Clin Neurophysiol, 39(3), 161-166.

Akataki, K., Mita, K., Watakabe, M., Itoh, K. (2001). Mechanomyogram and force relationship during voluntary isometric ramp contractions of the biceps brachii muscle. Europ J Appl Physiol, 84(1-2), 19-25.

Alexander, R.M. (1988). Elastic mechanisms in animal movement. Cambridge University Press, Cambridge.

Allen, D.G., Lee, J.A., Westerblad, H. (1989). Intracellular calcium and tension during fatigue in isolated single muscle fibres from Xenopus laevis. J Physiol, 415, 433-458.

Amis, A.A., Dowson, D., Wright, V. (1979). Muscle strength and musculo-skeletal geometry of the upper limb. Engineering in Medicine, 8, 41-47.

An, K.N., Hui, F.C., Morrey, B.F., Linscheid, R.L., Chao, E.Y. (1981). Muscles across the elbow joint: a biomechanical analysis. J Biomech, 14, 659-669.

An, K.N., Takahashi, K., Herigan, T.P., Chao, E.Y. (1984a). Determination of muscle orientations and moment arms. J Biomech Engineering, 106, 280-282.

An, K.N., Kwak, B.M., Chao, E.Y., Morrey, B.F. (1984b). Determination of muscle and joint forces: A new technique to solve the indeterminate problem. J Biomech Engineering, 106, 364-367.

Anderson, P., Sears, T.A. (1964). The mechanical properties and innervation of fast and slow motor units in the intercostal muscles of he cat. J Physiol (London), 173, 114-129.

Asmussen, E., Hansen, D., Lammert, O. (1965). The relation between isometric and dynamic muscle strength in man. Commun. Testing Observation Inst. Danish Natl. Assoc. Infantile Paralysis, 20.

Aukland, M., Reed, R.K. (1993). Interstitial-lymphatic mechanisms in the control of extra cellular fluid volume. Physiol Rev, 73, 1-78.

Bajd, T. (1996) Nihajni test spastičnosti. V Gregorič, M. (ur.). Klinična neurofiziologija I kineziologija v rehabilitaciji. 1. izd. Ljubljana, 215-221.

Balnave, C.D., Allen, D.G. (1996). The effect of muscle length on intracellular calcium an force in single fibres from mouse skeletal muscle. J Physiol (London), 492(3), 705-713.

Banus, M.G., Zetlin, A.M. (1938). The relation of isometric tension to length in skeletal muscle. J Cellular Compar Physiol, 12(3), 403-420.

Baratta, R.V., Solomonov, M., Zhou, B.H., Zhu, M. (1998). Methods to reduce the variability of EMG power spectrum estimates. J Electrom and Kinesiol, 8, 279-285.

Bárány, M. (1967). ATPase activity of myosin correlated with speed of muscle shortening. J General Physiol, 50, 197-218.

Barry, D.T., Geiringer, S.R., Ball, R.D. (1985). Acoustic myography: a noninvasive monitor of motor unit fatigue. Muscle & Nerve, 189-194.

Barry, D.T. (1987). Acoustic signals from frog skeletal muscle. Biophys J, 51, 769-773.

Barry, D.T., Gordon, K.E., Hinton, G.G. (1990). Acoustic and surface EMG diagnosis of pediatric muscle disease. Muscle & Nerve, 13, 286-290.

Barry, D.T. (1992). Vibrations and sounds evoked from muscle twitches. Electrom and Clin Neurophysiol, 32, 35-40.

Barry, D.T., Hill, T., Dukjin, I. (1992). Muscle fatigue measured with evoked muscle vibrations. Muscle & Nerve, 15, 303-309.

Baskin, R.J., Paolini, P.J. (1967). Volume change and pressure development in muscle during contraction. Am J Physiol, 213, 1025-1030.

Bawa, P., Calancie, B. (1983). Repetitive "doublet"s in human flexor carpi radialis muscle. J Physiol (London), 339, 123-132.

Belanger, A.Y., McComas A.J., Elder, G.B. (1983). Physiological properties of two antagonist human muscle groups. Eur J Appl Physiol, 51(3), 381-393.

Belanger, A.Y., McComas, A.J. (1985). A comparison of contractile properties in human arm and leg muscles. Eur J Appl Physiol, 54(3), 326-330.

Bellemare, F., Woods, J.J., Johansson, R.S., Bigland – Ritchie, B. (1983). Motor-unit discharge rates in maximal voluntary contractions of three human muscles. J Neurophysiol, 50, 1380-1392.

Benko, H., Štefančič, M., Obreza, P., Bajd, T., Karčnik, T., Šavrin, R. (1998). Hoja tetraplegičnih bolnikov s pomočjo FES. V Rehabilitation bei hoher Querschnittlähmung. Zaključno poročilo. Wien: Allgemeine Unfallversicherungsanstalt, 169-172.

Bennet, D.J., Gorassini, M., Prochazka, A. (1994). Catching a ball: contributions of intrinsic muscle stiffness, reflexes and high order responses. Canad J Physiol and Pharmacol, 72, 525-534.

Bernardi, M., Solomonow, M., Nguyen, G., Baratta, R. (1996). Motor unit recruitment strategy changes with skill acquisition. Eur J Appl Physiol, 74, 52-59.

Bernhard, C.G., Von Euler, U.S., Skoglund, C.R. (1941). Post-tetanic action potentials in mammalian muscle. Acta Physiol Scand 2, 284-288.

Bewick, G.S., Zammit, P.S., Tonge, D.A. (1993). Restoration of motor unit properties and fibre type distribution in reinnervated axolotl skeletal muscle. Develop Biol, 158(2), 288-300.

Biewener, A.A. (1998). Muscle function in vivo: A comparison of muscle used as springs for elastic energy savings versus muscle used to generate mechanical power. Am Zool, 38, 703-717.

Bigland, B., Lippold, O.C.J. (1954a). The relation between force velocity and integrated electrical activity in human muscles. J Physiol (London), 123, 214-224.

Bigland, B., Lippold, O.C.J. (1954b). Motor unit activity in the voluntary contraction of human muscle. J Physiol (London), 125, 322-335.

Bilodeau, M., Arsenault, A.B., Gravel, D., Bourbonnais, D. (1990). The influence of an increase in the level of force on the EMG power spectrum of elbow extensors. Eur J Appl Physiol, 61, 461-466.

Bilodeau, M., Cincera, M., Gervais, S., Arsenault, A.B., Gravel, D., Lepage, Y., McKinley, P. (1995). Changes in the electromyographic power spectrum caused by a progressive increase in the force level. Eur J Appl Physiol, 71, 113-123.

Bilodeau, M., Houck, J., Cuddeford, T., Sharma, S., Riley, N. (2002). Variations in the relationship between the frequency content of EMG signals and the rate of torque development in voluntary and elicited contractions. J Electrom and Kinesiol, 12, 137-145.

Bobbert, M.F., Huijing, P.A., Van Ingen Schenau, G.J. (1986). A model of human triceps surae muscle-tendon complex applied to jumping. J Biomech, 19, 887-898.

Bobbert, M.F., Van Zatwijk, J.P. (1994). Dependence of human maximal jump height on moment arms of the biarticular m. gastrocnemius; a simulation study. Human Mov Sci, 13, 696-716.

Bodine, S.C., R.R., Eldred, E., Edgerton, V.R. (1987). Maximal force as a function of anatomical features of motor units in the cat tibialis anterior. J Neurophysiol, 57, 1730-1745.

Botterman, B.R., Iwamoto, G.A., Gonyea, W.J. (1986). Gradation of isometric tension by different activation rates in motor units of cat flexor carpi radialis muscle. J Neurophysiol, 56, 494-506.

Botterman, B.R., Cope, T.C. (1988). Motor-unit stimulation patterns during fatiguing contractions of constant tension. J Neurophysiol, 60, 1198-1214.

Bowman, W.C., Goldberg, A.A., Raper, C. (1962). A comparison between the effect of a tetanus and the effects of sympathomimetics amines on fast. and slow-contracting skeletal muscles. J. Pharmacol. 19, 464-484.

Brown, G.L., Von Euler, U.S. (1938). The aftereffects of a tetanus on mammalian muscle. J Physiol (London) 93, 39-60.

Brown, I.E., Loeb, G.E. (1998). Post-activation potentiation: a clue for simplifying models of muscle dynamics. Am Zool, 38, 743-754.

Brown, I.E., Loeb, G.E. (*in press*). Measured and modeled properties of mammalian muscle. The effects of post activation potentiation on the time course and velocity dependencies of force production. J Muscle Res Cell Motil.

Buchthal, F., Lindhard, J. (1939). The physiology of striated muscle fibre. Det Kgl. Danske Videnskabernes Selskab. Biologiske Meddelelser XIV, 6. Kobenhaven Ejnar Munksgaard.

Buchthal, F. (1942). The mechanical properties of the single striated muscle fibre at rest and during contraction and their structural interpretation. Det Kgl. Danske Videnskabernes Selskab. Biologiske Meddelelser XVIII, 2. Kobenhaven Ejnar Munksgaard.

Buchthal, F., Kaiser, E. (1951). The rheology of the cross striated muscle fibre with particular reference to isotonic conditions. Det Kgl. Danske Videnskabernes Selskab. Biologiske Meddelelser XXI, 7. Kobenhaven Ejnar Munksgaard.

Buchtal, F., Schmalbruch, H. (1981). Contraction times and fibre types in intact human muscle. Acta Physiol Scand, 79, 435-452.

Buller, A.J., Lewis, D.M. (1965). The rate of tension development in isometric tetanic contractions of mammalian fast and slow skeletal muscle. J Physio. (London) 176, 337-354.

Buller, A.J., Dornhorst, A.C., Edwards, R., Kerr, D., Whelan, R.F. (1959). Fast and slow muscles in mammals. Nature (London), 183, 1516-1517.

Burke, R.E. (1967). Motor unit types of cat triceps surae muscle. J Physiol (London), 193, 141-160.

Burke, R.E., Levine, D.N., Zajac III, F.E., Tsairis, Engel, W.K. (1971). Mammalian motor units: physiological-histochemical correlation in three types in cat gastrocnemius. Science 174, 709-712.

Burke, R.E., Tsairis, P. (1973). Anatomy and innervation ratios in motor units of cat gastrocnemius. J Physiol (London) 234, 749-765.

Burke, R.E., Levine, D.N., Tsairis, P., Zajac III, F.E. (1973). Physiological types and histochemical profiles in motor units of the cat gastrocnemius. J Physiol (London) 234, 723-748.

Burke, R.E., Rudomin, P., Zajac III, F.E. (1976). The effect of activation history on tension production by individual muscle units. Brain Res, 109, 515-529.

Butler, D.L., Goods, E.S., Noyes, F.R., Zernicke, R.F. (1978). Biomechanics of ligaments and tendons. Exerc Sports Sci Rev, 6, 125-181.

Bülow, P.M., Norregaard, J., Danneskoild-Samsøe, B., Mehlsen, J. (1993). Twitch interpolation technique in testing of maximal muscle strength: influence of potentiation, force level, stimulus intensity, and preload. Eur J Appl Physiol Occup Physiol, 67, 462-467.

Bülow, P.M., Norregaard, J., Danneskoild-Samsøe, B., Mehlsen, J. (1995). The twitch interpolation technique for study of human quadriceps muscle. J Neurosci Meth, 62, 103-109.

Calvert, T.W., Chapman, A.E. (1977). Relationship between the surface EMG and force transients in muscle: Simulation and experimental studies. Proceedings of the IEEE, 65, 682-689.

Canaday, P.G., Fay, F.S. (1976). An ultrasensitive isometric force transducer for single smooth muscle cell mechanics. J Appl Physiol, 40, 243-246.

Chang, Y.W., Su, F.C., Wu, H.W., An, K.N. (1999). Optimum length of muscle contraction. Clin Biomech, 14, 537-542.

Charles, T., Leonard, P.T., Jennifer, U., Stephens, P.T., Sheri, L., Stroppel, P.T. (2001). Assessing the spastic condition of individuals with upper motoneuron involvent: validity of the mytonometer. Arch Phys Med Rehabil, 82, 1416-1420.

Cinderby, C.A., Comtois, A.S., Thomson, R.G., Grassino, A.E. (1996). Influence of the bipolar electrode transfer on the electromyogram power spectrum. Muscle & Nerve, 19, 290-301.

Clarkson, P.M., Kroll, W., Melchionda, A.M. (1981). Age, isometric strength, rate of tension development, and fibre type composition. J Gerontol, 36, 648-653.

Close, R.I. (1972a). Dynamic properties of mammalian skeletal muscle. Physiol Rev 52, 129-197.

Close, R.I. (1972b). The relations between sarcomere length and characteristics of isometric twitch contractions of frog sartorius muscle. J Physiol (London), 220(3), 745-762.

Corcos, D.M:, Jaric, S., Agarwal, G.C., Gottlieb, G.L. (1993). Principles for learning single joint movement. I. Enhanced performance by practice. Exp Brain Res, 94, 499-513.

Dahmane, R. (1997). Tipi mišičnih vlaken v skeletni mišici. Proteus, 60(3), 118-121.

Dahmane, R., Valenčič, V., Knez N., Eržen, I. (2000). Evaluation of the ability to make non-invasive estimation of muscle contractile properties on the basis of the muscle belly response. Med Biol Eng Comput, 39, 51-55.

Dahmane, R., Valenčič, V., Šimunić. B. (in press). Spatial fibre type distribution in normal human muscle: histochemical and tensiomyographical evaluation. Muscle & Nerve.

Dalton, P.A., Stokes, M.J. (1993). Frequency of acoustic myography during isometric contraction of fresh and fatigued muscle and during dynamic contractions. Muscle & Nerve, 16, 255-261.

Daminai, E., Margreth, A. (1994).Characterization study of the ryanodine receptor and of calsequestrin isoforms of mammalian skeletal muscles in relation to fibre types. J Muscle Res Cell Motil, 15, 86-101.

Darling, V.G., Cooke, J.D. (1987). Movement related EMGs become more variable during learning of fast accurate movements. J Motor Behav, 19, 311-331.

Day, J.W., Sakamoto, C., Parry, G.J., Lehmann-Horn, F., Iazzio, P.A. (2002). Force assessment in periodic paralysis after electrical muscle stimulation. Mayo Clinic Proceedings, 77(3), 232-240.

De Luca C.J., Foley P.J., Erim Z. (1996). Motor unit control properties in constant force isometric contractions. J Neuropshysiol; 76, 1503-1516.

De Luca, C.J., LeFever, R.S., McCue, M.P., Xenakis, A.P. (1982). Behavior of human motor units in different muscles during linearly varying contractions. J Physiol, 329, 113-128.

Delp, S.L., Loan, J.P. (1995). A graphic-based software system to develop and analyze models of musculoskeletal structures. Comp Biol Med, 25, 21-34.

Desmedt, J.E. (1967). The isometric twitch of human muscle in the normal and the dystrophic states. In Rxploratory Concepts in Muscular Dystrophy and Related Disorders, Edited by Milhorat, A.T., Amsterdam, 224-231

Desmedt, J.E., Godaux, E. (1977). Ballistic contractions in man: characteristic recruitment pattern of single motor units of the tibialis anterior muscle. J Physiol (London), 264, 673-693.

Desmedt, J.E., Godaux, E. (1978). Ballistic contractions in fast or slow human muscles: discharge patterns of single motor units. J Physiol, 285, 185-196.

Dimitrov, G.V., Dimitrova, N.A. (1998). Fundamentals of power spectra extracellular potentials produced by skeletal muscle fibre of finite length. Part II: Effect of parameters altering with functional state. Med Eng Phys, 20, 702-707.

Dimitrova, N.A., Dimitrov, G.V., Lateva, Z.C. (1991). Influence of the fibre length on the power spectrum of single fibre extracellular potentials. Electromyogr Clin Neurophysiol, 31, 387-398.

Dimitrova, N.A., Dimitrov, G.V., Nikitin, O.A. (2001). Longitudinal variations of characteristics frequencies of skeletal muscle fibre potentials detected by a bipolar electrode or multi-electrode. J Med Eng Techn, 25, 34-40.

Djordjevič, S., Valenčič, V., Godina, N., Jurčič-Zlobec, B. (1998). The comparison of dynamic characteristics of skeletal muscles in two groups of sprtsmen – sprinters and cyclists. Proceedings of 6th Vienna International Workshop on Functional Electrostymulation, 181-184.

Duchateau, J. Hainaut, K. (1986). Nonlinear summation of contractions in striated muscle. I. Twitch potentiation in human muscle. J Muscle Res Cell Motil, 7(1), 11-17.

Edgerton, V.R., Apor, P., Roy, R.R. (1990). Specific tension of human elbow flexor muscles. Acta Physiol Hun, 75, 205-216.

Edman, K.A.P., Reggiani, C., Schiaffino, S., Te Kronnie, G. (1988). Maximum velocity of shortening related to myosin isoform composition in frog skeletal muscle fibres. J Physiol, 95, 679-694.

Eisenberg, B.R., Kuda, A.M. (1977). Retrieval of cryostat sections for comparison of histochemistry and quantitative electron microscopy in a muscle fibre. J Histochem Cytochem 25, 1169-1177.

Elder, G.C.B., Bradbury, K., Roberts, R. (1982). Variability of fibre type distributions within human muscles. J Appl Physiol, 53(6),1473-1480.

Enoka, R.M. (2002). Neuromechanics of human movement. Human Kinetics, 3rd edition.

Erfanian, A., Chizeck, H.J., Hashemi, R.M. (1998). Using evoked EMG as a synthetic force sensor of isometric electrically stimulated muscle. IEEE Trans Biomed Eng, 45(2), 188-202.

Evans, C.L., Hill, A.V. (1914). The relation of length to tension development and heat production on contraction in muscle. J Physiol, 49, 10-16.

Farina, D., Merletti, R., Rainoldi, A., Buonocore, M., Casale, R. (1999). Two methods for the measurement of voluntary contraction torque in the biceps brachii muscle. Med Eng Phys, 21, 533-540.

Farina, D., Merletti, R., Nazzaro, M., Caruso, I. (2001). Effect of joint angle on EMG variables in leg and thigh muscles, IEEE Eng Med Biol Mag, 20, 62-71.

Farina, D., Madeline, T., Graven-Nielsen, T., Merletti, R., Arent-Nielsen, L. (2002). Standardising surface electromyogram recordings for assessment of activity and fatigue in the human upper trapezius muscle. Eur J Appl Physiol, 86, 469-478.

Faszczewski, A., Kędzior, K., Rzymkowski, C. (1994). Modeling of muscles co-operation under dynamic condition. Second World Congress of Biomechanics, I-179a, Amsterdam.

Fearn, L.A., Bartoo, M.L., Myers, J.A., Pollack, G.H. (1993). An optical fibre transducer for single myofibril force measurement. IEEE Trans Biomed Eng, 40(11), 1127-1132.

Fleckenstein, J.R., Shellock, F.G. (1991). Exertional muscle injuries: magnetic resonance imaging evaluation. Topics in Magnetic Resonance Imaging, 3, 50-70.

Ford, L.E., Huxley, A.F., Simmons, R.M. (1986). Tension transients during the rise of tetanic tension in frog muscle fibres. J Physiol (London), 372, 595-609.

Fowler, E.G., Gregor, R.J., Hodgson, J.A., Roy, R.R. (1993). Relationship between ankle muscle and joint kinetics during the stance phase of locomotion in the cat. J Biomech 26, 465-483.

Frangioni, J.V., Kwan-Gett, T.S., Dobrunz, L.E., McMahon, T.A. (1987). The mechanism of low-frequency sound production in muscle. Biophys J, 51, 775-783.

Freund, H.J., Büdingen, H.J., Dietz, V. (1975). Activity of single motor units from human forearm muscles during voluntary isometric contractions. J Neurophysiol, 38, 933-946.

Friederich, J.A., Brand, R.A. (1990). Muscle fibre architecture in the human lower limb. J Biomech, 23, 91-95.

Fuglevand, A.J., Macefield, V.G., Bigland-Ritchie, B. (1999). Force-frequency and fatigue properties of motor units in muscles that control digits of the human hand. J Neurophysiol, 81, 1718-1729.

Fukunaga, T., Roy, R.R., Shellock, F.G., Hodgson, J.A., Edgerton, V.R. (1996). Specific tension of human plantarfelxors and dorsiflexors. J Appl Physiol, 80, 158-165.

Fukunaga, T., Miyatami, M., Tachi, M., Kouzaki, M., Kawakami, Y., Kanehisha, H. (2001). Muscle volume is a major determinant of joint torque in humans. Acta Physiol Scand, 172(4), 249-255.

Gabriel, D.A. (2000). Reliability of SEMG spike parameters during concentric contractions. Electromyogr Clin Neurophysiol, 40, 423-430.

Gabriel, D.A. (2002). Changes in kinematic and EMG variability while practicing a maximal performance task. J Electromyogr Kinesiol, 12, 407-412.

Gans, C., Bock, W.J. (1965). The functional significance of muscle architecture: a functional analysis. Ergebnisse der Anatomie und Entwicklungsgeschichte, 38, 115-142.

Gatton, M.L., Pearcy, M.J., Pettet, G.J. (1999). Difficulties in estimating muscle forces from muscle cross-sectional area. An example using the psoas major muscle. Spine, 24(14), 1487-1493.

Gerbeaux, M., Turpin, E., Lensel-Corbeil, G. (1996). Musculo-articular modeling of the triceps brachii. J Biomech, 29, 171-180.

Gerdler,R.A., Robbins, N. (1978). Differences in neuromuscular transmission in red and white muscles. Brain Res, 142, 160-164.

Gerdle, D.A., Wretling, M.L., Heriksson-Larsen, K. (1988). Do the fibre type proportion and the angular velocity influence the mean power frequency of the electromyogram? Acta Physiol Scand, 134, 341-346.

Gerdle, B., Henriksson-Larsen, K., Lorentzon, R. (1991). Dependence of the mean power frequency of the electromyogram on muscle force and fibre type. Acta Physiol Scand, 142, 457-465.

Gerdle, B., Henriksson-Larsen, K., Lorentzon, R., Wretling, M.L. (1991). Dependence of the mean power frequency of the electromyogram on muscle force and fibre type. Acta physiol Scand, 142, 457-465.

Gerdle, B., Karlsson, S. (1994). The mean frequency of the EMG of the knee extensors is torque dependent both in the unfatigued and fatigued states. Clin Physiol, 14, 419-432.

Gerdle, B., Karlsson, S., Crenshaw, A.G., Fridén, J. (1997). The relationships between EMG and muscle morphology throughout sustained static knee extension at two submaximal force levels. Acta Physiol Scand, 160, 341-351.

Gerdle, B., Karlsson, S., Crenshaw, A.G., Elert, J., Fridén, J. (2000) The influences of muscle fibre proportions and areas upon EMG during maximal dynamic knee extensions. Eur J Appl Physiol, 81, 2-10.

Gielen, A.W.J. (1998). A continuum approach to the mechanics of contracting skeletal muscle. Ph.D. Thesis. University Press Facilities, Eindhoven.

Glerum, J.J., Van Mastrigt, R. (1990). Mechanical properties of mammalian single smooth muscle cells I. A low cost large range microforce transducer. J Musc Res Cell Mot, 11, 331-337.

Gordon, A.M., Huxley, A.F., Julian, F.J. (1966). The variation in isometric tension with sarcomere length in vertebrate muscle fibres. J Physiol (London), 184, 170-192.

Gordon, D.A. (1988). Analysis of force parameters used to assess the fatigability of mammalian motor units. Ph.D. dissertation. University of Arizona. Tuecson. AZ. USA.

Gordon, D.A., Enoka, R.M., Stuart, D.G. (1990). Motor-unit force potentiation in adult cats during a standard fatigue test. J Physiol (London), 421, 569-582.

Gonzales, R.V., Buchanan, T.S., Delp, S.L. (1997). How much muscle architecture and moment arms affect wrist flexion-extension moments. J Biomech, 30, 705-712.

Gonyea, W.J., Marushia, S.A., Dixon, J.A. (1981). Morphological organization and contractile properties of the wrist flexor muscles in the cat. Anatom Rec, 199(3), 321-339.

Greger, R., Windhorst, U. (1996). Comprehensive human physiology: from cellular mechanisms to integration. Volume 1, Springer – Verlag, Berlin, Heidelberg, Germany.

Griffiths, R.I. (1991). Shortening of muscle fibres during stretch of the active cat medialis gastrocnemius: the role of tendon compliance. J Physiol, 436, 219-236.

Guyton, A.C. (1976). Textbook of medical physiology. 9th edition, W.B. sounders company, Philadelphia, USA.

Gydikov, A.A., Kosarov, D. (1974). Some features of different motor units in human biceps brachii. Pflűgers Archiv, 347, 75-88.

Hagg, G.M. (1992). Interpretation of EMG spectral alterations and alteration indexes at sustained contraction. J Appl Physiol, 73, 1211-1217.

Hagberg, C., Eriksson, N., Gerdle, B., Hagberg, M., Johnson, B. (1987). Frequency analysis of EMG activity of muscles with different fibre type composition. Proceedings of the International Society of Biomechanics, 112.

Hamada, T. Sale, D., MacDougall, J.D., Tarnopolsky, M.A. (2000). Postactivation potentiation, fibre type and twitch contraction time in human knee extensor muscles. J Appl Physiol, 88(6), 2131-2137.

Hanchard, N.C., Williamson, M., Caley, R.W., Cooper, R.G. (1998). Electrical stimulation of human tibialis anterior: (A) contractile properties are stable over a range of submaximal voltages; (B) high- and low-frequency fatigue are inducible and reliably assessable at submaximal voltages. Clin Rehabil, 12(5), 413–27.

Hargens, A.R., Sejersted, O.M., Kardel, K.R., Blom, P., Hermansen, L. (1982). Intramuscular fluid pressure: a function of contraction force and tissue depth. Proceedings of 28th Annual Meeting of the Orthopedic Research Society, New Orleans.

Hasan, Z., Enoka, R.M. (1985). Isometric torque-angle relationship and movement-related activity of human elbow flexors: Implications for the equilibrium-point hypothesis. Exp Brain Res, 59, 441-450.

Hatze, H. (1981). Myocybernetic control models of skeletal muscle. University of South Africa Press, Pretoria.

Henneman E., 1980. Skeletal muscle: the servant of the nervous system. In: Mountcastle VB, editor. Med Physiol, 14, 674-702.

Herzog, W., Leonard, T.R. (1991). Validation of optimization models that estimate the forces exerted by synergistic muscles. J Biomech, 10, 529-539.

Herzog, W., Kamal, S., Clarke, H.D. (1992a). Myofilament lengths of cat skeletal muscle: theoretical considerations and functional demands of cat gastrocnemius, soleus and plantaris muscles. J Biomech, 25, 945-948.

Herzog, W., Leonard, T.R., Renaud, J.M., Wallace, J., Chaki, G., Bornemisza, S. (1992b). Force-length properties and functional demands of cat gastrocnemius, soleus and plantaris muscles. J Biomech, 25, 1329-1335.

Hill, A.V. (1938). The heat of shortening and the dynamic constants of muscle. Proc Roy Soc, 126, 136-195.

Hill, A.V. (1949). The abrupt transition from rest to activity in muscle. Proc Soc (London), B 136, 399-420.

Hill, A.V. (1953). The plateau of full activity during a muscle twitch. Proc Soc (London), B 141, 498-503.

Hill, A.V. (1970). First and last experiments in muscle mechanics. Cambridge University Press, Cambridge.

Hogan, N. (1990). Mechanical impedance of single and multi-articular systems. In: Winters, J., Woo, S. (Eds.), Mult Muscle Sys. Springer, New York, 149-164.

Hoyle, G. (1983). Muscles and their neural control. New York: Wiley.

Huijing, P.A., Ettema, G.J.C. (1988/1989). Length-force characteristics of aponeurosis in passive muscle and during isometric and slow dynamic contractions of rat gastrocnemius muscle. Acta Morphol Neerlando-Scand, 26, 51-62.

Huijing, P.A. (1998). Muscle, the motor of movement: properties in function, experiment and modeling. J Electromyogr Kinesiol, 8(2), 61-77.

Huijing, P.A. (1999). Muscle as a collagen fibre reinforced composite material: force transmission in muscle and whole limbs. J Biomech, 32, 329-345.

Huijing, P.A., Baan, G.C. (2001). Extramuscular myofascial force transmission within the rat anterior tibial compartment: proximo-distal differences in muscle force.

Hutchins, E.L., Gonzales, R.V., Barr, R.E. (1993). Comparison of experimental and analytical torque-angle relationship of the human elbow joint complex. Biomed Sci Instrument, 29, 17-24.

Huxley, A.F., Niedergerke, R. (1954). Structural changes in muscle during contraction. Interference microscopy of living muscle fibres. Nature, 173, 971-973.

Huxley, A.F., Hanson, J. (1954). Changes in cross-striations of muscle during contraction and stretch and their structural interpretation. Nature, 173, 973-976.

Huxley, H.E. (1956). Endeavour, 15(177).

Huxley, H.E. (1965). Scient Am, 213(18).

Huxley, H.E. (1969). The mechanism of molecular contraction: recent structural studies suggest a revealing model for cross-bridge action at variable filament spacing. Science, 164, 1356-1366.

Huxley, A.F. (2000). Mechanics and models of the myosin motor. Philosophical Trans Roy Soc, B355, 433-440.

Huxley, A.F. (1957). Muscle structure and theories of contraction. Prog Biophys Molecul Biol, 7, 255-318.

Huxley, A.F., Simmons, R.M. (1971). Proposed mechanism of force generation in striated muscle. Nature, 233, 533-538.

Huxley, A.F., Huxley, H.E. (1964). Organizers of a discussion of the physical and chemical basis of muscular contraction. Proc Roy Soc, B160, 433-542.

Ikai, M., Fukunaga, T. (1968). Calculation of muscle strength per unit cross-sectional area of human muscle by means of ultrasonic measurement. Internationale Zeitschrift fuer Angewandte Physiologie, 26, 26-32.

Ikai, M., Fukunaga, T. (1970). A study of training effect on strength per unit cross-sectional area muscle by means of ultrasonic measurement. Internationale Zeitschrift fuer Angewandte Physiologie, 28, 173-180.

Inbar, G.F., Allin, J., Kranz, H. (1987). Surface EMG spectral changes with muscle length. Med Biol Eng Comput, 25, 683-689.

Irwing, M., Piazzesi, G. (1997). Motions of the myosin heads that drive muscle contraction. News Physiol Sci, 12, 249-254.

Jacobs, R., Van Ingen Schenau, G.J. (1992a). Control of an external force in leg extensions in humans. J Physiol, 457, 611-626.

Jacobs, R., Van Ingen Schenau, G.J. (1992b). Intermuscular coordination in a sprint push-off. J Biomech, 25, 953-965.

James, R.S., Altringham, J.D., Goldspink, D.F. (1995). The mechanical properties of fast and slow skeletal muscles of the mouse in relation to their locomotory function. J Exp Biol, 198, 491-502.

Jensen, B.R. (1991). Isometric contractions of small muscle groups, (Ph.D. Thesis). Copnehagen: Danish National Institute of Occupational Health.

Johnson, M.A., Polgar, J., Weightman, D., Appleton, D. (1973). Data on the distribution of fibre types in thirty-six human muscles-an autopsy study. J Neurol Sci, 18, 111-129.

Joyce, G.C., Rack, P.M. (1969). Isotonic lengthening and shortening movements of cat soleus muscle. J Physiol, 204, 475-491.

Joyce, G.C., Rack, P.M., Westbury, D.R. (1969). The mechanical properties of cat soleus muscle during controlled lengthening and shortening movements. J Physiol, 204, 461-474.

Kadefors, R., Kaiser, E., Petersén, I. (1968). Dynamic spectrum analysis of myopotentials with special reference to muscle fatigue. Electromyogr, 8, 39-74.

Kamen, G., Sison, S.V., Du, C.C.D., Patten, C. (1995). Motor unit discharge behavior in older adults during maximal-effort contractions. J Appl Physiol, 79, 1908-1913.

Kanda, K., Hashizume, K. (1992). Factors causing difference in force output among motor units in the cat medial gastrocnemius muscle. J Physiol (London), 448, 677-695.

Karlsson, S., Gerdle, B. (2001). Mean frequency and signal amplitude of the surface EMG of the quadriceps muscles increase with increasing torque – a study using the continuous wavelet transform. J Electromyogr Kinesiol, 11, 131-140.

Kasprisin, J.E:, Grabiner, M.D. (2000). Joint angle-dependence of elbow flexor activation levels during isometric and isokinetic maximum voluntary contractions. Clin Biomech, 15, 743-749.

Kawakami, Y., Abe, T., Kuno, S.Y., Fukunaga, T. (1995). Training-induced changes in muscle architecture and specific tension. Eur J Appl Physiol, 72, 37-43.

Kawakami, Y., Lieber, R.L. (2000). Interaction between series compliance and sarcomere kinetics determines internal sarcomere shortening during fixed-end contraction. J Biomech, 33, 1249-1255.

Kanehisa, H., Nemoto, I., Okuyama, H., Ikegawa, S., Fukunaga, T. (1996). Force generation capacity of knee extensor muscles in speed skaters. Eur J Appl Physiol, 73, 544-551.

Keidel, M., Keidel, W.D. (1989). The computer-vibromyography as a biometric progress in studying muscle function. Biomed Tech (Berlin), 34, 107-116.

Ker, R.F., Alexander, R.McN., Bennet, M.B. (1988). Why are mammalian tendons so thick? J Zoo (London), 216, 309-324.

Ker, R.F. (1992). Tensile fibres: strings and straps. In: Vincent, J.F.V. (Ed.), Biomechanics-Materials: A Practical Approach, Oxford University Press, New York, 75-97.

Kernell, D., Eerbeek, O., Verhey, B.A. (1983). Relation between isometric force and stimulation rate in cat's hindlimb motor units of different twitch contraction time. Exp Brain Res, 50, 220-227.

Kerševan, K. (2002). Primerjava biomehanskega in mioelektričnega odziva mišice biceps brachii pri človeku. Magisterska naloga, Fakulteta za elektrotehniko, Ljubljana.

Kitamura, K., Tokunaga, M., Iwane, A.H., Yanagida, T. (1999). A single myosin head moves along an actin filament with regular steps of 5.3 nanometers. Nature, 397, 129-134.

Knaflitz, M., Merletti, R., De Luca, C.J. (1990). Inference of motor unit recruitment order in voluntary and electrically elicited contractions. J Appl Physiol, 68, 1657-1667.

Knez, N., Valenčič, V., Burger, H., Marinček, Č. (1994). Ponovljivost merjenja odzivov skeletnih mišic z merilnikom odmikov, ERK 94, 340-343.

Knez, N. (2000). Modeliranje odziva trebuha skeletne mišice na električno stimulacijo. Doktorska disertacija, Fakulteta za elektrotehniko, Univerza v Ljubljani, Ljubljana, Slovenija.

Knez, N., Valenčič, V., Godina, N., Djordjevič, S. (1999). Non-invasive measurement of muscle tension and its relevance in sport. Sport kinetics 1999: theories of human motor performance and their reflections in practice: book of abstracts, (Kinesiologija slovenica, 5), Strojnik, V., Ušaj, A. (ur.), Ljubljana, International Association of sport kinetics, Univerza v Ljubljani, Fakulteta za šport, 92.

Kogi, K., Hakamada, T. (1962). Slowing of surface electromyogram and muscle strength in muscle fatigue. Rep Inst Sci Labour Tokyo, 60, 27-41.

Kogovšek, N. (1991). Merjenje in modeliranje biomehanskih lastnosti skeletnih mišic, Prešernova nagrada.

Komi, P.V, Buskirk, E.R. (1970). Reproducibility of electromyographic measurements with inserted wire electrodes and surface electrodes. Electromyogr and Clin Neurophysiol, 10, 357-367.

Komi, P.V. (1973). Measurement of the force-velocity relationship in human muscle under concentric and eccentric contractions. Med Sport Biomech, Bassel, 8, 224-229.

Komi, P.V. (1990). Relevance of in vivo force measurement to human biomechanics. J Biomech 23, 23-34.

Komi, P., Viitsalo, J.H.T. (1976). Signal characteristics of EMG at different levels of muscle tension. Acta Physiol Scand, 96, 267-276.

Koo, T.K.K., Mak, A.F.T., Hung, L.K. (2002). In vivo determination of subject-specific musculotendon parameters: applications to the prime elbow flexors in normal and hemiparetic subjects. Clin Biomech, 17, 390-399.

Kouzaki, M., Shinohara, M., Fukunaga, T. (1999). Non-uniform mechanical activity of quadriceps muscle during fatigue by repeated maximal voluntary contraction in humans. Eur J Appl Physiol, 80, 9-15.

Kralj, A., Bajd, T. (1989). Functional electrical stimulation:standing and walking after spinal cord injury. Boca Raton (Florida): CRC Press.

Kralj, A., Bajd, T., Stanič, U., Ačimovič-Janežič, R., Turk, R. (1994). Functional electrical stimulation in the rehabilitation of patients with paraplegia and hemiplegia. V Illis, L. S. (ur.), Neurological rehabilitation, 2nd edition, Oxford (etc): Blackwell Scientific Publications, 519-535.

Kudina, L.P., Alexeeva, N.L. (1992a). After-potentials and control of repetitive firing in human motoneurones. Electroencephalogr Clin Neurophysiol, 85, 345-353.

Kudina, L.P., Alexeeva, N.L. (1992b). Repetitive “doublet”s of human motoneurones: analysis of interspike intervals and recruitment pattern. Electroencephalogr Clin Neurophysiol, 85, 243-247.

Kukulka C.G., Clamann H.P., 1981. Comparison of the recruitment and discharge properties of motor units in human biceps brachii and adductor pollicis during isometric contractions. Brain Res, 219, 45-55.

Kupa, E.J., Roy, H., Kadarin, S.C., De Luca, C.J. (1995). Effects of muscle fibre type and size on EMG median frequency and conduction velocity. J Appl Physiol, 79(1), 23-33.

Laframboise, J., Cafarelli, E. (1994). Differential effects of voluntary and involuntary activation on contractile characteristics of two human muscles. J Appl Physiol, 76, 1400-1402.

Lateva, Z.C., Dimitrova, N.A., Dimitrov, G.V. (1993). Effect of recording electrode position along a muscle fibre on surface potential power spectrum. J Electromyogr Kinesiol, 3, 195-204.

Lawrence, J.H., De Luca, C.J. (1983). Myoelectric signal versus force relationship in different human muscle. J Appl Physiol, 54, 1653-1659.

Lännergren, J., Smith, R.S. (1966). Types of muscle fibres in toad skeletal muscle. Acta Physiol Scand, 68, 263-274.

Lev-Tov, A., Pratt, C.A., Burke, R.E. (1988). The motor-unit population of the cat tenuissimus muscle. J Neurophysiol, 59, 1128-1142.

Lexell, J., Heriksson-Larsen, K., Sjostrom, M. (1983). Distribution of different fibre types in human skeletal muscles. Acta Physiol Scand, 117, 115-122.

Lieber, R.L., Boakes, J.L. (1988). Sarcomere length and joint kinematics during torque production in frog hindlimb. Am J Physiol, 254, C759-768.

Lieber, R.L., Leonard, M.E., Brown, C.G., Trestik, C.L. (1991). Frog semitendinosis tendon load-strain and stress-strain properties during passive loading. Am J Physiol, 261, C86-92.

Lieber, R.L., Loren, G.J:, Fridén, J. (1994). In vivo measurement of human wrist extensor muscle sarcomere length changes. J Neurophysiol, 71, 874-881.

Lindström, L., Magnusson, R., Petersén, I. (1970). Muscular fatigue and action potential conduction velocity changes studied with frequency analysis of EMG signals. Electromyogr, 10, 341-356.

Lippold, O.C.J. (1952). The relation between integrated action potentials in a human muscle and its isometric tension. J Physiol, 117, 492-499.

Loren, G.J., Lieber, R.L. (1995). Tendon biomechanical properties enhance human wrist muscle specialization. J Biomech, 28, 791.

MacIntosh, B.R., Gardiner, P.F. (1987). Post-tetanic potentiation and skeletal muscle fatigue: interactions with caffeine. J Physiol Pharmacol, 65(2), 260-268.

Maenhout, M., Hesselink, M.K.C., Oomens, C.W.J., Drost, M.R. (2000). Parameter identification of a distribution-moment approximation two-state Huxley model of the rat tibialis anterior muscle. In: Skeletal Muscle Mechanics: From Mechanism to Function. Herzog, W. (ed.), John Wiley & Sons, Ltd., Chichester, England.

Maganaris, C.N., Baltzopoulos, V., Sargeant, A.J. (1998a). Changes in achilles tendon moment arm from rest to maximum isometric plantarflexion: In vivo observations in man. J Physiol, 510, 977-985.

Maganaris, C.N., Baltzopoulos, V., Sargeant, A.J. (1998b). In vivo measurements of the triceps surae complex architecture in man: Implications for muscle function. J Physiol, 512, 603-614.

Maganaris, C.N., Baltzopoulos, V., Sargeant, A.J. (1998c). Differences in antagonistic ankle dorsiflexor co-activation between legs: Can they explain the moment deficit in the weaker plantarflexor leg? Exp Physiol, 83, 843-855.

Maganaris, C.N., Paul, J.P. (2000). In vivo human tendinous tissue stretch upon maximum muscle force generation. J Biomech, 33, 1453-1459.

Maganaris, C.N. (2001). Force-length characteristics of in vivo human skeletal muscle. Acta Physiol Scand, 172(4), 279-285.

Maganaris, C.N. (2002). Tensile properties of in vivo human tendinous tissue. J Biomech, 35, 1019-1027.

Mannion, A.F., Dumas, G.A., Stevenson, J.M., Cooper, R.G. (1998). The influence of muscle fibre size and type distribution on electromyographic measures of back muscle fatigability. Spine, 23, 576-584.

Marsden, C.D., Meadows, J.C. (1970). The effect of adrenaline on the contraction of human muscle. J Physiol (London), 207, 429-448.

Marsden C.D., Meadows J.C., Merton P.A., 1983. "Muscular Wisdom" that minimizes fatigue during prolonged effort in man: peak rates of motoneuron discharge and slowing of discharge during fatigue. Motor Control Mech Health Dis; 169-211.

Marsh, E., Sale, D., McComas, A.J., Quinlan, J. (1981). Influence of joint position on ankle dorsiflexion in humans. J Appl Physiol, 51(1), 160-167.

Masuda, T., Sadoyama, T., Shiraishi, M. (1996). Dependence of average muscle fibre conduction velocity on voluntary contraction force. J Electromyogr Kinesiol, 6, 267-276.

Matheson, G.O., Maffey-Ward, L., Mooney, M., Ladly, K., Fung, T., Zhang, Y. (1997). Vibromyography as a quantitative measure of muscle force production. Scand J Med, 29, 29-35.

Matjačič, Z., Bajd, T., Gregorič, M., Benko, H., Obreza, P. (1996). Trunk muscles strength evaluation in normal and paraplegic subject. V Miklavčič, D., Bajd, T., Stanič, U., Munih, M. (ur.), 9th international Coference on Mechanics in Medicine and Biology, Ljubljana, Slovenia, 437-440.

Maton, B., Pérès, G., Landjerit, B. (1987). Relationships between individual isometric muscle forces, EMG activity and joint torque in monkeys. Eur J Appl Physiol 56, 487-494.

Maton, B., Petitjean, M., Cnockaert, J.C. (1990). Phonomyogram and electromyogram relationships with isometric force reinvestigated in man. Eur J Appl Physiol, 60, 194-201.

Mazella, H. (1954). On the pressure developed by the contraction of striated muscle and its influence on muscular circulation. Archives Internationales de Physiologie, 62, 334-347.

McComas, A.J., Thomas, H.C. (1968). Fast and slow twitch muscle in man. J Neurol Sci, 7, 301-307.

McPhedran, A.M., Wuerker, R.B., Henneman, E. (1965). Properties of motor units in a homogeneous red muscle (sloeus) of the cat. J Neurophysiol, 28, 71-84.

Mela, P., Veltink, P.H., Huijing, P.A. (2001). The influence of stimulation frequency and ankle joint on the moment exerted by human dorsiflexor muscles. J Electromyogr Kinesiol, 11, 53-63.

Merletti, R., Knaflitz, M., De Luca, C.J. (1990). Myoelectric manifestations of fatigue in voluntary and electrically elicited contractions. J Appl Physiol, 69, 1810-1819.

Merletti, R., LoConte, L.R., Orizio, C. (1991). Indices of muscle fatigue. J Electromyogr Kinesiol, 1, 20-33.

Merletti, R., De Luca, C.J., Sathyan, D. (1994). Electrically evoked myoelectric signals in back muscles: effect of side dominance. J Appl Physiol, 77, 2104-2114.

Merletti, R., De Luca, C.J., Sathyan, D. (1995). Repeatability of electrically-evoked myoelectric signals in the human tibialis anterior muscle. J Electromyogr Kinesiol, 5(2), 67-80.

Miller, A.E.J., MacDougall, J.D., Tarnopolsky, M.A., Sale, D.G. (1993). Gender differences in strength and muscle fibre characteristics. Eur J Appl Physiol, 66, 254-262.

Milner-Brown, H., Stein, R.B. (1975). The relation between the surface electromyogram and muscular force. J Physiol (London), 246, 549-569.

Monster, A.W., Chan, H.C. (1977). Isometric force production by motor units of extensor digitorum communis muscle in man. J Neurophysiol, 40, 1432-1443.

Morgan, D.L. (1985). From sarcomeres to whole muscles. J Exp Biol, 115, 169-178.

Moritani, T., Muro, M. (1987). Motor unit activity and surface EMG power spectrum during increasing force contraction. Eur J Appl Physiol, 56, 200-265.

Munih, M., Kralj, B., Bajd, T. (1995). Calculated muscle activity during paraplegic standing optimised for minimal femur and tibia bone loading. V Granat, M.H., Conway, B.A., Barbenel, J.C. (ur.), BES Symposium on Electrical Stimulation, Clinical Systems, University of Strathclyde, Glasgow, 73-74.

Murray, W.M., Delp, S.L., Buchanan, T.S. (1995). Variation of muscle moment arms with elbow and forearm position. J Biomech, 28, 513-525.

Murray, W.M., Buchanan, T.S., Delp, S.L. (2000). The isometric functional capacity of muscles that cross the elbow. J Biomech, 33, 943-952.

Murray, W.M., Buchanan, T.S., Delp, S.L. (2002). Scaling of peak arms of elbow muscles with upper extremity bone dimensions. J Biomech, 35, 19-26.

Nakhostine, M., Styf, J.R., Van Leuven, S., Hergens, A.R., Gershuni, D.H. (1993). Intramuscular pressure varies with depth. The tibialis anterior muscle studied in twelve volunteers. Acta Orth Scand, 64, 377-381.

Nanthavanu, S., Deivanayagam, S. (1989). On assessment of muscle fatigue rate via various EMG frequency spectral parameters. Int J Indust Erg, 4, 213-224.

Narici, M.V., Roi, G.S., Landoni, L., Minetti, A.E., Cwerretelli, P. (1989). Changes in force, cross-sectional area and neural activation during strength training and detraining of the human quadriceps. Eur Appl Physiol, 59, 310-319.

Narici, M.V., Binzoni, T., Fasel, J, Terrier, F., Cerretelli, P. (1996). In vivo human gastrocnemius architecture with changing joint angle at rest and during graded isometric contraction, J Physiol, 496, 287-297.

Noyes, F.R. (1977). Functional properties of knee ligaments and alterations induced by immobilization. Clin Orth Rel Res, 123, 210-242.

Noyes, F.R., Butler, D.L., Grood, E.S., Zernicke, R.F., Hefzy, M.S. (1984). Biomechanical analysis of human ligament grafts used in knee ligament repairs and reconstructions. J Bone Joint Surg, 66-A, 344-352.

Oberg, T., Sandsjo, L., Kadefors, R. (1992). Arm movement and EMG mean power frequency in the trapezius muscle. A comparison between surface and intramuscular recording techniques. Electromyogr Clin Neurophysiol, 32, 87-92.

Okada, M. (1987). Effect of muscle length on surface EMG wave forms in isometric contractions. Eur J Appl Physiol, 56, 462-466.

Onishi, H., Yagi, R., Akasaka, K., Momose, K., Ihashi, K., Handa, Y. (2000). Relationship between EMG signals and force in human vastus lateralis muscle using multiple bipolar wire electrodes. J Electromyogr Kinesiol, 10, 59-67.

Orizio, C., Perini, R., Veicsteinas, A. (1989). Muscular sound and force relationship during isometric contraction in man. Eur J Appl Physiol, 58, 528-533.

Barr

Orizio, C. (1993). Muscle sound: bases for the introduction of a mechanomyographic signal in muscle studies. Crit Rev Biomed Eng, 21, 201-243.

Orizio, C., Solomonow, M., Baratta, R., Veicsteinas, A. (1993). Influence of motor units recruitment and firing rate on the soundmyogram and EMG characteristics in cat gastrocnemius. J Electromyogr Kinesiol, 2, 232-241.

Orizio, C., Liberati, D., Locatelli, C., DeGrandis, D., Veicsteinas, A. (1996). Surface mechanomyogram reflects muscle fibres twitches summation. J Biomech, 29(4), 475-481.

Orizio, C., Esposite, F., Paganotti, I., Marino, L., Rossi, B., Veicsteinas, A. (1997). Electrically-elicited surface mechanomyogram in myotonic dystrophy. Ital J Neurol Sci, 18, 185-190.

Orizio, C., Baratta, R., Zhou, B., Solomonow, M., Veicsteinas, A. (1999). Force and surface mechanomyogram relationship in cat gastrocnemius. J Electromyogr Kinesiol, 9, 131-140.

Orizio, C., Baratta, R.V., Zhou, B.H., Solomonow, M., Veicsteinas, A. (2000). Force and surface mechanomyogram frequency responses in cat gastrocnemius. J Biomech, 33, 427-433.

Orizio, C. (2002). Comments on the letter "Accelerometer and mechanomyogram". J Biomech, 3, 385.

Oster, G., Jaffe, J.S. (1980). Low frequency sounds from sustained contraction of human skeletal muscle. Biophys J, 30, 189-194.

Otten, E. (1988). Concepts and models of functional architecture in skeletal muscle. Exercise Sport Sci Rev, 16, 89-139.

Panenic, R., Gardiner, P.F. (1998). The case for adaptability of the neuromuscular junction to endurance exercise training. Canad J Appl Physiol, 23, 339-360.

Parker, P.A., Körner, L., Almström, C., Andersson, G., Johnsson, V., Herberts, P., Kadefors, R. (1982). Skeletal muscle force, pressure and myoelectric signal. Proceedings of the 5th Congress of ISEK, 32-34.

Parker, P.A., Körner, L., Kadefors, R. (1984). Estimation of muscle force from intramuscular total pressure. Med Biol Eng Comput, September 1984, 453-457.

Payne, C.M., Stern, L.Z., Curless, R.G., Hannapel, L.K. (1975). Ultrastructural fibre typing in normal and diseased muscle. J Neurol Sci, 25, 99-108.

Pernuš, F. (1997). Arrangement for fibre types in human skeletal muscle fascicles. V Zajc, B. (ur.), Zbornik šeste Elektrotehniške in računalniške konference ERK 1997, B339-342.

Petitjean, M., Maton, B., Fourment, A. (1998). Summation of elementary phonomyograms during isometric twitches in humans. Eur J Appl Physiol, 77, 527-535.

Praprotnik, U. (1999). Odziv mišice na električno stimulacijo pred in po obremenitvi. Diplomska delo, Fakulteta za šport, Ljubljana.

Putz, R., Pabst, R. (2001). Sobotta: Atlas of human anatomy. Putz, R., Pabst, R. (ed.).

Rack, P.M.H., Westbury, D.R. (1969). The effects of length and stimulus rate on tension in the isometric cat soleus muscle. J Physiol (London), 204, 443-460.

Rack, P.M.H., Westbury, D.R. (1984). Elastic properties of the cat soleus tendon and its effects on mechanical properties. J Physiol, 282, 253-261.

Rankin, L.L., Enoka, R.M., Volz, K.A., Stuart, D.G. (1988). Coexistence of twitch potentiation and tetanic force decline in rat hidlimb muscle. J Appl Physiol, 65, 2687-2695.

Ranvier, L. (1873). Propertiétés et structures différentes des muscles rouges et des muscles blancs, chez les lapins et chez les raies. C.R. Acad Sci (Paris), 77, 1030-1034.

Rainoldi, A., Nazzaro, M., Merletti, R., Farina, D., Caruso, I., Gaudenti, S. (2000). Geometrical factors in surface EMG of the vastus medialis and lateralis muscles. J Electromyogr Kinesiol, 10, 327-336.

Raschke, U., Don Chaffin, B. (1996). Support for a linear length-tension relation of the torso extensor muscles: an investigation of the length and velocity EMG-force relationships. J Biomech, 29(12), 1597-1604.

Rassier, D.E., Tubman, L.A., MacIntosh, B.R. (1997). Length-dependent potentiation and myosin light chain phosphorylation in rat gastrocnemius muscle. Am J Physiol, 273(1), C198-204.

Reberšek, S. (1984). Vpliv električne stimulacije in mehanskega gibanja na spastičnost mišic skočnega sklepa pri hemiplegičnih bolnikih. Disertacija, Ljubljana.

Reberšek, S., Stefanovska, N., Vodovnik, L., Gros, N. (1986). Some properties of spastic ankle joint muscles hemipeglia. Med Biol Eng Comput, 24, 19-26.

Rice, C.L., Cunningam, D.A., Taylor, A.W., Paterson, D.H. (1988). Comparison of the histochemical and contractile properties of human triceps surae. Eur J Appl Physiol, 58, 165-170.

Richardson, R.S., Frank, L.R., Haseler, L.J. (1998). Dynamic knee-extensor and cycle exercise: Functional MRI of muscular activity. Inter J Sport Med, 19, 182-187.

Riley, D.A., Bain, J.L.W., Thompson, J.L., Fitts, R.H., Widrick, J.J., Trappe, S.W., Trappe, T.A., Costill, D.L. (2000). Increased thin filament density and length in human atrophic soleus muscle fibres after spaceflight. J App Physiol, 88, 567-572.

Roszek, B., Huijing, P.A. (1997). Stimulation frequency history alters length-force characteristics of fully recruited rat muscle. J Electromyogr Kinesiol, 7(3), 161-177.

Roy, S.H., De Luca, C.J., Schneider, J. (1986). Effects of electrode location on myolectric conduction velocity and median frequency estimates. J Appl Physiol, 61, 1510-1517.

Sadamoto, T., Bonde-Petersen, F., Suzuki, Y. (1983). Skeletal muscle tension, flow, pressure and EMG during sustained isometric contractions in humans. Eur J Appl Physiol Occupat Physiol, 51, 395-408.

Sale, D., Quinlan, J., Marsh, E., McComas, A.J., Belanger, A.Y. (1982). Influence of joint position on ankle plantrflexion in humans. J Appl Physiol, 52(6), 1636-1642.

Salvenberg, H.H.C.M. (2000). Rise and relaxation times of twitches and tetani in submaximally recruited, mixed muscle: a computer model. In: Skeletal Muscle Mechanics: From Mechanism to Function. Herzog, W. (editor), John Wiley & Sons, Ltd., Chichester, England.

Sanchez, J.H., Solomonow, M., Baratta, R.V., D'Ambrosia, R. (1993). Control strategies of the elbow antagonist muscle pair during two types of increasing isometric contraction. J Electromyogr Kinesiol, 3, 33-40.

Schure, A. (1970). Impedance matching. John F. Rider Publisher, New York, 1-19.

Scott, S.H., Loeb, G.E. (1995). Mechanical properties of aponeurosis and tendon of the cat soleus muscle during whole-muscle isometric contractions. J Morphol, 224, 73-86.

Sejersted, O.M., Hargens, A.R., Kardel, K.R., Blom, P., Jensen, Ø., Hermansen, L. (1984). Intramuscular fluid pressure during isometric contraction of human skeletal muscle. J Appl Physiol, 56, 287-295.

Sejersted, O.M., Hargens, A.R. (1995). Intramuscular pressures for monitoring different tasks and muscle conditions. Plenum press, New York, 339-350.

Sherrington, C.S. (1898). J Physiol (London), 22, 319.

Sica, R.E.P., McComas, A.J. (1971). Fast and slow twitch units in a human muscle. J Neurol Neurosurg Psychiat, 34(2), 113-120.

Simoneau, J.A., Lortie, G., Boulay, M.R., Thibault, M.C., Thériault, G., Bouchard, C. (1985). Skeletal muscle histochemical and biochemical characteristics in sedentary male and female subjects. Can J Physiol Pharmacol, 63, 30-35.

Simoneau, J.A., Bouchard, C.H. (1989). Human variation in skeletal muscle fibre-type proportion and enzyme activities. Am J Physiol, 257, E567-572.

Sjöström, M. (1975). The thick myofilament fine structure in ultrathin cryo-sections. Umeå univ. med. diss. new ser. 3, 1-32.

Slomić, A., Rosenfalck, A., Buchthal, F. (1968). Electrical and mechanical responses of normal and myasthenic muscle, with particular reference to the staircase phenomenon, Brain Res, 10, 1-78.

Smith, R.S., Lännergren, J. (1968). Types of motor units in the skeletal muscle of Xenopus laevis. Nature (London), 217, 281-283.

Smith, T.G., Stokes, M.J. (1993). Technical aspects of acoustic myography (AMG) of human skeletal muscle: contact pressure and force/AMG relationships. J Neurosci Meth, 47, 92-95.

Spiegel, K.M., Stratton, J., Burke, J.R., Glendinning, D.S., Enoka, R.M. (1996). The influence of age on the assessment of motor unit activation in a human hand muscle. Exp Physiol, 81, 805-819.

Stefanovska, A., Reberšek, S., Bajd, T., Vodovnik, L. (1991). Effects of electrical stimulation on spasticity. Crit Rev Phys Rehabil Med, 3(1), 59-99.

Steinen, G.J.M., Kiers, J.L., Bottinelli, R., Reggiani, C. (1996). Myofibrillar ATPase activity in skinned human skeletal muscle fibres: Fibre type and temperature dependence. J Physiol, 493, 299-307.

Stephens, J.A., Stuart, D.G. (1975). The motor units of a cat medial gastrocnemius: speed-size relations and their significance for the recruitment order of motor units. Brain Res, 91, 177-195.

Stephenson, D.G., Williams, D.A. (1982). Effects of sarcomere length on the force-pCa relation in fast- and slow-twitch skinned muscle fibres from the rat. J Physiol (London), 233, 637-653.

Stephenson, D.G., Wendt, I.R. (1984). Length dependence of changes in sarcoplasmic calcium concentration and myofibrillar calcium sensitivity in striated muscle fibres. J Muscle Res Cell Motil, 5(3), 243-272.

Stensen, N., (1994). Elementorum myologiæ specimen sev musculi descriptio geometrica. Florence, 1667, cited by T. Kardel, Trans Am Philosoph Soc, 84, 1-252.

Strojnik, V., Komi, P.V. (1998). Neuromuscular fatigue after maximal stretch-shortening cycle exercise. J Appl Physiol: Respiratory, environmental and exercise physiology, 84(1), 344-350.

Stokes, M.J., Dalton, P.A. (1991). Acoustic myographic activity increases linearly up to maximal voluntary isometric force in the human quadriceps muscle. J Neuro Sci, 101, 163-167.

Suter, E., Herzog, W. (1997). Extent of muscle inhibition as a function of knee angle. J Electromyogr Kinesiol, 7, 123-130.

Swammerdam, J. (1994). Biblia naturae. Leiden, 1737, cited by T. Kardel, Trans Am Philosoph Soc, 84, 1-252.

Sweeney, H.L., Bowman, B.F., Stull, J.T. (1993). Myosin light chain phosphorylation in vertebrate striated muscle: regulation and function. Am J Physiol, 264(5), C1085-1095.

Šimunić, B., 2001. Analiza variabilnosti odzivov skeletnih mišic na električno stimulacijo. Magistrska naloga, FE - ULj.

Šimunić, B., Žagar, T., Valenčič, V. (2002). Vpliv izbire merilne točke na variabilnost merjenja odziva trebuha skeletne mišice kot odziv na električno stimulacijo. Zajc, B. (ur.), Zbornik ERK 2002, B325-328.

Tanji, J., Kato, M. (1973). Firing rate of individual motor units in voluntary contraction of abductor digiti minimi muscle in man. Exp Neurol, 40, 771-783.

Thomas, C.K. (1993). Huan motor units studied by spike-triggered averaging and intraneural moor axon stimulation. In Fatigue by Simon C. Gandevia et al., Plenium Press New York, 147-160

Thomas, C.K. (1997). Contractile properties of human thenar muscles paralyzed by spinal cord injury. Muscle & Nerve, July, 788-799.

Thomas, C.K., Johansson, R.S., Bigland-Ritcie, B. (1999). Pattern of pulses that maximize force output from single human thenar motor units. Am Physiol Soc, 3188-3195.

Thorstensson, A., Grimby, G., Karlsson, J. (1976). Force-velocity relations and fibre composition in human knee extensor muscles. J Appl Physiol, 40, 12-16.

Trotter, J.A. (1993). Functional morphology of force transmission in skeletal muscle. A brief review. Acta Anat (Basel), 146(4), 205-222.

Uchiyama, T., Bessho, T., Akazawa, K. (1998). Static torque-angle relation of human elbow joint estimated with artificial neural network technique. J Biomech, 31, 545-554.

Valenčič, V. (1990). Direct measurement of the skeletal muscle tonus. Advances in External Control of Human Extremities, Nauka, Beograd.

Valenčič, V., Knez, N. (1997). Measuring of skeletal muscles dynamic properties. Artific Org, 21, 240-242.

Valenčič, V., Vodovnik, L, Štefančič, M., Jelnikar, T. (1986). Impoved motor response due to chronic electrical stimulation of denervated tibialis anterior muscle in humans. Musle & Nerve, 9, 612-617.

Van Bavel, H., Drost, M.R., Wielders, J.D., Huyghe, J.M., Huson, A., Janssen, J.D. (1996). Strain distribution on rat medial gastrocnemius (MG) during passive stretch. J Biomech, 29, 1069-1074.

Van Bavel, H., Holzer, C.A.J., Van Leeuwem, J., Muijtjens, A.M.M., Willems, P.J.B., Drost, M.R. (1998). Quantification of local surface strains of cat gastrocnemius medialis during contraction. Netherlands J Zool, 48.

Van Cutsem, M., Feiereisen, P., Duchateau, J., Hainaut, K. (1997). Mechanical properties and behavior of motor units in the tibialis anterior during voluntary contractions. Canad J Appl Physiol, 22, 585-597.

Van Donkelaar, C.C., Willems, P.J.B., Muijtjens, A.M.M., Drost, M.R. (1999). Skeletal muscle transverse strain during isometric contraction at different lengths. J Biomech, 32, 755-762.

Van Donkelaar, C.C., Huyge, J.M., Vankan, W.J., Drost, M.R. (2001). Spatial interaction between tissue pressure and skeletal muscle perfusion during contraction. J Biomech, 34, 631-637.

Van Eijden, T.M.G.J., Turkawski, S.J.J., van Ruijven, L.J., Brugman, P. (2002). Passive force characteristics of an architecturally complex muscle. J Biomech, 35, 1183-1189.

Van Ingen Schenau, G.J., Van Soest, A.J., Gabriels, F.J.M. (1995). The control of multi-joint movements relies on detailed internal representations. Human Mov Sci, 14, 511-538.

Vandenboom, R., Houston, M.E. (1996). Phosphorylation of myosin and twitch potentiation in fatigued skeletal muscle. J Physiol Pharmacol, 74(12), 1315-1321.

Vandervoort, A.A., Quinlan, J., McComas, A.J. (1983). Twitch potentiation after voluntary contraction. Exp Neurol, 81(1), 141-152.

Viidik, A. (1973). Functional properties of collagenous tissues. Inter Rev Connective Tissue Res, 6, 127-215.

Wakeling, J.M., Nigg, B.M. (2001)Soft-tissue vibrations in the quadriceps measured with skin mounted transducers. J Biomech, 34, 539-543.

Wang, Y.P., Fuchs, F. (1994). Length, force and Ca(2+)-troponin C affinity in cardiac and slow skeletal muscle. Am J Physiol, 266(4), C1077-1082.

Warshaw, D.M. (1996). The in vitro motility assay: A window into the myosin molecular motor. News Physiol Sci, 11, 1-6.

Weber, W., Weber, E. (1836). Mechanik der menschlichen gehwerkzeuge. W. Fischer Verlag, Goettingen.

Wee, A.S., Ashley, R.A. (1990). Transmission of acoustic vibratory signals from a contracting muscle to relatively distant tissues. Electromyogr Clin Neurophysiol, 30, 303-306.

Weijs, W.A., Korfage, J.A.M., Langenbach, G.J. (1989). The functional significance of the position of the center of rotation for jaw opening and closing in the rabbit. J Anat, 162, 133-148.

Wetzel, P., Gros, G. (1998). Decay of Ca^{2+} and force transients in fast- end slow- twitch skeletal muscles from the rat, mouse and etruscan shrew. J Exp Biol, 201, 375-384.

Wilkie, D.R. (1950). The relation between force and velocity in human muscle. J Physiol (London), 110, 249-280.

Wollaston, W.H. (1980). On the duration of the muscle action. Philos Trans Roy Soc (London), 1810-1821.

Woittiez, R.D., Huijing, P.A., Rozendal, R.H. (1983). Influence of muscle architecture on the force-length diagram of mammalian muscle. Pflug Arch, 399, 275-279.

Wong, Y.M. (2001). Letter to the editor: Accelerometer and mechanomyogram. J Biomech 34, 557.

Wretling, M.L., Gerdle, B., Henriksson-Larsen, K. (1987). EMG: a non-invasive method for determination of fibre type proportion. Acta Physiol Scand, 131, 627-628.

Yamaguchi, G.T., Sawa, A.G.U., Moran, D.W., Fessler, M.J., Winters, J.M. (1990). A survey of human musculotendon actuator parameters. Multiple Muscle Systems: Biomechanics and Movement Organization. Winters, J.M., Woo, S.L-Y. (eds.), Springer-Verlag, New York, 713-773.

Yang, Z., Stull, J.T., Levine, R.J.C., Sweeney, H.L. (1998). Changes in interfilament spacing mimic the effect of myosin regulatory light chain phosphorylation in rabbit psoas fibres. J Struct Biol, 122, 139-148.

Yemm, D.P., DiCaprio, R.A., Fourtner, C.R. (1982). Resting tension and posture in arthropods. J Exp Biol, 96, 412-425.

Yoshitake, Y., Moritani, T. (1999). The muscle sound properties of different muscle fibre types during voluntary and electrically induced contractions. J Electromyogr Kinesiol, 9, 209-217.

You, G., Alexander, A.L., Laidlaw, D.H., Gmitro, A.F., Unger, E.C., Enoka, R.M. (1994). Sensitivity of muscle proton spin-spin relaxation time as an index of muscle activation. J Appl Physiol, 77, 84-92.

Zajac III, F.E., Young, J.L. (1980a). Properties of stimulus trains producing maximum tension-time area per pulse from single motor units in medial gastrocnemius muscle of the cat. J Neurophysiol, 43, 1206-1220.

Zajac III, F.E., Young, J.L. (1980a). Discharge properties of hindlimb motoneurons in decelerate cats during locomotion induced by mesencephalic stimulation. J Neurophysiol, 43, 1221-1235.

Zajac III, F.E. (1989). Muscle and tendon: properties, models, scaling, and application to biomechanics and motor control. CRC Crit Rev Biomech Eng, 17, 359-411.

Zepetnek, T.J., Hung, H.V., Erdebil, S., Gordon, T. (1992). Innervation ratio is an important determination of force in normal and reinnervated rat tibialis anterior muscles. J Neurophysiol, 67, 1385-1403.

Zhang, Y., Frank, C.B., Rangayyan, R.M., Bell, G.D. (1992). A comparative study of simultaneous vibromyography and electromyography with active human quadriceps. IEEE Trans Biomed Eng, 39, 1045-1052.

Zhang, Y., Frank, C.B., Rangayyan, R.M., Bell, G.D. (1996). Relationships of the vibromyogram to the surface electromyogram of the human rectus femoris muscle during voluntary isometric contraction. J Rehab Res Dev, 33(4), 395-403.

Zupan, A., Gregorič, M.,Valenčič, V. (1995). Long-lasting effects of electrical stimulation upon muscles of patients suffering from progressive muscular dystrophy. Clin Rehabil, 9, 102-109.

Zupan, A., Gregorič, M.,Valenčič, V., Vandot, S. (1993). Effects of electrical stimulation on muscles of children with Duchenne and Becker muscular dystrophy. Neuropediatrics, 24, 4.

Zuurbier, C.J., Huijing, P.A. (1992). Influence of muscle geometry on shortening speed of fibre, aponeurosis and muscle. J Biomech, 25, 1017-1026.

Zuurbier, C.J., Huijing, P.A. (1993). Changes in geometry of actively shortening unipennate rat gastrocnemius muscle. J Morphol, 218, 167-180.

Zuurbier, C.J., Everard, A.J., Van der Wees, P., Huijing, P.A. (1994). Length-force characteristics of the aponeurosis in the passive and active muscle condition and in the isolated condition. J Biomech, 27, 445-453.

Zwarts, M.J., Keidel, M. (1991). Relationship between electrical and vibratory output of muscle during voluntary contraction and fatigue. Muscle & Nerve, 14, 756-761.

Žefran, M., Bajd, T., Kralj, A. (1996). Kinematic modeling of four-point walking paterns in paraplegic subjects. IEEE trans man cybern, Part A, Syst humans, 26(6), 760-770.

URL: http://www.neurogenic.com, 2002.

8. Appendix

Appendix A: Force sensor for measuring MVC and ballistic MVC

Manufacturer	Globus Italia
Name	ERGO METER isometric dynamommeter
Sensitivity	100 g
Maximal load	200 kg
Data acquisition	via RS 232 interface

Figure 8.1: Measuring chair

Appendix B: Force sensor for measuring electrically evoked longitudinal responses in human

Manufacturer	World Precision Instruments, Inc
Name	FORT 5000 (Force Transducer)
Sensitivity	5 g
Maximal load	5 kg
Linearity	error < 0.1 %
Own frequency	300 Hz
Mass	8 g
Data acquisition	via diff. amplifier TBM4M (Appendix E)

Figure 8.2: Force sensor for measuring longitudinal responses of human skeletal muscles

Appendix C: Force sensor for measuring electrically evoked longitudinal responses of toad gastrocnemius

Manufacturer	World Precision Instruments, Inc
Name	FORT 250 (Force Transducer)
Sensitivity	0.25 g
Maximal load	250 g
Linearity	error < 0.1 %
Own frequency	300 Hz
Mass	8 g
Data acquisition	via diff. amplifier TBM4M (Appendix E)

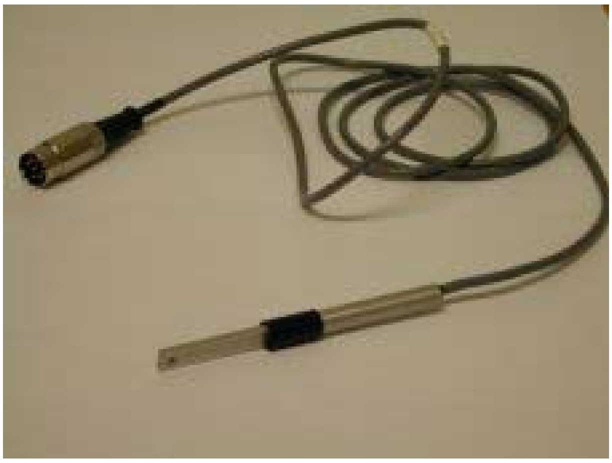

Figure 8.3: Force sensor for measuring longitudinal responses of toad gastrocnemius

Appendix D: Displacement sensor for measuring electrically evoked transverse responses of toad muscle belly

Manufacturer	World Precision Instruments, Inc
Name	DSPL (Displacement Transducer)
Lever length	24 mm
Principle	electromagnetic sensor
Noise amplitude	0.5 mV
Linearity	error < 2 %
Own frequency	28 Hz
Mass	2.5 g
Data acquisition	via diff. amplifier TBM4M (Appendix E)

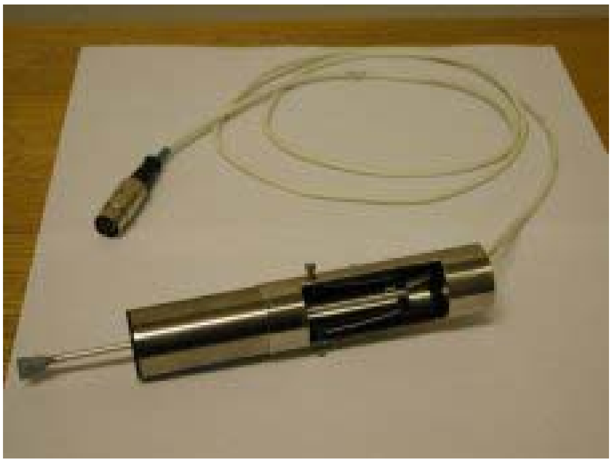

Figure 8.4: Displacement sensor for measuring transverse responses of toad muscle belly

Appendix E: Differential amplifier used for amplifying longitudinal (toad and human skeletal muscles) and transverse responses (toad muscles only)

Manufacturer	World Precision Instruments, Inc
Name	TBM4M (4-Channel Transducer Amplifier)
Channels	4
Amplification	x1, x10, x100, x1000
Noise amplitude	0.4 μV (0.1 do 10 Hz, x100)
Output voltage	± 10V
Input resistance	10^{10} Ω
Frequency band	1 MHz (x1), 80 kHz (x10), 10 kHz (x100), 1 kHz (x1000)
Linearity	error < 0.001 % (x1), < 0.01 % (x 1000)
Data acquisition	using input-output interface (Appendix F)

Figure 8.5: Differential amplifier TBM4M.

Appendix F: Input-output interface for data transfer and acquisition

Manufacturer	National Instruments, Inc
Name	DAQCard™ 1200 PCMCIA (Data Acquisition Card)
Analogue channels	8 inputs (2 of them duplex)
Duplex lines	24
Input voltage	± 5 V
Sampling frequency (analogue channels)	100 – 44100 Hz
Input resistance	10^{10} Ω
AD DA converter resolution	12 bit
Frequency band	250 kHz (x1 - x10), 150 kHz (x20), 60 kHz (x50), 30 kHz (x100)
Data acquisition	using Matlab 5.3, DAQ Toolbox, (Mathworks, Inc.)

Figure 8.6: Input-output interface for transferring collected data together with the connection-board (connecting BNC cables from measuring instruments).

Appendix G: Displacement sensor for monitoring electrically evoked transverse responses of human muscles

Manufacturer	RLS merilna tehnika d.o.o. (Rotary & Linear Motion Sensing Solution)
Name	Displacement Transducer
Principle	Optical lever
Optical lever length	42 mm
Output signal	A and B (TTL levels)
Own frequency	44 Hz
Resolution	2 µm
Error	2 µm (on the whole measuring range)
Maximal displacement velocity	1 m/s
Data acquisition	via counters and parallel computer interface

Figure 8.7: Displacement sensor for measuring muscle belly transverse enlargement.

Appendix H: PC

Manufacturer	Hewlett Packard
Name	Omnibook XE_2
Operating system	Microsoft Windows 98
Configuration	• Pentium Celeron 450 MHz, • 64 MB, • HDD: 5GB.

Figure 8.8: Personal computer with user interface.

Appendix I: Electrical stimulator

Manufacturer	EMF-Furlan&Co. d.o.o.
Name	TMG – S1
Output current	0 – 110 mA for 0 – 1000 Ω resistance
Output voltage	$Ui_{max} < 30$ V rms
Stimulus width	0.1 do 2 ms
Stimulus shape	rectangular, monophasic
Power supply (accumulator)	Ub = 12 V DC

Figure 8.9: Electrical stimulator TMG – S1 was used for generating electrical stimulation in protocols A and B and experiments on toad isolated gastrocnemius.

Appendix J: Measuring chair (Figure 8.1)

Manufacturer	Enraf Nonius BV
Model	Manumed

Appendix K: Software

Matlab 5.3 (*Mathworks, Inc.*)
Microsft Office (*Microsoft, Inc.*)
Mathematica